CHARACTERIZATION OF THE CATALYST USED IN PASSIVE AUTOCATALYTIC RECOMBINERS FOR HYDROGEN MITIGATION IN A NUCLEAR REACTOR AND FORMULATION OF A METHOD FOR CONTAINMENT ANALYSIS

By

VIKRAM SHUKLA

ENGG01201404010

Bhabha Atomic Research Centre, Mumbai

A thesis submitted to the

Board of Studies in Engineering Sciences

In partial fulfillment of requirements

for the Degree of

DOCTOR OF PHILOSOPHY

of

HOMI BHABHA NATIONAL INSTITUTE

May, 2021

Homi Bhabha National Institute[1]

Recommendations of the Viva Voce Committee

As members of the Viva Voce Committee, we certify that we have read the dissertation prepared by **Vikram Shukla** entitled "*Characterization of the Catalyst used in Passive Autocatalytic Recombiners for Hydrogen Mitigation in a Nuclear Reactor and Formulation of a Method for Containment Analysis*" and recommend that it may be accepted as fulfilling the thesis requirement for the award of Degree of Doctor of Philosophy.

Chairman - Prof. S. Banerjee Srikumar Banerjee

Guide / Convener - Prof. N. K. Maheshwari Naresh Kr. Maheshwari 4/5/2021

Co-guide - Dr. Salil Varma Salil Varma 04/05/2021

Examiner - Prof. M. R. Ravi

Member 1- Prof. G. Sugilal G Sugilal 4/5/21

Member 2- Prof. Rajeev kapoor Rajeev Kapoor

Tech. Adviser - Shri Sunil Ganju Sunil Ganju 04/05/2021

Final approval and acceptance of this thesis is contingent upon the candidate's submission of the final copies of the thesis to HBNI.

We hereby certify that we have read this thesis prepared under our direction and recommend that it may be accepted as fulfilling the thesis requirement.

Date: 04/05/2021

Place: Mumbai

Salil Varma 04/05/2021
Dr. Salil Varma
Co-guide

Naresh Kr. Maheshwari
Prof. N. K. Maheshwari
Guide

STATEMENT BY AUTHOR

This dissertation has been submitted in partial fulfillment of requirements for an advanced degree at Homi Bhabha National Institute (HBNI) and is deposited in the Library to be made available to borrowers under rules of the HBNI.

Brief quotations from this dissertation are allowable without special permission, provided that accurate acknowledgement of source is made. Requests for permission for extended quotation from or reproduction of this manuscript in whole or in part may be granted by the Competent Authority of HBNI when in his or her judgment the proposed use of the material is in the interests of scholarship. In all other instances, however, permission must be obtained from the author.

Vikram Shukla

DECLARATION

I, hereby declare that the investigation presented in the thesis has been carried out by me. The work is original and has not been submitted earlier as a whole or in part for a degree / diploma at this or any other Institution / University.

Vikram Shukla

List of Publications arising from the thesis

Journal

1. Development And Validation Of CFD Model For Catalytic Recombiner Against Experimental Results, **V. Shukla**, D. Tyagi, S. Varma, S. Ganju, N. K. Maheshwari, Chemical Engineering Journal 407 (2021) 127216
2. Evaluation Of Reaction Kinetics For The Catalyst Used In PCRD And Study Of Channel Affect On The Same, **V. Shukla**, D. Tyagi, S. Varma, B Saha, A N Shirsat, S. Ganju, S. Sengupta, S. Bhattacharya, N. K. Maheshwari, International Journal of Hydrogen Energy 45/15 (2020) 8584-8594
3. Affect Of Recombiner Location On Its Performance In Closed Containment Under Dry And Steam Conditions, **V. Shukla**, S. Ganju, S. Varma, S. Sengupta, N. K. Maheshwari, International Journal of Hydrogen Energy 44/47 (2019) 25957-25973

Conferences

1. CFD Evaluation of Inlet Gas Conditions Effect on Passive Catalytic Recombiner Device Efficiency, **V. Shukla**, S. Ganju, S. Varma, N. K. Maheshwari, 8th International and 47th National Conference on Fluid Mechanics and Fluid Power, IIT Guwahati, India (2020)
2. Study of Channel Affect on Kinetics of PCRD Catalyst, **V. Shukla**, D. Tyagi, S. Varma, B Saha, A N Shirsat, S. Ganju, N. K. Maheshwari, 64th DAE Solid State Physics Symposium, IIT Jodhpur, India (2019)

Vikram Shukla

Dedicated

To

My beloved

Family

ACKNOWLEDGEMENTS

I take this opportunity to express my sincere gratitude towards my guide, Prof. N. K. Maheshwari and co-guide Dr. Salil Varma for their precious guidance, perennial motivation and constant support. I feel short of words to extend my deep and humble gratitude towards my technology advisor Shri Sunil Ganju (SO/H, DAE) for introducing me to this exciting research field and for his never ending guidance, help, encouragement and support. I am highly obliged and thankful towards Dr. Sujay Bhattacharya (Director RPG & Head, RRDPD, BARC) and Dr. Samiran Sengupta (Head PDS, RRDPD, BARC) for their strong support and motivation during the tenure of this work.

I express my sincere gratitude to the Chairman Prof. S. Banerjee, Prof. G. Sugilal, Prof. Rajeev Kapoor, members of the Doctoral committee and former members Prof. G. K. Dey and Prof. Smt. S. B. Roy. Their valuable suggestions during the internal reviews paved the way for making this research work successful.

It is an emotional moment for me to remember the precious guidance and encouragement provided by late Shri S. G. Markandeya (my M Tech. guide) who helped me inculcate the fundamentals of the subject. I am also grateful Shri S. B. Chafle (former Head PDS, RRDPD, BARC) for granting me the opportunity to undertake this research activity.

I extend my special thanks to my friend Deepak Tyagi and other collogues of FCMCS, Chemistry Division BARC, for their timely help and support in performing the experiments related to this research work. I am also thankful and obliged to my friend and senior collogue Shri Bhuvaneshwar Gera for his never ending help and technical suggestions. My special thanks are due for my collogue and friend Shri D. S. Saini for his selfless and timely technical help for the modifications required in the experimental setup. I am also grateful towards all my friendly and supporting collogues from Process Design Section of RRDPD BARC, for their constant support and motivation.

I am grateful to Dr. J. Chattopadhyay (Head, RSD) and Shri Vishnu Varma (Head, CSS, RSD) for providing me the opportunity to perform and complete theoretical studies related to the work. I am also thankful to Dr. Arun Murthy and Dr. Anil Kumar from m/s Transoft International, Bangalore for their help and consultations regarding the use of computer software FLUIDYN-MP.

Finally, I wish to express my heartfelt gratitude towards my late grandparents, my caring parents and my dear sister who have always been the source of inspiration and motivation for me. I my thankful beyond words towards my loving wife and two sweet daughters for their love, support and understanding which gave me courage and motivation to accomplish this endeavor with zeal and perseverance.

Vikram Shukla

TABLE OF CONTENTS

CONTENTS **Page No.**

EXECUTIVE SUMMARY

A majority of the Nuclear Power Plants presently operational around the world are based on the concept of light/heavy water as coolant and moderator. These reactors are designed with highest standards of industrial and nuclear safety. But during certain postulated severe accidents, they are prone to release of large amounts of hydrogen which gets generated primarily by metal water reaction between fuel clad and steam at elevated temperatures. It is also generated by the radiolysis of water in a gradual but prolonged process. Hydrogen being a very low density gas has a tendency to rise up and form hydrogen rich pockets in the topmost regions of the containment. This could cause combustion/detonation inside the containment posing a threat to its integrity. Out of the various methodologies investigated to mitigate this hydrogen buildup, the use of Passive Catalytic Recombiner Device (PCRD) is the most promising and accepted one. PCRD works on the principle of passively oxidising hydrogen with the oxygen from ambient air over a catalytic surface to form steam. The presence of catalyst enables oxidation of hydrogen at a faster rate at lesser temperatures and thus eliminates the risk of hydrogen combustion inside containment.

Research has been underway around the world for the design, development, performance enhancement and optimum utilization of PCRDs. Different recombiner catalysts have been developed, which have specific reaction kinetics. This chemical kinetics of the catalyst used plays significant role in the performance and efficiency of any recombiner. While the PCRDs developed and deployed in various water-based reactors around the world have been amply characterised with respect to the reaction kinetics and overall recombiner behaviour, there is a need to generate reaction kinetics

for the PCRD catalyst developed for the Indian Pressurised Heavy Water Reactors (IPHWRs). Containment analysis based on Computational Fluid Dynamics model needs to be carried out for analyzing various effects of PCRDs on the overall containment atmosphere during accident scenarios. However, the use of detailed CFD models for simulating PCRD performance in reactor containment is computationally extensive due to the fact that PCRD catalyst plates have thickness of the order of sub-millimeter while the geometries where PCRDs need to be placed have volume in thousands of cubic meters. Hence, innovative and more practical approaches need to be devised for faster analysis. Researchers world-wide have used manufacturer correlations for their respective recombiners for evolving such CFD based hybrid approaches. Hence, similar correlation is required for the Indian PCRD also.

To address the above issues, a detailed CFD based recombiner model has first been developed and validated against data from REKO 3 experiments reported in open literature. The validated model is applied to assess the most suitable recombiner location within a closed cylindrical geometry having pre-filled hydrogen-air-steam mixture. It is found that PCRD placed near bottom of the vessel gives better uniformity of hydrogen concentration inside vessel. The investigation is vital for selecting the PCRD locations for hydrogen mitigation in severe accident scenarios.

The experimental studies have been carried out to determine reaction kinetics of hydrogen recombination on the surface of in-house catalyst developed for PCRD. These catalytic plates are made of 80 mesh SS wire gauze substrate having Pt-Pd catalyst coated by simultaneous electroless deposition method. Characterization of the catalyst shows that it has a noble metal loading of 0.8 wt% with a Pt-Pd ratio of 2:1

and has rough spherical particles of size 0.1 - 1 micron. For generation of kinetics data, a catalytic plate has been placed inside a stainless-steel vessel to carry out hydrogen recombination reaction with known amount of hydrogen and air concentrations in the vessel. The activation energy of recombination reaction for catalyst is found out to be 18.1 kJ/mol and pre exponential factor is 2.14. Behavior of multiple catalytic plates stacked in parallel inside vessel has also been evaluated. This has been achieved by placing four parallel catalytic plates with a gap of 10 mm between each of them. The outer surfaces of the two corner plates are blocked to avoid the lateral diffusion of hydrogen from sideways. The activation energy in this case is found out to be 20.6 kJ/mol, while the pre-exponential factor is 6.1. These values signify faster reaction rate than single catalytic plate due to higher mass transfer because of natural convection established between the catalytic plates.

The reaction kinetics for catalytic plates placed in parallel is written as a single step Arrhenius equation and incorporated into the CFD model. This fine-tuned model has been validated against data from in-house experiments. The validated CFD model has then been used to perform simulations for a parametric study involving various inlet conditions. Values of all variables at the outlet of recombiner obtained as result of about 50 simulations with different inlet conditions are tabulated as a data matrix. This data matrix has been processed to derive the correlations for hydrogen conversion as well as outlet variable conditions for PCRD as functions of inlet variables. These correlations have been compiled for the PCRD developed. The results of the developed empirical correlations are compared against the CFD simulations with reactions kinetics model and found to be within accuracy range of ±20%. These results indicate that conversion efficiency does not change significantly with concentration of steam at the inlet. On the other hand, it is highly dependent on the hydrogen concentration at inlet. This is because, higher hydrogen concentration causes faster reaction rate leading to the increase in catalyst temperature and in turn, further improvement in reaction kinetics.

The developed empirical correlation is incorporated into a general purpose CFD code to formulate a new hybrid approach for predicting the PCRD performance inside closed geometries. In the hybrid approach, the fluid domain of the environment (like reactor containment) is modeled using CFD code, while the volume of PCRD inside the domain is not meshed. The approach has been demonstrated by simulating a room having two compartments and an interconnecting window, with each compartment having one recombiner. The results indicate that values of different variables at recombiner outlet as obtained during the simulation match very closely with the values calculated by the stand alone empirical correlation. This signifies that the hybrid approach has been correctly implemented and gives the results as intended. The simulation gives faster results as compared to detailed recombiner model as it obliviates the complexity of fine meshing inside PCRD while using CFD for capturing hydrogen distribution and other thermodynamic processes inside the closed geometry. Thus, it serves as a vital tool for speedy containment analysis for hydrogen recombination studies.

LIST OF FIGURES

LIST OF TABLES

ABBREVIATIONS

ASME	American Society of Mechanical Engineers
AECL	Atomic Energy of Canada Limited
BARC	Bhabha Atomic Research Centre
BWR	Boiling Water Reactor
CANDU	Canadian Deuterium Uranium
CEA	Commissariat à l'Énergie Atomique
CFD	Computational Fluid Dynamics
CSNI	Committee on the Safety of Nuclear Installations
DOM	Discrete Ordinates Method
ECCS	Emergency Core Cooling System
EDTA	Ethylene-Diamine-Tetraacetic Acid
EPR	European Pressurized Reactor
EURATOM	European Atomic Energy Community
FZJ	Forschungszentrum Jeulich
FZK	Forschungszentrum Karlsruhe
GRS	Gesellschaft für Anlagen- und Reaktorsicherheit (Plant and Reactor Safety Society)
HDR	Decommissioned High-temperature Reactor plant
HEM	Homogeneous Equilibrium Model
HPCM	High Porosity Cell Material
HRTF	Hydrogen Recombiner Test Facility
HYMIS	Hydrogen Mitigation Studies
IAEA	International Atomic Energy Agency

IRSN	Institut de radioprotection et de sûreté nucléaire
KNT	Korea Nuclear Technology
LOCA	Loss Of Coolant Accident
LWR	Light Water Reactor
MBH	Mit Beschränkter Haftung (With Limited Liability)
NEA	Nuclear Energy Agency
NIS	Ingenieurgesellschaft mbH (Hanau, Germany)
NPP	Nuclear Power Plant
OECD	Organisation for Economic Co-operation and Development
PAR	Passive Autocatalytic Recombiner
PCRD	Passive Catalytic Recombiner Device
PHWR	Pressurized Heavy Water Reactor
PWR	Pressurized Water Reactor
RSM	Reynolds Stress equation Model
RTE	Radiative Transfer Equation

NOMENCLATURE

A_j = pre-exponential factor for j^{th} reaction
Cp = specific heat at constant pressure
C_μ = constant
$[D]$ = conductivity matrix
E_j = activation energy for j^{th} reaction
F_{rs} = view factor
h_f = film coefficient
h_r = film coefficient due to radiation
I = total radiation intensity
i = any conserved species (scalar)
K = thermal conductivity
k = turbulence kinetic energy
k_T = reaction rate constant at temperature T
L = vector operator
M_i = molecular weight of species i [kg/kmol]
n = refractive index
p = pressure
Q_{rj} = heat of reaction of j^{th} reaction in terms of leading reactant [J/kmol]
q_r = radiating flux coming onto the structure
q = heat flux vector = $k\nabla T$
$\dddot{q}$ = volumetric heat generation rate
r = position vector
R = universal gas constant
R_j = reaction rate of reaction j in terms of leading reactant [$kmol/m^3s$]
S = surface of solid
s = direction vector/path length
s' = scattering direction vector
S_i = source term for species i
S_T = source term for temperature
S_U = source term for momentum equation

T = temperature
t = time
T_f = temperature of the surrounding fluid
T_r = temperature of the radiating surface
t_{pc} = relaxation time for phase change
U or V = velocity vector
vol = volume of solid element
ν_{ji} = species rate exponents
w^m = quadrature weights associated with the direction,
X_i = mass fraction of species i
x_i = mole fraction of species i
ε = dissipation rate of *k*
ε_r = emissivity of the radiating surface
ε_s = emissivity of the structure
ρ = density
τ = the viscous stress tensor
$\dot{\gamma}$ = the rate-of-strain (or rate-of-deformation) tensor
μ = effective viscosity
μ_t = eddy viscosity
κ = dilatational viscosity
δ = unit tensor
δT = allowable virtual temperature change
ΔH_f = heat of formation
κ_a = absorption coefficient
κ_s = scattering coefficient
Γ_ϕ = exchange coefficient for ϕ
σ = Stefan-Boltzmann constant
σ^ϕ = Prandtl number for ϕ
Ω' = solid angle
Φ = phase function

CHAPTER 1

Introduction

1.1 Introduction

Nuclear Power Plants (NPPs) are designed to achieve highest level of industrial as well as nuclear safety to minimize damage to the environment and population during their normal operation as well as in the event of any accidents. They are provided with several Engineered Safety Features to prevent and handle situations arising from accidents. The reactor containment building is designed to withstand the pressure and temperature arising from large amount of steam released during a Loss of Coolant Accident (LOCA) or Main Steam Line Break. However, in the event of certain postulated severe accidents scenarios involving LOCA followed by delay or failure of Emergency Core Cooling System (ECCS), there is a likelihood of significant overheating of fuel leading to partial or complete core melting. Subsequently, there is a possible release of large amount of hydrogen (IAEA-TecDoc-1196) in the containment primarily by the clad-oxidation reaction (due to metal water reaction at high clad temperature) as well as by radiolysis of water. The released hydrogen being much lighter than air is expected to move upwards due to buoyancy and get non-uniformly distributed in the complex network of interconnected rooms/halls, corridors, stair-ways, passages inside the containment. This can lead to formation of hydrogen rich pockets (IAEA-TecDoc-1661) in several localized areas of the building. Hydrogen behavior issues during severe accidents have become a widely researched topic in the field of nuclear reactor safety owing to possible damage to the integrity of reactor containment by hydrogen fire as witnessed in major nuclear accidents of Three Miles Island, and Fukushima witnessed by world so far.

1.2 Hydrogen Behavior Issues in Nuclear Power Plants

The hydrogen generated during an accident in the NPP of Three Mile Island (TMI) in USA, by the clad oxidation reaction got ignited within the containment building and resulted in a pressure spike. Fortunately, the containment building could withstand the resulting pressure spike without any damage. The disastrous effects of hydrogen combustion were also experienced in the accident and the post tsunami nuclear accident at Japan's Fukushima Daiichi nuclear power plant. These accidents unleashed worldwide research and studies to address the following issues related to hydrogen behavior during severe accident scenarios.

1.2.1 Hydrogen generation

During a severe accident involving unavailability of heat sink, large amounts of hydrogen gets released in very short time from the metal-water reaction between fuel clad at prevailing elevated temperatures and super-heated steam formed due to overheating of coolant water.

$$Zr\ (s) + 2H_2O\ (g) \rightarrow ZrO_2\ (s) + 2H_2\ (g)\ ;\ \Delta H = -616\ \text{kJ/mol} \qquad (1.1)$$

Since the above reaction is exothermic in nature, it leads to a cascading effect causing accelerated hydrogen generation. In the Indian context, in a typical 220 MW PHWR, the amount of hydrogen generation by this source is estimated to be 45 kg of hydrogen in initial 3000 seconds in case of LOCA followed by ECCS failure and cumulative 300 kg in 10 hours in case of LOCA plus ECCS and moderator cooling failure (BARC's internal Report).

Additionally, hydrogen also gets generated by the radiolysis of water due to γ-radiation. This process is gradual and prevails over extended duration.

$$H_2O \rightarrow [H_2O]^* \longrightarrow H\bullet + OH\bullet \qquad (1.2)$$

For a typical 220 MW PHWR, the amount of hydrogen generated by means of radiolysis is estimated to be 2 kg of hydrogen in 30000 seconds. This process continues for longer duration even after the reactor coolant is exhausted and core decay heat is being removed by the water injected from external means.

1.2.2 Hydrogen distribution:

The transport behavior of hydrogen in closed geometries is a complex fluid dynamics problem that governs the local and global hydrogen concentration values inside reactor containment building. The processes of natural convection along with forced convection and molecular diffusion over a long time, mainly determines the distribution of hydrogen in the containment. When hydrogen is introduced at lower elevations inside containment building, the average molecular weight of the resulting gas mixture is lowered. The resultant lower gas mixture density in this region of the containment leads to rapid natural convection currents and causes stratification of the containment atmosphere (NEA/CSNI/R-2014-8).

Molecular diffusion due to the stratified concentration gradient causesgases to diffuse from regions of high concentration to low concentration regions. Diffusion effects fall off very rapidly with increase in the size geometry concerned as the time for molecular diffusion mixing is proportional to the square of length scale. Thus, it would take days to attain a well mixed atmosphere in the containment. The temperature induced stratification taking place simultaneously inside the containment inhibits this homogenization process. Moreover, the presence of condensing steam also affects the hydrogen distribution behavior due to induced turbulence.

1.2.3 Hydrogen combustion/detonation:

Hydrogen in air has very wide flammability limits as depicted in Table 1.1. However, during severe accident conditions, large amount of steam is also present inside reactor containment. The flammability limits for a hydrogen-air-steam mixture are depicted by the ternary diagram Shapiro-Moffette (1957) given in Figure 1.1 below.

Table 1.1: Flammability limits of hydrogen in dry air

H_2 Conc. in air	**Event**
0 – 4.1 %	Non-combustible
4.1 –13.5%	Deflagration
13.5 – 70%	Detonation
70 –74%	Deflagration
74 – 100%	Non-Combustible

Hydrogen has very low energy requirement for ignition. Moreover, the low radiant heat, very high heat of combustion, high thermal conductivity and specific heat and high buoyancy add to the difficulty of controlling hydrogen fires. Thus, any combustion and/or detonation of H_2-air-steam mixture within the containment building can cause damage to the concrete containment building and affect its integrity.

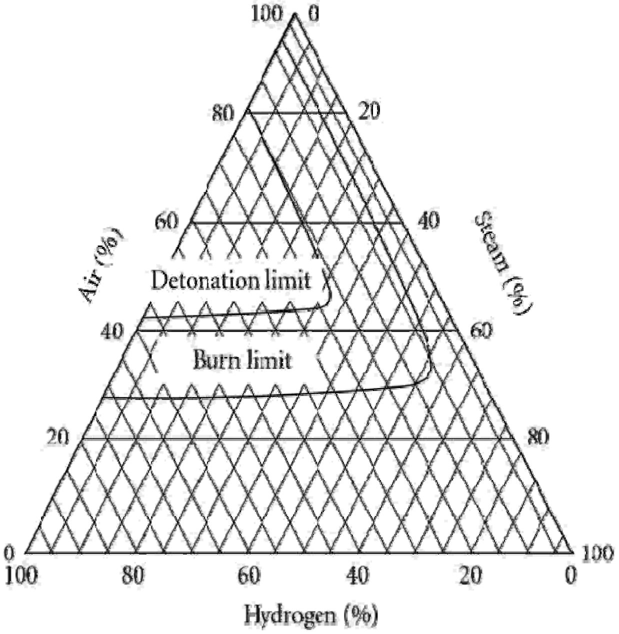

Fig. 1.1: Ternary diagram for hydrogen/air/steam/mixtures at 300 K and 1 bar; Shapiro - Moffette (1957)

1.2.4 Hydrogen mitigation:

Many approaches and technologies have been investigated and developed to mitigate the phenomenon of hydrogen buildup inside reactor containment during severe accidents (NEA/CSNI/R-96-9). Some of the important approaches are as follows: -

- **Deliberate Ignition:** In this approach hydrogen is deliberately ignited before it reaches dangerous concentration levels in the gas mixture. The problem associated with this method is that containment atmospheres under severe accident scenario are steam laden and the igniters fail to perform under wet atmospheric conditions. Additionally, if somehow ignition is achieved, the other main issue is that hydrogen-air-steam gas mixtures leaner than 4% (v/v) in hydrogen are very difficult to ignite while in mixtures beyond 8% (v/v) hydrogen are very difficult to control once ignited and may lead to detonation.

- **Homogenization (mixing)**: As mentioned earlier, due to its peculiar properties, hydrogen tends to form high concentration pockets in localised regions inside containment, so this method targets diffusing such pockets by homogenizing the containment atmosphere. Mixing can be achieved by using fans which have the disadvantage of dependence on electrical power, which in most accident scenarios, may not be available. Moreover, operation of fans can cause an electrical spark, which itself may be a source of ignition to the hydrogen mixture.
- **Inerting**: In this approach, the containment atmosphere is replaced with inert gases like pure nitrogen or carbon dioxide before every startup which deprives the containment atmosphere of oxygen and hence any existing flame gets starved of the supporting oxygen and combustion is prevented. The main drawback associated with this method is that it causes restrictions on entry of operators in the reactor building for any maintenance work. Also, it is possible only in smaller containments like that of BWRs where the total gas volume is relatively low.
- **Helium Injection:** This method involves injecting helium in the lower portions of the containment which serves the advantage of both of the above two methods. Firstly, it reduces the overall density of gas mixture in the lower region and promotes natural convection towards upper regions of the containment causing homogenization. Secondly, being inert, it also deprives the gas mixtures of the oxidizer by reducing oxygen levels in the regions of

low density where hydrogen is present. The main disadvantage of the method is its sluggish effectiveness. Also, it is not a passive system as it has dependence on the remote activation of number of valves. Additionally, it requires storage of large quantity of helium in the plant.

- Passive Catalytic Recombiner Devices (PCRDs)

1.3 Passive Catalytic Recombiner Devices

PCRDs work on the principle of passively recombining (oxidizing) the released hydrogen with the oxygen present in containment atmosphere on catalytic surfaces to form steam and release heat. Here the oxidation of hydrogen takes place at low (room) temperatures due to the presence of catalyst and the thermodynamic consequences of a high temperature hydrogen-oxygen reaction (like deflagration or detonation gets eliminated. The device consists of a box which has several catalytic plates stacked in parallel inside it and is open from bottom and top. Being exothermic in nature, the hydrogen-oxygen reaction taking place on the catalyst plates heats them up and this in turn, heats up the hydrogen-air (or oxygen) mixture flowing over the plates. The steam formed on catalytic surface mixes with the outgoing gases and reduces the effective concentration of hydrogen in the gas mixture. This hot gas mixture rises through the channels between parallel catalyst plates by buoyancy setting up a natural convection loop across the recombiner box.. The upward movement of hot leaner gas mixture towards box outlet at the top causes low pressure inside the box. This causes cold, hydrogen rich mixture to be sucked in through the box inlet at the bottom. Consequently, the overall hydrogen gas concentration in the vicinity of the device keeps on getting depleted in a passive manner. The catalyst used for this purpose is primarily platinum and palladium or a suitable combination of the two. A schematic of the recombiner device is illustrated in Figure. 1.2.

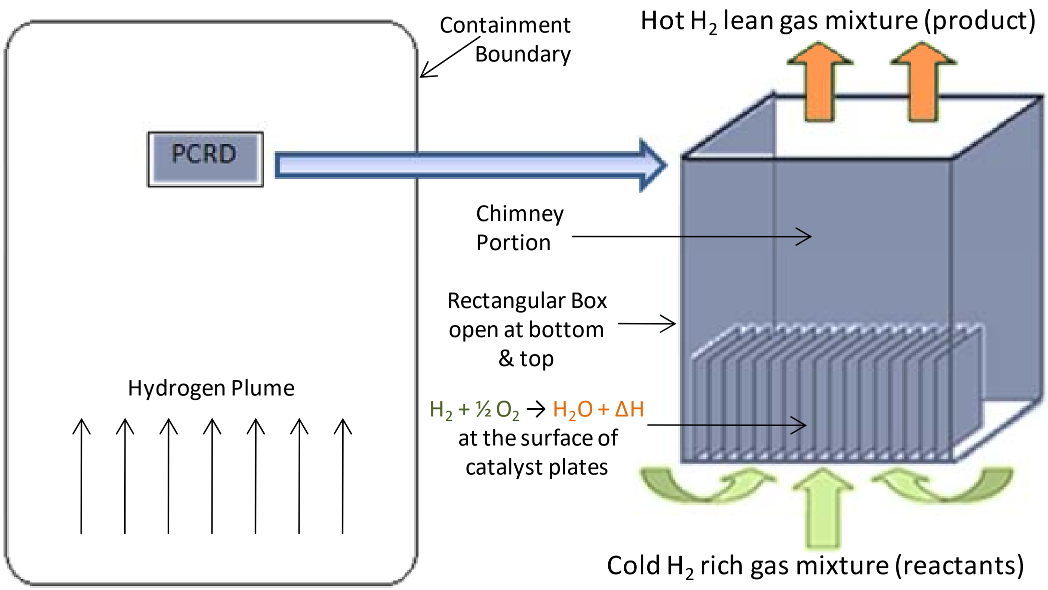

Fig. 1.2: Schematic of PCRD

These devices have emerged as the most promising technology for hydrogen mitigation due to their following inherent features:

- They are passive in nature as they do not require any external power for their functioning or any external stimulus for their startup.
- They can function well over wide range of hydrogen concentrations. This happens due to the exothermic nature of the recombination reaction and positive dependence of reaction kinetics on temperature. Hence more is the hydrogen concentration, more is the exothermic heat release and the more is the rate of reaction which intern further rises the temperature and improves the reaction rate. Moreover, the same promotes enhanced natural circulation causing quick homogenization of the nearby atmosphere. The only care while

designing these devices that should be taken is that the maximum temperature attained at the catalytic surface needs to be limited below the self ignition temperature of the gas mixture.

- They are simple in construction and easy in application as they do not have any dynamic components. Hence their handling, installation and maintenance are relatively easy.

1.4 Current Scenario and Research Priorities

In the recent times, research on hydrogen mitigation techniques for nuclear reactor containments has blossomed into an exclusive and significant area of research. Major priorities for research and development in the field of hydrogen recombiner technology currently being worked upon worldwide are focused on optimizing the design and type of recombiner to be selected for specific containment geometries. As part of the technology development program for hydrogen management in Indian PHWRs also, experimental as well as analytical studies are underway.

Different kinds of catalysts have been developed around the world for deployment in hydrogen recombiners. The reaction kinetics of the surface reaction taking place on these catalysts is specific to their method of manufacturing and the type of catalyst and the substrate employed. It has a strong bearing on the performance of recombiners and can vary significantly for different PCRD catalysts. Hence detailed CFD models of hydrogen recombiners with literature-based reaction kinetics can qualitatively predict the behavior of PCRD inside a closed geometry but it is vital to use accurate and specific reaction kinetics of the catalyst used in recombiner being modeled to get accurate quantitative prediction of PCRD performance.

CFD based containment analysis needs to be carried out for optimizing the choice between using a greater number of recombiners of smaller size and using fewer ones of relatively larger size to cater to the amount of hydrogen released inside a reactor containment. However, using full scale three dimensional recombiner model for simulating PCRD performance in a large reactor containment is computationally extensive. This is because the catalyst plates used in PCRD are very thin, having thickness of the order of sub-millimeter while the geometries where PCRDs need to be placed are very large having volume in thousands of cubic meters. Since, many parametric studies are to be carried out to ascertain the appropriate location and number of recombiner boxes to be placed inside containment building to mitigate hydrogen. Thus, it is practically impossible to use this approach for containment analysis involving thousands of cubic meters of domain volume and hours of transient simulation.

Hence, innovative and more practical approaches need to be devised for capturing multi physics phenomena using CFD in a more computationally economical manner. This can be achieved by using some sort of lumped model for the PCRD while modelling the rest of the geometry where PCRDs are placed using a detailed CFD approach. Use of such a coupled approach can obviate the need of using fine mesh for modelling recombiners and can serve as a vital tool to predict the effect of PCRDs on hydrogen distribution inside reactor containment. Analysis of the thermal hydraulic performance of recombiners and hydrogen distribution behaviour in the large multi-compartment containment volumes may thus become less time-intensive.

In the context of Indian NPPs, the development of PCRD has been undertaken for hydrogen management in the operating and upcoming Pressurised Heavy Water Reactors (PHWRs). While the PCRDs developed and deployed in various water-based reactors around the world have been amply characterised with respect to the reaction kinetics and overall recombiner behaviour, there is a need to generate reaction kinetics for the catalysts used in our PCRDs and also develop theoretical models for characterising the recombiner behaviour in the Indian context. Hybrid approach combining computational fluid Dynamics (CFD) and empirical formulation for reaction kinetic is also required to be developed for the hydrogen behaviour analysis in the containment of our PHWRs.

The above discussion on current scenario pertaining to hydrogen mitigation using passive recombiner devices can be summarised into following gap areas in this field:

- Use of detailed CFD approach has not been widely used so far to analyse the multi physics processes associated with the working of recombiner devices.
- Chemical kinetics for the reactions involved is specific to the type of catalyst substrate employed and method of manufacturing.
- To accurately predict the behaviour of the developed catalyst to be used in IPHWRs, kinetic data of the same has to be generated.
- There is a need to study the affect of recombiner location on its behaviour to find out the optimum location of recombiner inside closed geometries to ensure its reasonably best performance is extracted.

- The use of CFD tools for studies involving actual recombiners modelled in relatively larger geometries is computationally very extensive and it is practically impossible to use this approach for containment analysis.
- Innovative methods need to be developed for carrying out such studies with more practical approach.

1.5 Objectives of the Present Studies

In order to address the above gap areas in the field of research related to PCRDs for hydrogen mitigation during severe accidents, the studies under this thesis have been aimed to achieve the following objectives:

- Experimental evaluation of the reaction kinetics and characterisation of the catalyst developed for recombiner.
- Experimental studies to determine the channel effect between parallel catalytic plates of a recombiner box and developing a rate equation for the in-house catalyst device.
- Development of a CFD model to study the influence of recombiner location on its performance inside closed geometry.
- Incorporation of parallel catalytic plate reaction kinetics into the detailed CFD model and validation of this model against experimental data.
- Use of this validated CFD model to formulate an empirical model for the recombiner box which can be plugged into any general CFD code.

Thus, the successful completion of the work will make available, a hybrid tool for speedy severe accident containment analysis using any commercial CFD software by drastically reducing the meshing requirement in such studies.

1.6 Structure of The Thesis

This thesis presents details of the various studies performed to achieve the above-mentioned objectives as part of the present work. The thesis is organized in remaining chapters with the following contents:

Chapter 2 presents a literature review of the experimental and analytical studies related to catalytic hydrogen recombination. Details of recombiner designs, experimental evaluation and modeling approaches adopted by various researchers are highlighted in this chapter. The studies have been divided under four separate topics, viz., a) Catalyst development and recombiner design, b) Experimental studies, c) Analytical studies on recombiner performance and d) Performance studies using hybrid approach with CFD. These studies have been used to draw guidelines for the various studies carried out in the present work.

Chapter 3 presents salient features of the CFD based detailed recombiner model developed as a part of the ongoing research, its validation against data from open literature. The validated and optimized model is then applied to assess the suitable location for placing a PCRD within a closed geometry to extract its reasonably best performance and efficiency. Simulations performed for different PCRD positions within a closed vessel under dry as well as steam laden conditions have been presented in this chapter. The results indicate that recombiner gives better performance when places near the bottom of the vessel and causes uniform hydrogen distribution inside the vessel.

Chapter 4 focuses on experimental evaluation of reaction kinetics associated with hydrogen-oxygen recombination on surface of the developed PCRD catalyst. Details of the experimental setup and the methodology used to perform various experiments are presented in this chapter. Reaction kinetics of the surface reaction has been evaluated for the SS wire mesh substrate based Pt- Pd catalyst. Behaviour of catalyst plates stacked in parallel inside PCRD is evaluated. Overall affect is empirically approximated as single step Arrhenius equation. The results indicate that catalytic plates stacked in parallel give better reaction kinetics owing the formation of natural convection flow between the parallel channels.

Chapter 5 describes the incorporation of reaction kinetics of catalytic plates stacked in parallel inside PCRD in the form of single step Arrhenius equation developed in Chapter 4 into the detailed CFD model described in Chapter 3. The updated CFD model has been validated against data from the experiments involving four catalyst plates placed in parallel. The results indicate that initial hydrogen concentration has a strong bearing on the overall transient of hydrogen recombination.

Chapter 6 presents simulations involving parametric study using the updated and validated CFD model from Chapter 5 to generate a data matrix involving various inlet conditions. This data matrix has then been used to derive the correlation for hydrogen conversion as well as outlet variables of PCRD as functions of inlet variables. These correlations have been compiled in the form of an empirical model for specific PCRD. The results of the correlations have been compared against the simulation results from detailed CFD model. It is found that hydrogen conversion efficiency across the recombiner is independent of steam concentration while it increases rapidly with hydrogen concentration.

Chapter 7 demonstrates the use of empirical model for PCRD from Chapter 6 in conjunction with commercial CFD code to predict the performance of multiple PCRDs inside a multi compartment closed geometry. It describes the methodology behind the hybrid approach of speedy containment analysis for hydrogen mitigation using PCRDs. It is found that the hybrid approach gives faster results as compared to conventional CFD model due to lesser meshing requirement.

The conclusions drawn from various studies carried out as part of this work have been presented in Chapter 8 along with recommendations and the future scope of work.

CHAPTER 2

Literature Review

2.1 Introduction

Experimental studies together with well validated analytical models based on empirical, semi-empirical and more detailed 2D or 3D numerical approaches have gained significance particularly in the post Fukushima safety era for understanding the behavior and evaluating the performance of catalytic recombiners. A detailed literature survey was undertaken to comprehend and summarize experimental as well as analytical research on state-of-the-art techniques for hydrogen recombination. The intent was to formulate directions and set yard stick for pursuing activities related to the present work.

The literature studies carried out within the scope of present work have been divided under four separate topics, viz., a) Catalyst development and recombiner design, b) Experimental studies, c) Analytical studies on recombiner performance and d) Performance studies using hybrid approach with CFD. The literature studies are presented in brief as they are intended to bring out the major contributions to the subjects and are required to bring out the gap areas. A summary of the literature studies for experimental and analytical work carried is given below.

2.2 Catalyst Development And Recombiner Design

Johann Wolfgang Dobereiner at the University of Gena in Germany was the first to study the catalytic features of platinum for hydrogen oxidation almost more than a century back. However, as reported by Chakraborty (1991), this principle was first applied for mitigating hydrogen in NPPs in Germany in 1986. GRS (Gesellschaft fuer Anlagen- und Reaktorsicherheit) by developing the first conceptual recombiner based on a sandwich type design comprising of stainless steel carrier plates deposited with thin layers of platinum, vanadium and palladium. These plates were placed in a box having inert atmosphere to prevent contamination of the catalyst during plant operation. These plates were automatically unfolded and lowered during an accident. As reported in IAEA-Tecdoc-1196, Siemens developed a box type recombiner that employed thin walled stainless steel foils provided with a coating of catalytically active metal (such as platinum). Numerous such catalytic plates placed vertically were arranged in parallel at the bottom of a metal housing. The metal housing was designed such that gas mixture enters through the opening provided at the bottom and leaves through the opening at the top. NIS (Ingenieurgesellschaft mbH) also developed a similar module consisting of a hollow stainless steel box structure open at bottom and top having a large number of catalyst cartridges (in the form of thin vertical beds of catalyst coated pellets) installed at the bottom. The open passages between the cartridges were provided for the strong buoyancy induced gas-mixture flow through the box towards a tall dome shaped chimney at the top portion to drive the flow out. The cartridge was a rectangular shaped box structure provided with wire screen to hold the Pd-Pt coated alumina granulates. This type of catalyst offers a very large catalyst surface area (100m^2/g) of pellet although the active catalyst surface area participating in the catalytic reaction was estimated to be about 5m^2/g.

Subsequently, other countries also started their own R&D for recombiner development. In Canada two types of catalytic recombiner models have been developed based on natural convection and on forced convection. The catalyst developed by AECL consists of small platinum crystallites on a hydrophobic high surface area support, bonded to a stainless-steel screen. For the forced convection test, catalyst element was an open cylindrical module formed by wrapping alternate layers of flat and corrugated screen to provide cylindrical passages in between the catalyst layers. On the other hand, the catalyst elements for natural convection test were in the form of loose thin plates. The auto initiation capacity of the recombiner device even at a temperature of 15^0C, in condensing atmosphere and having hydrogen concentration as low as 1% is remarkable. Thus, the AECL design for recombiner appears as an effective means to remove hydrogen right from the onset of hydrogen production.

In Russia, flat plate type recombiners comprising of catalytically activated high porosity cell material (HPCM) in 1.2 m^3 cylindrical shaped reaction vessel were investigated at the Kurchatov Institute of Technology; Baronov (2006). Effective hydrogen combination was indicated with sufficiently small volumes of HPCM in both dry and wet air experiments. The HPCM samples made of stainless steel and nichrome were polyhedron with a characteristic cell scale of approximately 1 mm size with periodically repeating cells. These cells were highly porous (90%) structure with low specific gravity due to less wall material compared to overall cell volume. The walls of cell were coated with aluminium oxide and platinum layer deposited by magnetronic and electrochemical technique.

As reported by Belapurkar (2000), the first type of catalyst device developed in India was based on a chemically coated polyester curtain which was proposed to be kept in a rolled position and would roll down in the event of an accident. However, due to the low melting temperature of polyester cloth, this device could not perform beyond 150°C and hence, could be used for very low hydrogen concentrations only. Subsequently, metal substrate-based catalyst with three different techniques for deposition of the Pt-Pd catalyst on polyester Dewit (1996), cordierite honeycomb Belapurkar (2008) and stainless steel gauze Sanap (2011) were developed. Low surface area catalysts having Pt + Pd deposited over stainless-steel wire gauze simultaneously and sequentially, using single bath electroless reduction was developed. Effect of preparation route on overall morphology of noble metal coating was evaluated in detail by Sanap et al. (2011). This catalyst having Pt - Pd deposited simultaneously over stainless-steel wire gauze has been selected for evaluation of kinetics data for modelling of PCRDs in the present work.

Kweonha et al. (2016) proposed a new design of honeycomb catalyst Passive Autocatalytic Recombiner (PAR) made by the Korea Nuclear Technology (KNT) Inc. They added two slices of plate to the bottom of PAR model, to reflect and promote the gas flow into PAR. The new concept of PAR proved to have a better hydrogen removal performance compared to the original PAR. Zhengfeng (2017) reported a new kind of catalyst sheet based on stainless steel supported Pd nano-clusters prepared by electroless deposition route. The catalyst sheets prepared by them showed high activity and good stability when operated above 500 ^{0}C for 24 hr or continuous operating for 25 days. They also demonstrated that the start-up time for H_2-O_2 recombination reaction was less than 1 min and the catalytic efficiency was more than 90% for these catalytic sheets after exposure to methanal, iodine vapour and $BaSO_4$ aerosol. More recently, Peijian (2019) reported a super hydrophobic Pd@CeO_2/Al_2O_3 catalyst coating prepared through a self-assembly method and the grafting of 1H,1H,2H,2H-perfluorooctyltriethoxysilane. As per their study, this coating showed excellent potential for the mitigation of hydrogen containing various poisons during a nuclear accident.

2.3 Experimental Studies

Different designs of catalysts and recombiners have been tested in lab-scale and engineering scale experiments carried out by individual countries as well as in collaborative work as summarized by Markandeya (1993). As reported by Drinovac (2006) the qualification experiments for various recombiner devices have been performed in the HDR facility, Battele Frankfurt test facility and the REKO facility. Reinecke published a paper in 2004 based on experiments carried at REKO facilities at Forschungs Zentrum, Juelich (FZJ) involving innovative hydrogen recombiners as safety devices in the containments of light water reactors.

Experiments on sandwich type plates: The samples of sandwich type plates developed in Germany, as reported by Chakraborty (1991) were tested in laboratory scale test setup. Two series of experiments, described as ‘demonstration test’ and ‘convection test’, were performed in HDR test facility to demonstrate the functioning of the catalytic plates in large volumes. The experiments revealed that existing plate-type PAR systems had the risk of igniting the combustible containment atmosphere due to the local overheating of the catalyst elements caused by exothermic reaction heat. This was because their recombiner systems could not limit the system temperatures. Solution to this was provided by means of catalytic coated thermal insulation elements. These were prepared using coating technique for the catalyst as proposed in the THINCAT project within the 5th EURATOM Framework, Fischer (2003).

Experiments on box type recombiner-Siemens design: Performance of prototype device developed by Siemens in single compartment geometry under different environmental conditions was demonstrated using experiments in 12 m^3 cylindrical vessel. Following the single compartment tests, further detailed experiments were performed to optimize the recombiner size in the Battelle Model-containment Test Facility. As mentioned in IAEA-Techdoc-1196, Siemens also developed a simple, easy to test, portable test facility for quick in service inspection of the foils within few minutes at the sight itself. Performance results obtained from the several qualification tests of the box type recombiner revealed that the recombiner capacity increases with hydrogen concentration and is not much affected by the presence of steam. Moreover recombiners contribute towards mixing of the stratified gas components. In the event of large hydrogen release rates, the catalytic recombiners may themselves represent potential source of ignition and hence recommended only in combination with the catalytic igniters by Siemens.

Experiments on box-type recombiner-NIS design: As reported by Drinovac (2006), the NIS design of recombiner was tested in single compartment geometry as well as in multi-compartment Battelle Model-Containment Test Facility. The tests confirmed good start-up behavior and efficient removal of hydrogen. To confirm that the recombiner does not perform as igniter, a special test was carried out which indicated that even for hydrogen concentration of 10 % v/v and steam concentration of 42 % v/v with catalyst temperature of about 600 ^{0}C, ignition did not occur.

Experiments on AECL designed Recombiners: For the forced convective type recombiners, the conversion efficiencies approaching 100 % for hydrogen concentration as low as 1%, with gas residence time with the catalyst element of the order of about 100 ms or less, are claimed to have been achieved by AECL (IAEA-Techdoc-1196). The catalyst designed by AECL is also claimed to function without damage for transient temperatures of up to 600 ^{0}C. The 100 % conversion of each volume percent of hydrogen in the gas mixtures is observed to warm up the flowing air stream by approximately 90 ^{0}C for hydrogen concentration above 1%. From these experiments it is claimed that at hydrogen concentrations higher than 5%, the gas mixture would ignite due to high temperatures. Thus there would not be any damage to the catalyst.

As reported by Ganju et al. (2000) experimental studies related to hydrogen/helium dispersion and performance evaluation of catalytic recombiners under dry atmospheric conditions were performed in HYMIS (Hydrogen Mitigation Studies) Test Facility comprising a 7 m tall and 2 m diameter steel vessel.

2.4 Analytical Studies on Recombiner Performance

On the analytical front also, many researchers have put in dedicated efforts in this field and have published their studies. Presently Computational Fluid Dynamics (CFD) based models for the recombiners are being used to perform analytical/numerical studies to assess the nature and extent of flow, recombination reaction and heat transfer associated with PCRDs. However, initial codes in this field were based on one dimensional models (Wolf, 1991) for the gas flow inside the channels between catalyst plates of recombiner box. They used simple algorithms for

Navier-Stokes equations to calculate mass, momentum, energy balances and equation of state. Soon, Field codes based on two dimensional models of the recombiner were developed (Andreani, 2003) and were closer to the actual phenomena and gave satisfactory qualitative predictions of the phenomena. However, these lumped parameter models were not capable to capture the molecular hydrogen transport into the surrounding gas mixture, convective and diffusive transport of the gases inside the interconnected compartments of containment and effect of condensing steam on the transport phenomena of hydrogen and other gases. Consequently, detailed CFD models for hydrogen mitigation involving recombiners in closed geometries have gained importance due to their ability to capture all these local phenomena. Such studies are helpful for ascertaining the size, number and location of recombiner boxes that need to be deployed in a containment to effectively mitigate hydrogen build up during severe accident scenario. Such studies are preferable over experiments as they avoid the risk involved with handling of hydrogen.

Some of the initial works in this field were reported by Travis et al. (1998) and Royl et al. (1999) using the CFD tool GASFLOW which was used for three-dimensional analysis of steam/hydrogen transport in presence of catalytic recombiners. They applied it to situations involving transport and distribution of combustible gas mixtures to study gas dynamic behavior (1) under low-velocity, buoyancy-driven flows, as well as sonic flows or diffusion dominated flows; and (2) during chemically reacting flows, including deflagrations. Royl et al. (2002) subsequently applied the code in mechanistic 3-D analysis of steam/hydrogen distributions under severe accident conditions with hydrogen mitigation involving a large number of catalytic recombiners at various locations in two types of PWR containments of German design. Valdepanas et al. (2007) worked on improvements in the CFD code CFX-4 for analysis of hydrogen behavior within the NPP containments by implementation of models for transport and physical phenomena like steam condensation onto walls in presence of non-condensable gases, heat conduction, fog and rain formation, material properties and criteria for assessing the hydrogen combustion regime expected. Royl et al. (2008) carried out validation of the GASFLOW code with test data from the PANDA facility covering steam/air and steam/helium/air mixtures. Breitung et al. (2005) presented a detailed step by step procedure for mechanistic analysis of hydrogen behavior and mitigation during accidents and highlighted the application of CFD codes for hydrogen behavior modeling. Heitsch et al. (2010), with an intention of demonstrating the utility of CFD codes to model gas movement inside containment during a severe accident, presented a detailed study on CFD calculations using GASFLOW, FLUENT and CFX for the Paks NPP.

Gera et al. (2009) developed a code for hydrogen recombiner modeling. They first performed 2D modeling and validated it against REKO 3 experiments (from Drinovac, 2006) and then reported the development of a 3D model (Gera et al., 2011 a) for the hydrogen recombiner for the assessment of the PAR performance in terms of maximum temperature of catalyst surface and outlet hydrogen concentration. The code was used to study the mechanism of catalytic recombination and tested for two literature-quoted experiments. Mimouni et al. (2011) published CFD based recombiner modeling and its validation on the H_2-Par and Kali-H_2 experiments (from Reinecke, 2010). Here they presented numerical assessments of the recombiner models implemented in CFD solvers NEPTUNE_CFD and Code Saturne. Reinecke et al. (2011) presented simulation of the efficiency of hydrogen recombiners as safety devices. They investigated the applicability of Passive Autocatalytic Recombiner (PAR) on GARAGE experiment, using ANSYS-CFX and REKO-DIREKT codes. Rożeń (2013) presented modeling of a PAR for hydrogen mitigation by CFD methods using four turbulence models (k-ω, k-e, intermittency, RSM) for simulations of: gas flow, heat and mass transport, and chemical surface reactions. Reinecke (2013) investigated the effectiveness of PAR for fuel cell applications. For this purpose, they simulated a hydrogen release scenario based on experiments performed by CEA in the GARAGE facility (France) with and without PAR by implementing the in-house code REKO-DIREKT in CFD code ANSYS-CFX. Meynet et al. (2014) performed the numerical simulation to study the impact of oxygen starvation (i.e. low oxygen/nitrogen ratio) on the PAR efficiency and gas-phase ignition limit using a dedicated CFD code named SPARK. Klauck et al. (2014) reported experimental and numerical study on the effect of carbon monoxide on recombiner performance. Parallel catalytic reactions of H_2 and CO on the catalyst surface were studied in a series of experiments. The authors also used three different numerical codes REKO-DIREKT (JÜLICH/RWTH), SPARK (IRSN), and CFX (ANSYS) for the simulation of CO/H_2 recombination to capture the poisoning effects observed in the experiments. Orszulik et al. (2015) carried out numerical modeling of PAR based on the REKO 3 experiments using ANSYS-FLUENT and also tuned the model to get PAR performance in accordance to their own experimental results. Reinecke (2016) carried out validation of REKO-DIREKT code for simulation of PAR operational behavior against small-scale experiments performed at Forsc-hungszentrum Juelich in the REKO facilities (Drinovac, 2006). Hoyes et al. (2016) investigated the capabilities of CFD models for predicting hydrogen stratification in a containment vessel using data from the NEA/OECD SETH2 MISTRA experiments. Mehdi (2016) investigated hydrogen mitigation system during large break loss-of-coolant accident for a two-loop pressurized water reactor. They used MELCOR 1.8.6 code to assess core degradation and containment behaviour during the large break loss-of-coolant accident without the actuation of the safety injection system except for accumulators in Beznau nuclear power plant. During this situation, hydrogen distribution in containment and performance of hydrogen reduction system were evaluated by them.

Agrawal et al. (2017) developed a conceptual design of an innovative PAR which uses pool boiling of water to enhance heat transfer from the catalyst surface and limit its temperature. Additionally, an in-house numerical code called HDS couples CFD model with models for reaction kinetics and water pool boiling heat transfer was used to carry out numerical analysis of the same. Mahdi (2017) determined the minimum number and the best configurations of PAR for the effective design of the containment in a pressurized water reactor through a large number of sensitivity analyses. In this regard, they developed a nodalization for best estimate modelling by MELCOR integrated code. McMinn (2017) used Modular Accident Analysis Program version 5.04(MAAP5.04) software, to calculate flammable gas generation, migration and combustion risk within a containment. They calculated the number of PARs needed in a large dry PWR containment in order to prevent significant flammable gas combustion events. Halouane et al. (2018) implemented a CFD PAR model in the ANSYS Fluent code using a correlation given by the PAR manufacturer. In the model, PAR unit was considered as a channel where the reaction takes place without any chemistry details. The CFD model was validated against two experimental tests (HR2 and HR5), which were performed in the THAI facility in the frame of the OECD/NEA THAI project. Rożeń (2018) used CFD to study the dynamic behavior of a plate-type Areva FR-380 recombiner in a quiescent environment. His CFD model was able to identify the phenomenon of downward gas flow through the PAR metal casing in the initial phase of the start-up period and to correlate the magnitude and duration of this effect with the rate of increase of hydrogen concentration in the environment. Avdeenkov (2018) constructed and justified, a simple engineering thermo-hydraulic model of hydrogen removal in the operation of a passive autocatalytic recombiner based on the available experimental data. The paper presented the application results of the model applied in RELAP, TRACE and CORSAR codes. These were used for multifactor and full-scale calculations of the dynamics of emergency processes during release of hydrogen into nuclear power plant. A passive containment cooling system (PCCS) combined with hydrogen mitigation system has been suggested by Revankar (2019) that will passively remove containment heat load as well as mitigate hydrogen gas generated and accumulated in the containment atmosphere during a prolonged station blackout. They made use of atmospheric air as ultimate heat sink to reject the PCCS heat, which in turn transfers heat from the containment. In the proposed design a finned vertical tube type PCCS system submersed in pool water is considered with supply of pool water lasting three days following which airflow cools PCCS tubes for long term. The PCCS inlet flow path has a catalytic recombiner that is effective during first few days for hydrogen generation and accumulation in the containment. Zhi'ao (2019) through their study identified hydrogen risk and optimized hydrogen mitigation systems in the CPR1000 nuclear power plant during shutdown conditions before the opening of vessel head. A detailed MELCOR input was developed, which included detailed containment nodalization, accurate configuration of the PAR systems, and realistic boundary conditions based on design data and technical specifications. They also proposed two strategies to improve the hydrogen mitigation systems.

From the above survey, it is understood that the catalytic plates inside recombiner are very fine in thickness and in order to fully resolve the recombination processes, a very fine mesh size is required inside the recombiner channels to simulate geometric details of the recombiner. However, in order to carry out containment analysis for hydrogen mitigation using recombiners, these are to be modeled inside very large containment volume which would result in very large number of mesh elements. Thus, such calculations would require large computational times for completion. With the developments in the capabilities of CFD codes and improvements in computer power, these calculations have now become possible but are still impractical as the clock time needed for such simulations is of the order of many months, even when using parallel processors. Hence more practical approaches need to be developed and used where in the need of fine mesh to completely resolve the internals of recombiner is done away with. In such an approach, empirical models for recombiner can be suitable coupled with multi-dimensional CFD codes for detailed and speedy containment analysis.

2.5 Performance studies using hybrid approach with CFD

A one-dimensional recombiner model was implemented in ASTEC and COCOSYS codes as reported by Allelein (2008) where the recombiner is subdivided into three segments namely entry, catalytic plates and chimney along the height. The model considers the catalytic plates as well as the structure of the housing and heat transfer between the surrounding gas and the structures is calculated using free and forced convection, condensation and radiation. The Arrhenius-like form of the reaction equation as given by Heitsch (2000):

$$r = a\, A C_{H2}^{n1} C_{O2}^{n2} \exp\left(-\Delta E / R\, T\right) \qquad (2.1)$$

Where, C_{H2}^{n1} and C_{O2}^{n2} stands for the hydrogen and oxygen concentrations, respectively. The constants a, n1, n2, the plate surface 'A' and the activation energy ΔE are adjusted according to the experiment. Detailed and simplified models implemented in ASTEC have been validated on the basis of H2PAR tests as described by Plumecocq (2005).

Similar correlations can also be implemented by means of volumetric sinks and sources of energy, mass and momentum or as a 'black-box' model directly in other lumped parameter and CFD codes as described by Kudriakov et al. (2008). They used the TONUS code for hydrogen risk analysis. Several benchmark exercises based on experimental results obtained on large-scale facilities, such as MISTRA, TOSQAN and RUT, were performed by them. These studies were used as verification and assessment procedures for modeling and numerical approaches of the TONUS code. In order to facilitate the derivation of simplified ('black-box') models for long-term severe accident analyses numerous integral experiments were carried out. These experiments were aimed to investigate the global behavior of a recombiner in a larger environment for studying aspects such as the efficiency of hydrogen removal, start-up conditions, poisoning, oxygen starvation, steam and water impact. A summary of such experiments as reported by Reinecke (2010) is presented table 2.1.

Table 2.1: Integral PAR experiments

Facility	**Country-institution**	**Shape**	**Volume**	**Wall material**
LSVCTF	Canada-AECL	Rectangular	120 m^3	Steel
BMC	Germany-BATTELLE	Cylinder	625 m^3	Concrete
H2PAR	France-IPSN	Cylinder	8 m^3	Terphane
KALI-H2	France-CEA	Cylinder	15.6 m^3	Steel

The empirical correlations derived from these experiments describe the hydrogen consumption rate for a reference PAR type as a function of the gas composition, temperature and pressure. The hydrogen consumption rates for different recombiner types as proposed by the respective manufacturers are given by the following empirical correlations as mentioned by Bachellerie (2003)

AECL:

$$r_{H2} = \left(0.15196\ C_{H2} + 0.0126\ C_{H2}^{2}\right)(298/T)^{1.10974} \times p^{0.57769} (kg/h) \tag{2.2}$$

AREWA:

$$r_{H2} = \acute{\eta}\ \min(X_{H2}, 2X_{O2}, 8)\ (Ap + B) \tanh\ (X_{H2} - 0.5)(g/s) \tag{2.3}$$

NIS:

$$r_{H2} = 1.134\ C_{H2}^{1.307}(P/R\ T)(g/s) \tag{2.4}$$

Where X_i is the concentration (vol. %) and C_i the volume fraction (m^3) of the hydrogen and oxygen, respectively, p is the pressure (Pa), T the absolute temperature (K) and A and B and the other constants are model parameters which include all the residual influences and conditions during the validation experiments and depend on the recombiner model. In the AREVA approach η can be used to describe PAR efficiency under different conditions (e.g. oxygen deficiency or spray).

In 2011 Iyer et al. have presented the formulation of a model compatible with CFD code FLUENT to simulate hydrogen distribution and mitigation using a Passive Catalytic Recombiner in the Nuclear power plant containments. They compared the solution from two competing models, one a single step reaction and the other a multiple reaction model. A new single step rate expression was also derived from the detailed mechanism after simplifying it for the problem under consideration. The paper also considered diffusion-controlled model which assumes rapid reaction rates for which the surface chemistry is not required at all. In order to find the best suited approach to model the surface chemistry, CFD simulations were performed with FLUENT code using available experimental data from the literature. Gera et al. (2011 b) used a simplified approach to model PCRD in PARIS 1 benchmark geometry. They defined the volume having recombiner with porosity to apply source and sink terms for species and heat energy. Due to porous zone at catalytic section the heat released during recombination reaction is partly added to the solid mass of the catalyst plates and partly transferred to the surrounding fluid. In another paper, Gera et al. (2011 c) used a different approach to model PCRD in PARIS 1 benchmark geometry. They modeled PCRD as box with a single solid plate with the same mass as that of the combined number of catalyst plates inside PCRD. They also used empirically obtained pressure resistance term in addition to the hydrogen conversion correlation for PCRD.

2.6 Findings & Directions

The detailed literature survey of the experimental as well as analytical work carried out around the world for development and performance studies related to hydrogen recombiner devices reveals following observations regarding the current status of research in this field.

- Many diverse catalyst types and designs have been developed around the world by various countries for recombiners to be deployed in their respective nuclear plants.
- Chemical kinetics of the catalyst involved plays significant role in the performance and efficiency of any recombiner but the same is not widely reported in literature.
- Experimental studies are limited to the evaluation of newly developed catalysts and recombiner designs but can’t be utilised for performance evaluation and behavioural studies involving wide hydrogen concentration ranges due to the risk involved with handling hydrogen. Hence more emphasis is required on accurate and practical theoretical studies for the same.
- Lumped parameter codes have been used to study gross effect of recombiner devices on hydrogen distribution inside closed geometries.
- Use of CFD has gained importance in recent times to evaluate the simultaneous chemical, thermodynamic and transport phenomena-based processes occurring in and around recombiner devices.
- CFD based analytical tools have been used to study the behaviour of passive catalytic recombiners on standalone basis.
- Detailed CFD models for recombiners placed inside closed geometries have been sparingly reported in the literature due to their extravagant computational requirements.

- Researchers have used manufacturer correlations for their respective recombiners to develop hybrid approaches involving lumped approach for recombiners in conjunction with CFD modelling of the closed geometries where these devices are placed.
- Different approaches based on vivid assumptions have been reported in literature for the lumped model of recombiners placed in CFD domain of the closed geometry.

It can be concluded from the literature survey performed that chemical kinetics of the catalyst used plays significant role in the performance and efficiency of any recombiner. Hence there is a need to generate reaction kinetics for the catalyst developed for our recombiners. Secondly researchers world-wide have used manufacturer correlations for their respective recombiners for evolving CFD based hybrid approaches for analysis of recombiner behaviour. Similar correlations are to be developed for our PCRD. Accordingly, the objectives of the project, as described earlier have been formulated in a stage-wise manner. Subsequent to the generation of reaction kinetics and development of the empirical model for recombiner, the developed hybrid scheme based on CFD is envisaged which can become a powerful numerical tool for speedy containment analysis involving many recombiners.

CHAPTER 3

Development of CFD Model & Optimization of Recombiner Location

3.1 Introduction

Experimental as well as theoretical studies have gained paramount importance in recent years to understand and predict the performance behaviour of hydrogen recombiners. While the experimental studies have been used to evaluate the newly developed catalysts and recombiner designs, they have a limited scope. This is because they can’t be utilised for performance studies involving wide hydrogen concentration ranges owing to the risk involved with hydrogen handling. Hence more emphasis is laid on accurate theoretical studies to substitute them. Use of CFD has increased in recent times to evaluate the simultaneous chemical, thermodynamic and transport phenomena-based processes occurring in and around recombiner devices. CFD based analytical tools have been used to study the behaviour of Passive Catalytic Recombiners Devices (PCRDs) on standalone basis. For example, Orszulik et al. (2015) carried out numerical modeling of PAR based on the REKO 3 experiments using ANSYS-FLUENT and also tuned the model to get PAR performance in accordance to their own experimental results. Reinecke (2016) carried out validation of REKO-DIREKT code for simulation of PAR operational behavior against small-scale experiments performed at Forsc-hungszentrum Juelich in the REKO facilities (Drinovac, 2006). Detailed CFD models for recombiners placed inside large geometries have been sparingly reported in the literature due to their extravagant computational requirements.

CFD models are required for containment analysis of Nuclear Power Plants (NPPs) involving hydrogen recombination and steam atmospheres in the containment of a nuclear reactor. While considering steam inside the containment atmosphere, the local heat transfer and fluid flow phenomena are also required to be accounted during the model development. Such models resolve the stratification related issues in a typical steam laden containment during the severe accident scenario. Such computational tools can be built to predict some of safety related important information particularly in the context of hydrogen transport and mitigation behavior. These issues include: hydrogen transport behavior in and around the recombiners, effectiveness of homogenization of the gas mixture, catalyst temperature, determination of containment pressure from safety point of view and likely progression of the post-accident scenario.

As a part of the ongoing activities related to the present research, a CFD based recombiner model is developed. This chapter presents the salient features of detailed recombiner model and its validation against data from open literature. The validated and optimized model is then applied to assess the suitable location for placing a PCRD within a closed geometry to extract its reasonably best performance and efficiency. Simulations performed for different PCRD positions within a closed vessel under dry as well as steam laden conditions are presented in the later portion of the chapter.

3.2 Working Principle of Recombiner Device

A typical PCRD consists of a rectangular enclosure which is open at bottom and top. The Pt-Pd coated thin catalytic stainless-steel plates are stacked in parallel at the bottom portion of the box with a fixed gap between the plates. The ambient gas mixture (hydrogen-steam-air) enters the box at bottom and leaves the box from the top. As mixture comes in contact with catalytic plates, the exothermic oxidation reaction takes place on the catalyst surface. Part of the exothermic heat is dissipated to the surrounding gas mixture by convection and radiation causing rise in its temperature. This causes initiation of buoyancy induced gas movement in upward direction. The upward movement creates low pressure inside the box. This induces more and more hydrogen rich colder mixture to enter the box from the bottom and hot gas mixture lean in hydrogen to exit from top of the box. Consequently, the overall hydrogen gas concentration in vicinity of the recombiner box keeps on depleting passively. A schematic representation of the phenomena taking place inside a recombiner device is illustrated in Figure 3.1.

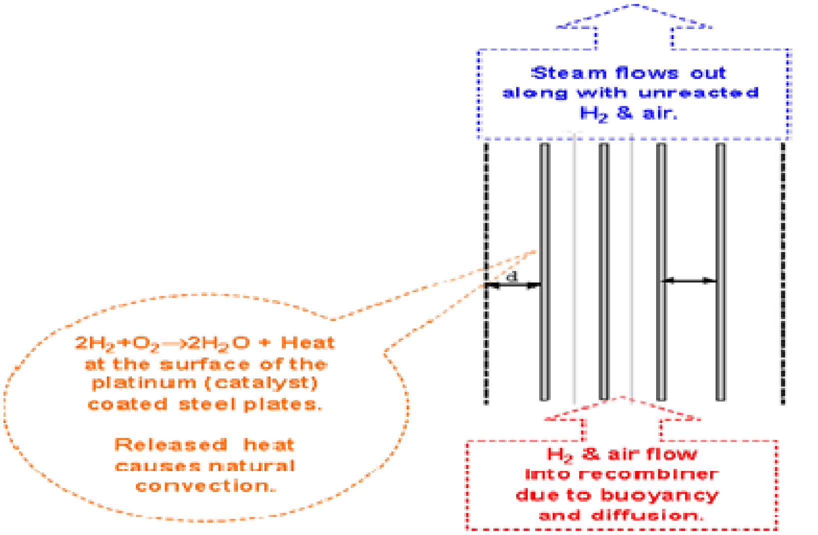

Fig. 3.1: Phenomena involved in a PCRD

3.3 Numerical Model

The whole process of hydrogen mitigation using recombiners is dominated by transport phenomena such as movement of gas mixture by buoyancy through the box, catalytic oxidation reaction, dissipation of exothermic heat on to the solid catalyst plate and steam condensation. Hence, the equations required for modeling the recombiner include: buoyancy and gravity; multi species transport and diffusion; chemical reaction modeling via source and sink terms for the species involved; and conjugate heat transfer. Since the interest of the present work is to determine the effect of condensation on gas distribution and pressure changes due to turbulence created by condensing steam, the homogeneous mixture model is chosen over other models such as interface tracking models and Eulerian two fluid model. The numerical model for recombiner has been developed using commercial CFD software FLUIDYN-MP that uses Finite Volume (FVM) based fluid flow solver and Finite Element Method (FEM) based solver for thermal analysis of structures. The flow and structural solvers are coupled by exchanging the heat flux at each time step. A basic description of the model is presented below.

3.3.1 Model Description

Since the recombiner model consists of solid catalyst plates surrounded by gaseous fluid, the domain is divided as fluid and solid. The solid domain comprises of the catalyst plates and the recombiner box while the fluid domain comprises of rest of the region. The fluid region is assumed to be a compressible gas mixture of four ideal gases namely hydrogen, nitrogen, oxygen and water vapour. Ideal gas equation states that $p = \rho R_u T/M$, where p is the pressure, ρ is the density, R_u is the universal gas constant, T is the temperature and M is the molecular weight. Thus, the local density inside the fluid region changes as per local pressure, temperature and gas mixture composition. Hence, the flow has been considered as compressible flow. Thermal conductivities of individual gas components are dependent on their respective Prandtl numbers. This approach has been used due to the large variation expected in temperature due to exothermic reaction. To account for the density difference between individual gas components of the mixture, Buoyancy Gravity model is used with suitable reference density. To capture flow in the fluid domain, the compressible form of Navier-Stokes equations and turbulence model, described below, are solved along with the ideal gas equation of state of the form $\rho = f(p,T)$.

The physical problems studied in this work involve relatively low volume fractions of the liquid phase, except possibly at the walls, and this liquid phase will normally be well mixed. The bulk condensation model is based on the concept of thermodynamic super saturation of the steam in gaseous environment with an empirical relaxation constant for incipient bulk condensation initiation. The wall condensation is based on wall condensation theory in conjunction with the gas mixture transport towards the wall by diffusive and convective modes.

The surface reaction at the catalyst plate is modelled at the fluid-solid interface by assigning source terms for the involved species at fluid cells adjacent to the interface. On the other hand, solid nodes at the interface are assigned the exothermic heat released during the surface reaction. In order to calculate the source and sink terms for chemical species and heat energy, the reaction rate is determined by the Arrhenius equation based on the local temperature and species concentration at each time step as. To account for the conjugate heat transfer between the solid and fluid domain, Finite Element Method is used to solve heat transport in the solid domain. At each time step, the heat fluxes are exchanged between solid and fluid domains based on the local temperature difference between solid nodes and fluid cells at the interface.

3.3.2 Modelling of Gas Transport

The movement of this gas mixture can be mathematically represented by conservation equation of mass (continuity equation) and momentum for three-dimensional space as follows

$$\frac{\partial \rho}{\partial t} + \nabla \cdot (\rho U) = 0 \tag{3.1}$$

$$\frac{\partial (\rho U)}{\partial t} + \nabla \cdot (\rho U U) = \nabla \cdot \tau - \nabla p + S_U \tag{3.2}$$

$$\tau \quad = \mu \dot{\gamma} - \left(\tfrac{2}{3}\mu - \kappa\right)(\nabla \cdot U)\,\delta \tag{3.3}$$

$$\dot{\gamma} \quad = \nabla \mathbf{U} + (\nabla \mathbf{U})^T \tag{3.4}$$

where, ρ is density, U is the velocity vector, p is pressure, τ is the viscous stress tensor, $\dot{\gamma}$ is the rate-of-strain (or rate-of-deformation) tensor, $\nabla \mathbf{U}$ is the velocity gradient tensor, $(\nabla \mathbf{U})^T$ is the transpose of the velocity gradient tensor, $(\nabla . \mathbf{U})$ is the divergence of the velocity vector, μ is effective viscosity, κ is the dilatational viscosity (=0 according to Stokes), δ is the unit tensor, S_U is the source term for momentum equation and t is time. Since, the fluid velocity is expected to vary in different directions at various places and may depend on the time t, generalized form of Newton's law of viscosity is used here. These are important, because the flow involves small passages between the plates with varying velocity gradients and the frictional losses may play an important role in the performance of the recombiner.

The energy conservation inside fluid domain can be represented by Eq. (3.5), as given by Bird (2002):

$$\mathrm{Cp}\left[\frac{\partial(\rho \mathrm{T})}{\partial \mathrm{t}}+\nabla \cdot(\rho \mathrm{UT})\right]=\nabla \cdot \mathrm{q}-\left[\frac{\partial(\ln \rho)}{\partial(\ln \mathrm{T})}\right]_{\mathrm{p}}\left[\frac{\partial \mathrm{p}}{\partial \mathrm{t}}+\mathrm{U} \cdot \nabla \mathrm{p}\right]+\mathrm{S}_{\mathrm{T}} \tag{3.5}$$

where, T is temperature, Cp is the specific heat at constant pressure, q is the heat flux vector (= K∇T), K is thermal conductivity and S_T is the source term for temperature. The pressure work term in the energy equation is included due to the expected pressure changes arising from phase change between water to water vapor and in case of any jet flow encountered for modeling the accident conditions. The temeprature source term is obtained in terms of divergence of heat flux vector from descrete ordinates method to account for the thermal radiation in the fluid domain. Additionaly temperature source at the fluid interface with solid catalyst plates is also obtained from the heat of the recombination reaction as given by Eq. (3.8).

The fluid comprises of multiple species and the phenomena involves source of some species in the form of chemical reaction and phase change between water and its vapor. The conservation of species in the fluid domain is given by equation Eq. (3.6):

$$\frac{\partial(\rho \mathrm{X}_{\mathrm{i}})}{\partial \mathrm{t}}+\nabla \cdot(\rho \mathrm{UX}_{\mathrm{i}})=-\nabla \cdot(\Gamma_{\mathrm{i}} \nabla \mathrm{X}_{\mathrm{i}})+\mathrm{S}_{\mathrm{i}} \tag{3.6}$$

where, X_i is the mass fraction of species i and S_i is the source term for species i. The species equations include those for individual gaseous species, except for a carrier species. The source/sink terms for hydrogen and oxygen are computed using Eq. (3.8). While the source term for water vapor arising from chemical reaction is computed using Eq. (3.8) and that arising from phase change is given by Eq. (3.24) explained later.

3.3.3 Modeling of Catalytic Recombination

The recombination reaction on catalyst surface is a multi-step process. But the CFD model deals with the overall phenomena associated with recombination. Hence the recombination reaction has been modeled using single step chemistry with an aim to reasonably capture the overall phenomena in a computationally economical manner without losing on the accuracy of results. The reaction rate is usually expressed in terms of the concentrations of the reactants and/or products, and catalyst temperature. The rate of a reaction, R_j, can be computed in 3 ways in the code: (i) by chemical kinetics, (ii) controlled by the mixing of the reactants and (iii) combination of (i) and (ii). In the Arrhenius model used in the present work, the reaction rate is completely determined by chemical kinetics. Hence, rate of a reaction, R_j, is given by:

$$R_j = A_j e^{-E_j/RT} \prod_i x_i^{\nu_{ji}} \qquad (3.7)$$

where, A_j is the pre-exponential factor, E_j is the activation energy, R is the universal gas constant, x_i denotes the mole fraction of species i and ν_{ji} depicts the species rate exponents. Aj, Ej, ν_{ji} are experimentally determined parameters. The source terms for the temperature and species concentrations in Eq. (3.5) and (3.6) respectively are expressed as follows:

$$S_i = \sum_j R_j(\nu_{2i} - \nu_{1i})M_i$$

$$S_T = \frac{1}{Cp}\sum_j Q_{rj}R_j \tag{3.8}$$

where, R_j is the reaction rate of reaction j in terms of leading reactant [kmol/m^{3}s], M_i is the molecular weight of species i [kg/kmol], Q_{rj} is the heat of reaction of jth reaction in terms of leading reactant [J/kmol]. It is calculated using heat of formation ΔH_f, of reactants and products as per Eq. (3.9)

$$Q_{rj} = \sum_i \Delta H_{f_i}(\nu_{2i} - \nu_{1i}) \tag{3.9}$$

However, in the present case the recombination reaction of hydrogen and oxygen is modeled as single step reaction (given by Eq. (4.3) later) hence reaction 'j' here is only the recombination reaction of H_2. Here, H_2 and O_2 are the reactants and H_2O is the product. Thus, the source term in the species conservation equation for hydrogen obtained as per Eq. (3.8) is R_{H_2} (R_j as per Eq. 3.8) multiplied by 0 – 1 ($\nu_{2i} - \nu_{1i}$) and molecular weight of hydrogen M_{H_2} i.e. 2. Similarly, as per Eq. (3.8) the source term for oxygen is taken as reaction rate R_{H_2} multiplied by (0 - 0.5) (as per Eq. (4.3) later) and its molecular weight 32. The source term for water vapor arising from the reaction is taken as reaction rate R_{H_2} multiplied by (1 - 0) and its molecular weight i.e. 18.

The source term for temperature is also computed as per Eq. (3.8). Here, the heat of formation is zero for diatomic gases H_2 and O_2 as they are in their elemental form. The heat of recombination reaction is 242 kJ/mol, as per Eq. (4.3). These terms are computed and used at the fluid-solid interface at every time-step.

The reaction has been modeled earlier by a detailed reaction mechanism as reported by Heitsch (2000) and Appel et al. (2002). For developing the CFD model, a single step global reaction rate expression as reported by Schefer (1982) has been used. It has been done so that the accuracy of the model established by validating it against available literature data. This approach assumes a single step reaction from the stable reactants to the stable products without considering any of the intermediate reactions. So the species considered in the reaction are hydrogen, oxygen and water vapor. The rate of the catalytic reaction in the present case is given by the following expression given by Schefer [1982].

$$R_{H_2} = 14\exp.\left(\frac{-16.1\mathrm{x}10^6}{RT}\right)[H_2] = \frac{-d[H_2]}{dt} \qquad (3.10)$$

where, R_{H_2} is the rate of recombination reaction.

This temperature function in Eq. (3.10) has been used in the numerical model to obtain the value of reaction rate based on local concentration and temperature at each time step during the simulation.

Schefer's equation is a generic single step formulation. The values for activation energy and pre exponential factor are catalyst specific. The Schefer's equation has been used as it has been widely referred in literature. However, the results from Schefer's data are accurate enough to give the general trend for behavior of PCRD and its dependence on location for better performance.

3.3.4 Modeling of Heat Transfer and Radiation

The highly exothermic reaction of hydrogen and oxygen heats up the catalyst surface as well as the gas mixture surrounding it. Equation (3.5) represents energy conservation which defines the adjoining gas mixture.

Figure 3.2 shows the basic heat transfer mechanism involved in the process. Heat source is added directly to the catalytic walls. Heat is transported due to conduction inside the catalyst plates and due to convection through the gas phase inside the flow channels. Conjugate heat transfer model has been considered for representing convective heat dissipation from solid plates to gas phase.

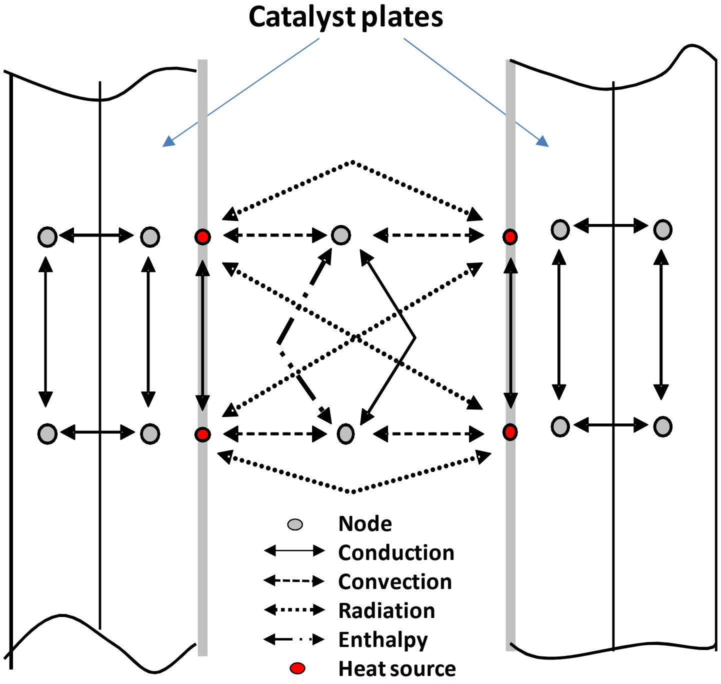

Fig. 3.2: Modes of Heat transfer in the recombiner model

The catalytic plates being at much higher temperature compared to the surrounding gas as well as the box, also radiate heat to the gas as well as box walls. The radiative transfer equation (RTE) for an absorbing, emitting, and scattering medium is given by Eq. (3.11):

$$\frac{dI(r,s)}{ds} + (\kappa_a + \kappa_s)I(r,s) = \kappa_a n^2 \frac{\sigma T^4}{\pi} + \frac{\kappa_s}{4\pi}\int_0^{4\pi} I(r,s')\,\Phi\,(r,s)d\Omega \qquad (3.11)$$

where, I is the total radiation intensity, **r** is position vector, s is the direction vector, **s'** is the scattering direction vector, s is path length, κ_a is the absorption coefficient, κ_s is scattering coefficient, n is refractive index, σ is Stefan-Boltzmann constant = 5.672e-8W/m^{2}K^4, T is temperature, Φ is the phase function, Ω is solid angle and (κ_a+κ_s) is the optical thickness or opacity of the medium. Here, absorption is only due to tri-atomic water vapor molecules, but their presence in significant quantities is possible in accident scenarios involving even more than 50% v/v steam. On the other hand, presence of aerosols in the containment atmosphere is possible during the accident scenarios, the same has not been simulated in the present model and hence the scattering term from the above equation is neglected in the solution. Solving the Radiative Transfer Equation with spectral accuracy is computationally prohibitive for this coupled multi-dimensional problem. Hence, the RTE is solved by the Discrete Ordinates Method, which is based on a discrete representation of the directional variation of the radiative intensity. A solution to the radiation transport problem can be found by solving the equation of transfer for a set of discrete directions spanning the total solid angle range of *4π*. The integrals over solid angle are approximated by numerical quadrature as $\int_{4\pi} f(\Omega)d\Omega \cong \sum_{m=1}^{M} w^m f(\Omega^m)$ where, w^m is quadrature weights associated with the direction, Ω^m. The transfer equation for radiation energy (in non-dimensional form) passing in a specified direction $\vec{\Omega}$ through a small differential volume, in three dimensional co-ordinates is written as a finite difference equation. From this, the outgoing radiation intensity from the wall is calculated. Once the radiation intensity field is obtained, the total incident radiation, radiative flux, and the divergence of radiative flux in the rectangular domain is obtained. The divergence of radiative flux for the assumptions of emitting, absorbing and non-scattering gray medium is shown below.

$$\nabla . q_r(x,y,z) = \alpha(x,y,z)\left[4\sigma T^4(x,y,z) - G(x,y,z)\right] \tag{3.12}$$

where, ε is the emissivity, α is the absorptivity of the wall surface and G(x,y,z) is the incident radiation. This divergence of heat flux arising due to thermal radiation is used as source term in the energy equation Eq. (3.5).

3.3.5 Modelling of Turbulence

The recombiner model is intended to simulate the performance of PCRD inside closed geometry of reactor containment during accident scenario. The domain encounters turbulence induced due to steam condensation. Hydrogen distribution inside the fluid domain while reaching up to the PCRD is affected by this turbulence. While the flow inside the parallel channels of PCRD is primarily laminar, it accelerates in the vicinity of PCRD due to buoyancy induced natural convection flow generated by temperature rise inside the PCRD. The model has been developed to handle turbulent flows typically encountered by hydrogen distribution. The choice of the turbulence model has been based on previous studies involving hydrogen distribution and comparison of results with open literature data.

Turbulent flows affect the transport of momentum. Chen-Kim model from the *k*-ε family of turbulence models has been used as it is found to give better results compared to other turbulence models for hydrogen distribution inside similar geometries. In the Reynolds averaging approach used here, the Navier-Stokes equations are averaged over time. The model employs the Boussinesq eddy viscosity model to approximate the Reynolds stress as:

$$\rho\overline{u_i^{'}u_j^{'}} = \mu_t\left(\frac{\partial\overline{u}_i}{\partial x_j} + \frac{\partial\overline{u}_j}{\partial x_i}\right) - \frac{2}{3}\rho\delta_{ij}k \tag{3.13}$$

where, μ_t is eddy viscosity and k is the turbulence kinetic energy ($= \frac{1}{2}\rho\overline{u_i^{'}u_i^{'}}$)

The eddy viscosity is determined as:

$$\mu_t = \rho C_\mu \frac{k^2}{\varepsilon} \tag{3.14}$$

where, ε is the dissipation rate of k and C_μ is constant.

The turbulence model solves for k and ε. The governing equations of these are of following generic form:

$$\frac{\partial(\rho\phi)}{\partial t} + \nabla\cdot(\rho\mathbf{U}\phi) = \nabla\cdot(\Gamma_\phi\nabla\phi) + S_\phi \tag{3.15}$$

where, $\Gamma_\phi = (\mu_l/\sigma^\phi_l + \mu_t/\sigma^\phi_t)$, is the exchange coefficient for ϕ and σ^ϕ is the Prandtl number for ϕ. Taking ϕ as k and ε respectively, values of their source terms and various constants of the turbulence model mentioned above are given in Table 3.1.

Table 3.1: Different terms in equations for the Chen-Kim form of *k*-ε model

S_k	S_ε	Constants
$\rho(P_k - \varepsilon)$ $P_k = \nu_t \dot{\gamma} : \nabla \mathbf{U}$	$\frac{\rho\varepsilon}{k}\left(C_{\varepsilon 1} P_k - C_{\varepsilon 2}\varepsilon\right) + C_{\varepsilon 4}\frac{\rho P_k^2}{k}$	$C_\mu = 0.09$ $C_{\varepsilon 1}$=1.15, $C_{\varepsilon 2}$ =1.9 $C_{\varepsilon 4} = 0.25$ $\sigma^k = 0.75$, $\sigma^\varepsilon = 1.15$

Chen and Kim modification to the standard *k*-ε model improves the dynamic response of the ε equation by introducing an additional time scale (*k*/P_k). In addition, several of the standard model coefficients are adjusted. The Chen and Kim modification involves addition of a source term to the ε equation that allows the turbulence distortion ratio (P_k/ε) to exert an influence on the production rate of ε. According to them the extra source term represents the energy transfer rate from large-scale to small-scale turbulence controlled by the production-range time scale and the dissipation-range time-scale.

3.3.6 Modelling of Heat Transfer in solid domain

As seen in Figure 3.2, exothermic heat of recombination reaction is applied as the nodal heat source at the fluid-solid interface. In FLUIDYN software, the heat transfer in solid is solved by FEM. The thermal solver is a Finite Element code for transient thermal analysis in a structure. In present work 8-noded hexahedral elements were used. The solid material properties are taken as temperature dependent (specified as a polynomial function). 3-D transient heat conduction equation is solved for catalyst plates. The thermal energy balance in an elemental volume of solid, surrounded by fluid is given by the following governing equation:

$$\rho C_p\left[\frac{\partial T}{\partial t}\right]=\nabla .q+\dddot{q} \tag{3.16}$$

where, ρ = density of the solid, C_p is the specific heat of solid, T is the temperature in the solid, t is time, q is heat flux vector and $\dddot{q}$ is volumetric heat generation rate. From Fourier's Law of heat conduction, the heat flux due to heat conduction can be written as:

$$q = k\nabla T \tag{3.17}$$

where, k is the thermal conductivity of the solid. For the convective surface present as a boundary to the solid, the convective flux that enters the solid from the fluid according to Newton's Law of Cooling is:

$$q_f = h_f (T_f - T) \tag{3.18}$$

where, h_f is the film coefficient, T_f is the temperature of the surrounding fluid and T is the temperature of the solid. Similarly, the radiative flux that enters the solid is:

$$q_r = h_r (T_r - T) \tag{3.19}$$

where, h_r is film coefficient due to radiation (explained in the following section), similar to h_f, T_r is the temperature of the radiating surface, T is the temperature of the solid. The transient heat transfer analysis involving solution of the above equations along with suitable boundary conditions has been performed using finite element method with implicit scheme which is more suitable due to stability and convergence.

3.3.6.1 Radiation Heat Transfer Coefficient

The thermal radiation transport through the participating medium (i.e., the gas mixture) is modeled using DOM. But, the radiation incident on the solid surfaces (i.e. fluid-structure interface at plate surfaces) is transferred to the plate by making it a boundary heat flux. This boundary heat flux is written in terms of a heat transfer coefficient and an effective fluid temperature. This radiation heat transfer coefficient is defined in analogy to convection heat transfer coefficient as $q_r = h_r (T_r - T_s)$ where, q_r is the radiating flux coming onto the structure with temperature T_s from a radiating surface at a temperature T_r. In accordance with the Stefan Boltzmann Law:

$$q_r = \sigma\, \varepsilon_r \varepsilon_s F_{rs} \left(T_r^4 - T_s^4\right) \tag{3.20}$$

where, σ is the Stefan Boltzmann constant, ε_r is the emissivity of the radiating surface and ε_s is the emissivity of the structure, T_r and T_s are the respective temperatures at the radiating surface and structure boundary. F_{rs} is the corresponding view factor.

$$\begin{aligned} q_r &= \sigma\, \varepsilon_r \varepsilon_s F_{rs} \left(T_r^4 - T_s^4\right) \\ &= \sigma\, \varepsilon_r \varepsilon_s F_{rs} \left(T_r^2 + T_s^2\right)\left(T_r^2 - T_s^2\right) \\ &= \sigma\, \varepsilon_r \varepsilon_s F_{rs} \left(T_r^2 + T_s^2\right)\left(T_r + T_s\right)\left(T_r - T_s\right) \\ &= h_r \left(T_r - T_s\right) \end{aligned}$$

Thus it can be seen that the radiation film coefficient can be expressed as:

$$h_r = \sigma\, \varepsilon_r \varepsilon_s F_{rs} \left(T_r^2 + T_s^2\right)\left(T_r + T_s\right) \tag{3.21}$$

For thermal analysis, the initial temperature of solid is taken to be the same as the initial fluid temperature. The algebraic equation has been solved by Pre-conditioned Conjugate Gradient (PCCG) solver with convergence criteria of 10^{-12}.

3.3.7 Homogeneous Equilibrium Model (HEM) & Wall Film Model

Stand-alone recombiner does not involve any condensation or evaporation as the internals are at higher temperatures owing to the exothermic heat of recombination reaction and the steam formed remains in the gas phase only. Thus the model does not need any steam condensation model. However, since this model is intended to be used inside closed geometries to understand the recombiner behavior in wet atmospheres also, handling of two-phase conditions becomes essential. Since the interest here is to determine the effect of condensation on gas distribution due to turbulence created by condensing steam and the pressure changes due to it, the inter-phase tracking approach has not be followed here and Eulerain multiphase approach has been adopted.

Flows involving phase change are modeled using homogeneous equilibrium model (HEM) (Fluidyn Mp Users Manual-2009), for phase changes in the bulk domain and wall film model for those occurring near or at the walls. The phase change, evaporation and condensation, is modeled by adding the appropriate source or sink term to the species equations for the liquid phase and the equation for the corresponding vapor. The assumptions used in these models are: (i) both phases are in thermodynamic equilibrium, and hence have same pressure and temperature, (ii) there is no well-defined interface between the two phases and (iii) the fluid, defined as a mixture of gases. As the species representing liquid water in the HEM is not a gas, the equation of state has been modified to the form $p = f(\rho, T, \theta)$. The density ρ is the mixture density, i.e., the sum of the macroscopic densities for each individual species including the liquid water (Royl et al. 1999). The equation of state for mixture of gases is modified to account for the presence of the liquid water. The general equation of state thus becomes (Travis et al. 1998),

$$p = \frac{T \sum_{i}^{i \neq h2ol} R_i \rho_i}{\theta} = \frac{\rho T \sum_{i}^{i \neq h2ol} R_i X_i}{\theta} \tag{3.22}$$

where, ρ_i is the density of water vapor at the instantaneous pressure temperature conditions of the cell and X_i is the mass fraction of water vapor in the multi species gas mixture solved by Eq. (3.6). The volume fraction of the gaseous mixture is calculated as

$$\theta = 1 - \theta_l = 1 - \frac{\rho_{h2ol}}{\rho_{h2ol}^{thermo}} \tag{3.23}$$

Where, ρ_{h2ol}^{thermo} is 1000 kg/m^3. The transport equations are solved only for the gaseous species. In order that HEM thermodynamics is correct, the expression for the liquid water specific internal energy is derived such that the difference between the vapor and liquid specific internal energies is matched by the same difference between the vapor and liquid saturation curve from the steam tables.

3.3.7.1 Bulk Condensation and Evaporation Models

The phase change takes place if the local thermodynamic state is different from the saturation condition. Ideally at a point, the phase change could be instantaneous and the state may always be in equilibrium. However, in a finite control volume the extent of phase change and the speed at which the fluid attains the equilibrium depends on the local mass and heat exchange rates and hence on mixing. To take care of this, the bulk condensation model is based on the concept of thermodynamic super saturation of the steam in gaseous environment with an empirical relaxation constant for incipient bulk condensation initiation. Thus, the finite rate of phase change leads to a non-zero relaxation time to reach the saturation state. Value of the empirical relaxation time constant, t_{pc}, is chosen based on the specific problem such that at every time step a stable solution is obtained. A value of 0.1 is found to be appropriate for t_{pc} for phase change in large containments. Also, the source term calculation considers the appropriate limits based on the instantaneous quantities available for evaporation and condensation. The mass source and sink term, in kg/(m^{3}s), for steam to be used in Eq. (3.6) is given by:

$$S_{h2og} = \left(\rho_{sat} - \rho_{h2og,gas}\right) \Big/ t_{pc}, \tag{3.24}$$

$$\rho_{sat} = \frac{p_{sat}}{R_{h2og} T} \tag{3.25}$$

$$p_{sat} = 10^5 e^{\frac{c_2 T - c_1}{c_3 T}} \tag{3.26}$$

The mass source and sink term, in kg/(m^{3}s), for liquid water is given by:

$$S_{h2ol} = -S_{h2og} \tag{3.27}$$

The enthalpy of water vapor is taken as the sum of enthalpy of liquid water and enthalpy of latent heat of evaporation. So, internal energy source term is derived using the liquid water and water vapor's enthalpy values, read from the code database.

3.3.7.2 Wall Film Model

The convective heat transfer coefficient is obtained by using Reynolds analogy formulation and the mass transfer coefficient is calculated based on Chilton-Colburn empirical analogy between heat and mass transfer,

The wall condensation/vaporization rate $\in_s$, is given by:

$$\in_s = \max\left\{-\frac{\delta_s^n A_s \rho_{h_2ol}^{thermo}}{2dt}, h_d A_s \left(\rho_{h_2og,gas} - \rho_{s,sat}\right)\right\} \tag{3.28}$$

The mass source or sink term for steam, in kg/(m^{3}s), due to phase change involving structural surfaces, is given by (for all the surfaces):

$$S_{str,h2og} = -\frac{1}{V}\sum_s \in_s \tag{3.29}$$

The internal energy source or sink term, in J/(m^{3}s) is given by (for all the surfaces)

$$S_{str,ie} = -\frac{1}{V}\sum_s \max\left\{\begin{matrix} \in_s I_{h_2og}(T_s) \\ h_d A_s \left(\rho_{h_2og,gas} - \rho_{s,sat}\right) I_{h_2og}(T) \end{matrix}\right\} \tag{3.30}$$

The work done by the gas mixture due to wall condensation, in J/(m^{3}s), is given by (for all the surfaces)

$$S_{work} = -\frac{1}{V}\sum_s \in_s R_{h_2og} T \tag{3.31}$$

When the wall film thickness exceeds the critical film thickness (critical film thickness, $\delta_{critical}$, is the maximum wall film thickness, which is allowed to stick with the wall face) then the excess water is drained out from the wall. The following equations give the mass and energy sink term for liquid water to drain out the excess wall film thickness. The mass sink term for liquid water, in kg/(m^{3}s) is given by (for all the surfaces)

$$S_{h2ol,drain} = \frac{1}{Vdt} A_s \rho_{h_2ol}^{thermo} \left(\delta_s^n - \delta_{critical} \right) \tag{3.32}$$

The internal energy sink term, in J/(m^{3}s) is given by (for all the surfaces)

$$S_{ie,drain} = S_{h2ol,drain} I_{h_2ol}(T) \tag{3.33}$$

Wall film thickness,

$$\delta_s^{n+1} = \delta_s^n + \frac{\in_s dt}{A_s \rho_{h_2ol}^{thermo}} \tag{3.34}$$

3.4 Validation of Recombiner Model

The detailed CFD model for catalytic recombiner has been validated by comparing the results of the analysis against the experimental data obtained in REKO-3 facility (Drinovac, 2006). The facility consists of a vertical flow channel with a rectangular cross section 46 X 146 mm. The channel is 504 mm high. This facility has three modules (Module1, Module2, and Module3). Module1 works as inlet and feeds gas mixture to Module 2, which contains four catalytic plates where hydrogen recombines with oxygen to form water. Module3 works as outlet. The whole unit is thermally insulated on the sides to prevent heat losses. Four catalyst sheets (stainless steel sheets coated with wash coat/platinum catalyst material) having dimensions of 143 mm x 143 mm x 1.5 mm are used in the experiments. The facility has been used to investigate the behavior of a recombiner under controlled conditions.

The geometry for numerical computations is shown in figure 3.3. For the model development and validation, various simulations were performed with increasing complexity of simulation in which a dry gas mixture of air and hydrogen was fed to the recombiner. These simulations differed in number of channels, gas transport properties and heat losses to the ambient.

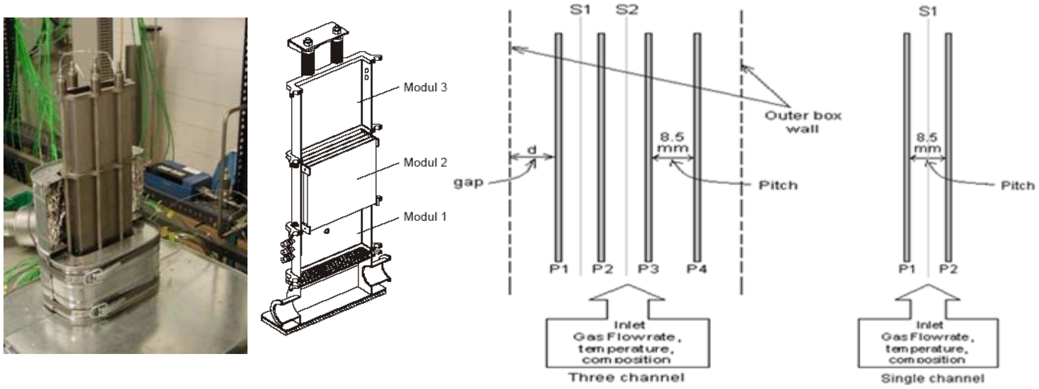

(a) (b) (c) (d)

Fig. 3.3: (a) REKO 3 Experimental facility (Drinovac, 2006), (b) Schematic, (c) Geometry for simulation of 3 channel and (d) single channel case

Since the geometry of recombiner with parallel plates is close to regular orthogonal shape, a structured grid approach has been used here as this allows better control of the mesh size near and away from the plate walls by use of appropriate power laws.

In order to simulate REKO-3 prototype results using the present analytical model, 4 catalyst plates along with walls of the facility were considered. For simulation purpose, only plates P1, P2 and the left box wall were chosen, since the system has symmetry with plane S2 as shown in Figure 3.3. The temperature profiles were calculated at the surfaces of P1 and P2, while hydrogen concentrations were calculated along planes S1 and S2. Mesh was selected based on mesh independence study. Table 3.2 shows the mesh parameters tested in the mesh independence test and the Figure 3.4 shows results of mesh independence test.

Table 3.2: Mesh Parameters for mesh independence study

Grid	Element size	
	Along the flow direction (mm)	Perpendicular to flow direction (mm)
G1	20	0.5
G2	15	0.25
G3	10	0.15

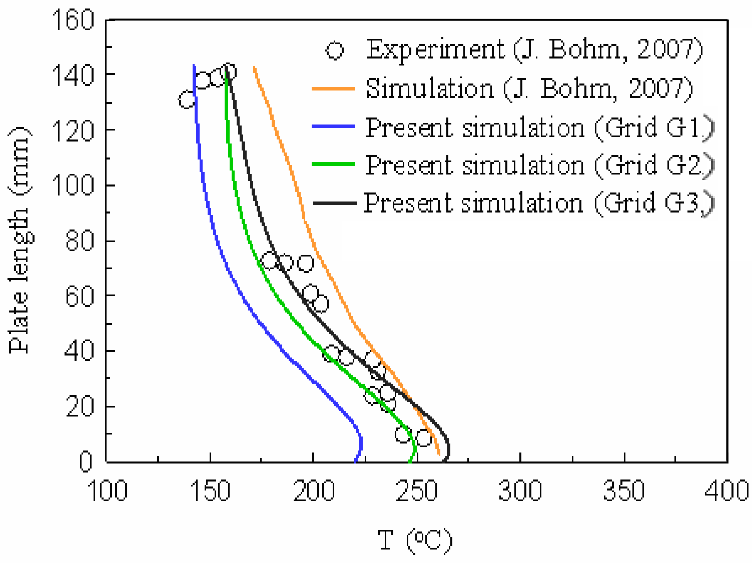

(a)

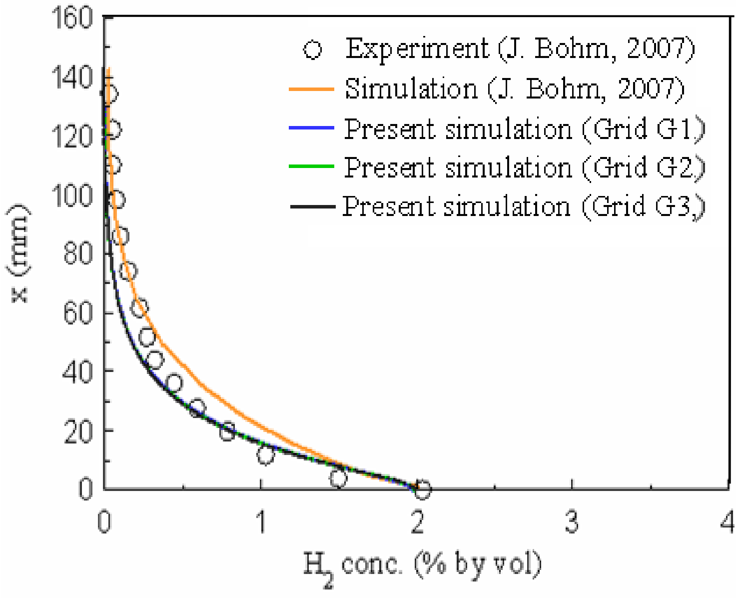

(b)

Fig. 3.4: (a) Plate temperature profiles & (b) Hydrogen concentration profiles for three meshes

The results have been compared against experimental as well as simulation results reported by Bohm (2007). On the basis of this comparison, Grid G2 is found good enough for accurate predictions. Still to improve the confidence, mesh parameters for the model were selected as per grid G3.

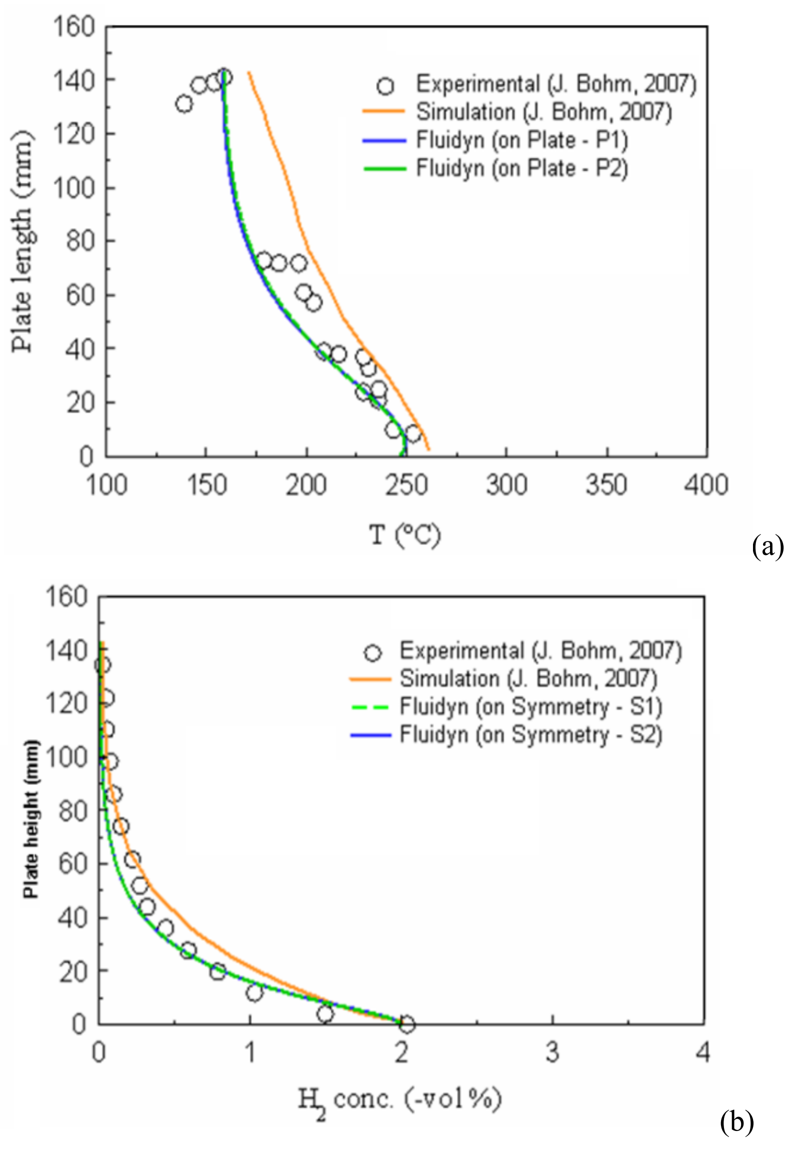

Fig. 3.5: (a) Profiles of catalytic plate temperature and (b) hydrogen concentration

As part of the studies for three channel geometry, several simulations were performed by changing the gap between the catalyst plate and the box wall as this dimension is not reported in the respective references. The outer wall of the box was modeled by an insulated boundary. Typical results for the temperature and concentration profiles are given in Figure 3.5. As can be seen from these results, only the lower portion of the catalytic plate is seen to be participating in the catalytic reaction. This can be attributed to lower inlet H_2 concentrations (2%) used in the reported experiment.

Several parametric studies were also performed for a single channel to study the effect of (i) inlet concentration and (ii) inlet flow velocity of hydrogen. These were also compared against experimental data. Typical results are presented in Figure 3.6.

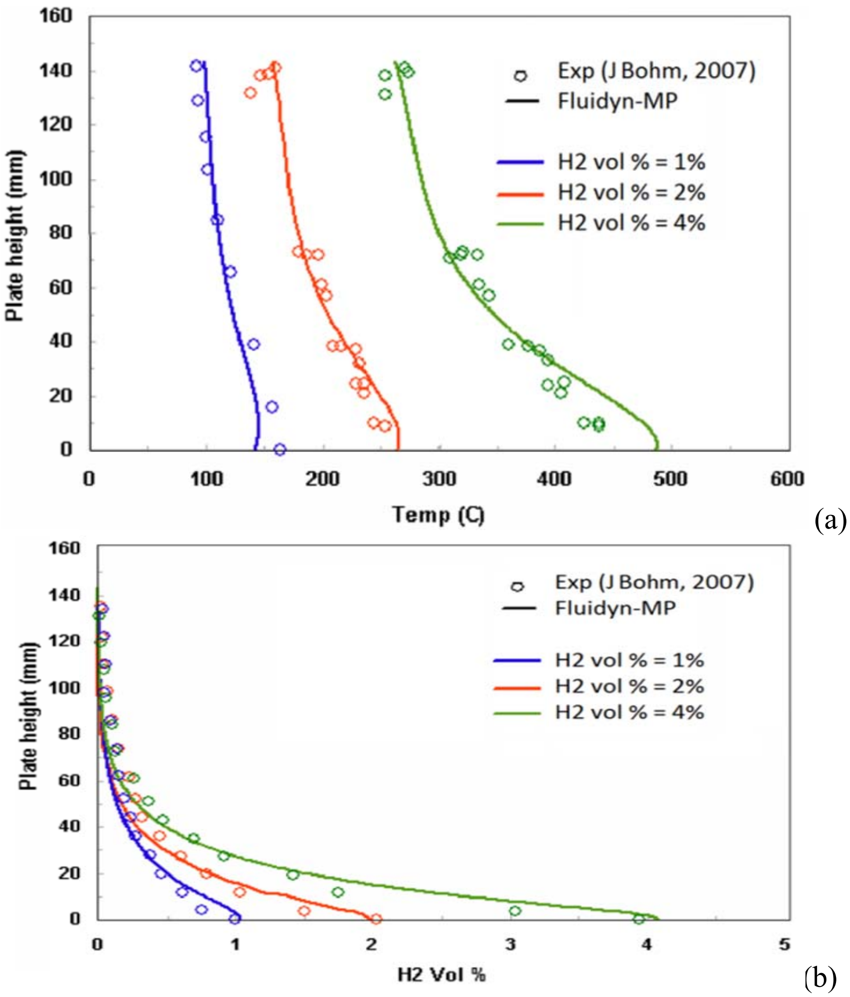

Fig. 3.6: (a) Catalytic plate temperature and (b) hydrogen concentrations with different concentrations of H_2 at the inlet

It can be seen that the steady state concentration profiles are matching well with experimental results for all the values of concentrations at inlet. The temperature profiles for the cases with 1% (v/v) and 2% (v/v) H_2 cases are closer to experiments but this is not the case for 4% (v/v). The model predicts higher temperatures at the leading edge of the plate for the higher concentration case. This could be attributed to the limitation of the single step reaction model to predict a multi step recombination process. It might cause high reaction rate and hence higher temperatures on encountering high hydrogen concentration as against the actual scenario where the forward reaction may develop slightly further from the leading edge of the plate after rise in plate temperature. Another reason may be the dependence of gas diffusivity on temperatures which was not accounted for in the simulation. Since the availability of hydrogen is less in the upper part of the plate (Figure 3.5), plate temperatures are less here. As there is no significant change in diffusivity, the results in this region of the plate match well with the experimental results.

3.5 Application of CFD Model

After validating the model developed in the CFD code FLUIDYN-MP, the recombiner model has been applied to simulate PCRD performance inside a closed geometry. For this purpose, the geometry of Hydrogen Recombiner Test Facility (HRTF) has been selected. HRTF is a facility to assess the performance of the PCRD. It is aimed at optimizing the recombiner design and its performance and to generate an extensive database for validation and fine-tuning of numerical models of nuclear reactor containment problems.

HRTF is a cylindrical carbon steel vessel of 3 m diameter and around 9 m height with torispherical top and bottom heads. The vessel has a volume of 60 m^3. The facility contains a recombiner device which comprises of a rectangular box made of stainless-steel sheets open at top and bottom. The approximate dimensions of the box are 400 mm x 700 mm x 1000 mm. At the lower portion of this box, catalytic plates are stacked at a pitch of 10 mm between them. Plates are coated with platinum/palladium catalyst. The gas is free to enter and exit at bottom and top ends of the box respectively. Figure 3.7 shows the locations of recombiner in HRTF as well as the schematic of recombiner box.

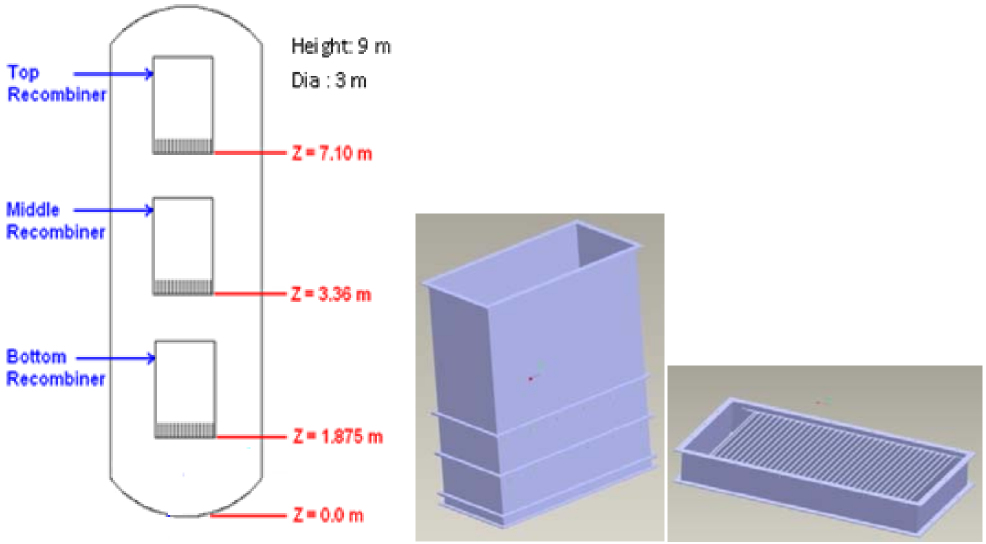

(a) (b)

Fig. 3.7: (a) Locations of PCRD in HRTF and (b) Schematic of recombiner box

The recombiner can be hung in the vessel at three heights (near top, middle & near bottom). The facility also has a steam supply unit comprising of an electrical boiler for supplying saturated steam to vessel. Steam condensation in the vessel due to loss of heat from the walls is minimized by insulating the vessel from outside.

3.5.1 Cases Simulated in Present Work

The present simulations aim to evaluate the performance of the recombiner at different locations in dry and wet conditions. Since the gas mixture is present uniformly all over the geometry for premixed cases, simulation domain has been considered as quarter symmetry. In dry condition, the insulated vessel walls are assumed to be at the vessel gas temperature. Whereas wet condition include non-condensing hydrogen–air–steam gas mixture in the containment as the vessel walls are kept insulated (adiabatic). The conditions used for dry as well as wet cases are given in Table 3.3.

Table 3.3: Inputs for dry & wet condition cases

	Pressure (bar)	Temperature (^oC)	Concentration (% v/v)		
			H_2	Steam	Air
Dry case	1.165	30	8	-	92
Wet Case	2.168	105	8	50	42

3.5.2 Geometry and Mesh

For premix cases, as hydrogen injector is not considered and the central axis of recombiner box passes through the central axis of containment, hence quarter symmetry is considered. Hexahedral elements were considered for modeling fluid as well as structural domain. The mesh for recombiner geometry having thin catalyst plates was selected based grid sensitivity study performed during validation exercise of the recombiner model. Similarly the mesh for modeling the vessel geometry was also selected based on a separate mesh sensitivity study for hydrogen distribution inside the closed vessel. Fine mesh was used in the regions where gradients were sharp especially between the plates and at inlet of the recombiner box. Other than these regions, relatively coarse mesh was used to reduce computational time. As fine mesh is not required at all parts of the domain, a non-conformal mesh was considered surrounding the recombiner box to maintain sufficient fine mesh inside the box and coarse mesh outside it. Thus, number of elements in the domain could be reduced without compromising the ability to capture gradients between the catalyst plates. Table 3.4 explains the details about the mesh used for premix cases.

Table 3.4: Mesh Details

Scenario	**Recombiner Position**	**Fluid**		**Structure**	
		Elements	**Nodes**	**Elements**	**Nodes**
Premix Cases	***Bottom***	97119	127302	6700	12042
	Middle	97218	127525	6700	12042
	Top	97119	127302	6700	12042

3.5.3 Fluid Configuration

The fluid has been considered as compressible mixture of gases containing hydrogen, nitrogen, oxygen, and water vapor. Buoyancy Gravity model has been considered for correct diffusion of hydrogen as it is a low-density gas. The appropriate reference density used for both dry as well as wet condition cases are provided below.

Ref. density for dry condition = 1.2341

Ref. density for wet condition= 1.4678

k–ε Chen-Kim model is considered for predicting turbulence parameters inside the domain however k-ω model was also tried but k-ε model was found better during validation studies. More complex models are difficult to use because of their high computational requirements adding to the complexity and sluggishness of solution. Homogeneous Equilibrium Model (HEM) is used for bulk evaporation and condensation.

3.5.4 Initial Conditions

Table 3.5: Initial Conditions

Fluid Domain			
Scenario	**Variable**	**Dry Condition**	**Wet Condition**
Premix Cases	*Pressure (kPa)*	116.524	216.837
	Temperature (K)	303.0	378.0
	Vol. fr. of H_2	8 %	8 %
	Vol. fr. of N_2	72.68 %	33.18 %
	Vol. fr. of O_2	19.32 %	8.82 %
	Vol. fr. of Steam	---	50 %
Structural Domain			
Scenario	**Variable**	**Dry Condition**	**Wet Condition**
Premix	*Temperature (K)*	303.0	378.0

3.5.5 Boundary Conditions

The outer walls of the domain are applied with adiabatic no-slip wall condition. The interface of the catalyst plates and surrounding fluid domain has been taken as no-slip isothermal wall with surface reaction applied at the interface. It may be noted here that isothermal here means specific boundary condition for the surface reaction at the interface, wherein, heat flux between solid and fluid is exchanged at each time step based on their temperature difference to keep the fluid and solid temperatures same at the interface. Symmetric boundary condition has been applied on the faces representing symmetry. For the solution of thermal radiation using DOM, an emissivity of 0.8 has been assigned to the surfaces. For recombiner box, to represent the symmetrical condition at symmetrical faces, adiabatic boundary condition (i.e. heat flux = 0) has been applied.

3.5.6 Method of solution

In order to solve the set of non-dimensional governing equations, pressure based 1st Order Euler Implicit solver (i.e. MP-NSNT) has been used for transient simulation. Pressure-velocity coupling is handled by Semi-Implicit Method for Pressure Linked Equations-Consistent (SIMPLEC). Convection is solved using 2nd order Upwind Differencing Scheme (UDS). Table 3.6 gives the solver parameters used in the simulations.

Table 3.6: Solver parameters for different flow variables

Variable	Number of inner iterations	Convergence criterion for inner iterations	Relaxation factor	Convection scheme
Pressure	2000	0.01	0.3	UDS
U (axial velocity)	20	0.1	0.3	UDS
V (transverse velocity)	20	0.1	0.3	UDS
W (transverse velocity)	20	0.1	0.3	UDS
Temperature	20	0.1	0.3	UDS
H_2	20	0.1	0.3	UDS
O_2	20	0.1	0.3	UDS
H_2O	20	0.1	0.3	UDS

The above convergence criteria are for inner iterations of the line by line solver. At every time step, multiple outer iterations are performed for all the variables. The accuracy and convergence is checked by the drop in residuals between subsequent outer iterations during each time step.

3.6 Results and Discussions

For dry as well as steam laden environment conditions, three recombiner locations have been considered for simulation i.e. top, middle and bottom recombiner position. Hence total six cases have been considered for simulation. For comparison between these cases, the contours and vectors have been plotted on symmetrical planes. Trace point locations have been considered in fluid as well as in structural domain to get the time history of variables like concentration of hydrogen, steam and temperature etc. The selected locations of the trace points are different for each scenario depending on the location of the recombiner box. For example, in case where recombiner is placed near top of the vessel, Figure 3.8 shows the location of trace points placed in fluid as well as on catalyst plates. Trace points in fluid domain were considered at top and bottom of the vessel, below and above the catalyst plates, and above the recombiner box like as shown in front view of vessel. Trace point locations in top view explain about the distribution of trace points at each elevation. Similarly the trace points on catalyst plates were considered at all four corners and at center as well.

The trace points on catalyst plate were considered on two plates in such a way that one is near to symmetry plane (Plate – 36) and the other one near to recombiner box wall (Plate – 1). All other cases for middle and bottom recombiner positions in dry as well as wet conditions were also analyzed in same manner with respect to the location of trace points and other parameters to be analyzed in the results.

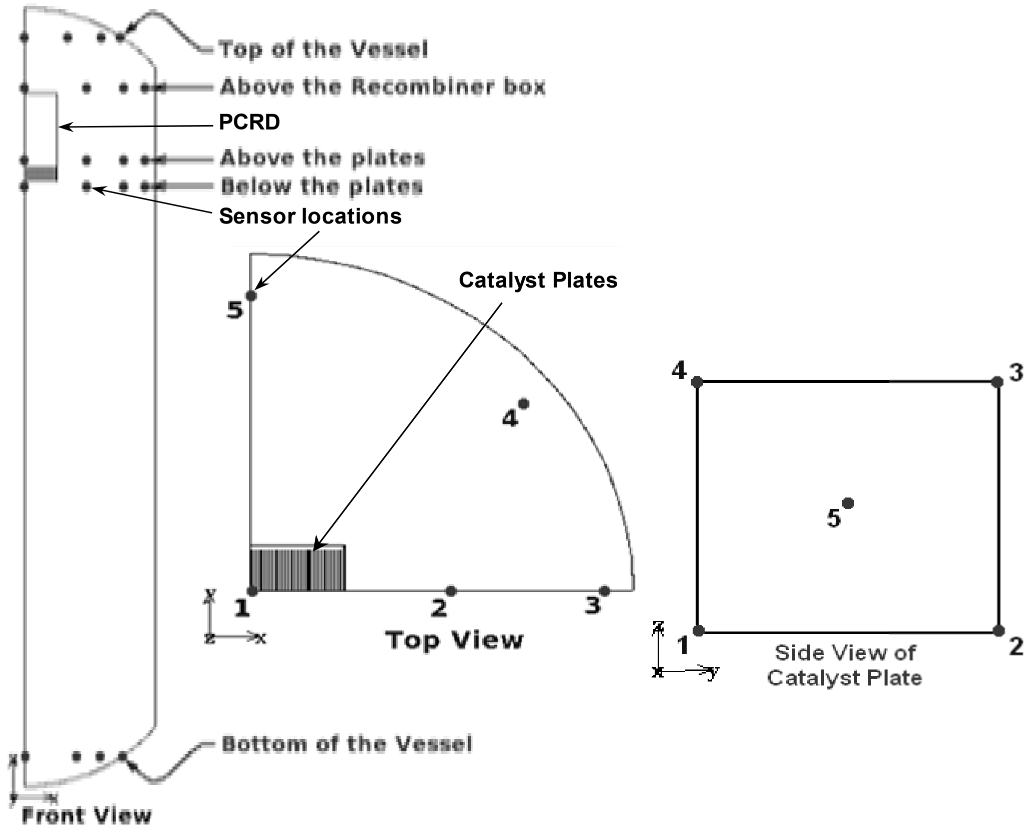

Fig. 3.8: Location of sensor points in fluid and catalyst plates for top recombiner case

For the transient analysis of various cases, 1200 seconds have been fixed as the simulation time. This is because as the concentration decreases, the temperature comes down and hence the rate of recombination reaction decreases due to temperature dependence of reaction kinetics. This leads to progressive sluggishness of the transient. One of the initial cases was run for a longer duration but it was observed that the trends are mostly captured during the initial time when concentration is more. Hence it was decided to run all the cases for 20 minutes of simulation to capture the transient for comparison purpose. Moreover, the simulation for 1200 seconds itself takes around 6 months for each case to complete. Hence it is not practical to carry out simulation of longer duration.

3.6.1 Cases for Dry Condition with Premixed Hydrogen

Figure 3.9 shows the comparative contour plots for hydrogen concentration after 1200 seconds for three dry cases having different recombiner positions. This figure shows that case having bottom positioned recombiner in the facility consumed the maximum hydrogen during 1200s for dry cases.

Initially as the 8% hydrogen in air mixture is present uniformly in the vessel, the reaction starts immediately at the catalyst plates. This exothermic reaction leads to increase in temperature. This change in temperature drives the flow due to buoyancy causing hot product gas moving out of the recombiner box from the top and fresh hydrogen rich gas entering the recombiner from bottom. The product gases travel upward due to natural convection, till they reach the top of vessel. During this travel they displace the hydrogen already present in this region. Thus a natural convection loop is developed wherein hot gases move upward near the axis of the vessel and the colder gases (rich in premixed hydrogen) move downwards near the vessel walls. So at initial time the velocities in the box accelerate and attain a maximum and then decreases to stabilize at a lower value. The time duration for the natural convection loop to establish and flow stabilization is different for three cases having different recombiner positions.

For the top recombiner case, the velocities in the box attain a maximum of 1.6 m/s and then decreases to low value of around 0.5 m/s. For the bottom recombiner case, velocity attains a maximum of 3.0 m/s and decreases up to around 1.0 m/s. The flow stabilization takes place during 100s to 700s for the top recombiner case. Whereas, for the bottom recombiner case, due to the large amount of hydrogen present above the recombiner box, the process of hot product gases replacing and pushing hydrogen downward continues for the entire simulation time.

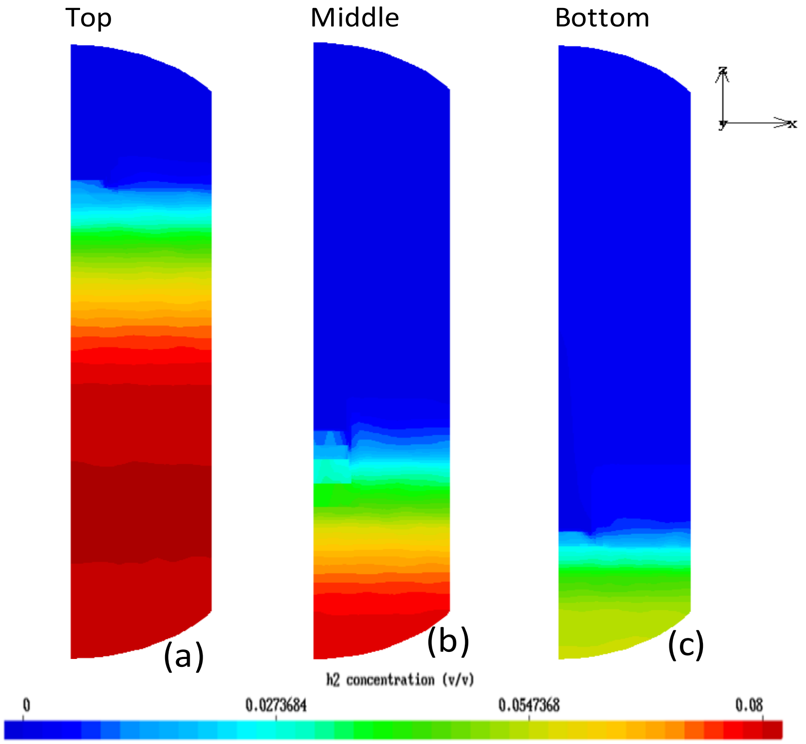

Fig. 3.9: H_2 concentration (v/v) Contours at 1200s on ZX-Symmetry plane for (a) top, (b) middle and (c) bottom recombiner positions in dry cases

The maximum concentration of hydrogen in the facility by the end of 1200s is present at the bottom of the vessel. In top and middle positioned recombiner cases, it is similar to the initial concentration of hydrogen (8% v/v), whereas in bottom positioned recombiner, its maximum concentration in the domain reduced to around 5% v/v for dry cases. This is primarily due to the hot gases coming out of recombiner box moving upwards and promoting better buoyancy driven flows for lower recombiner position. The effect is not prominent for the case having recombiner box at top location as the hot gases coming out from the box are already near the top of vessel and hence are not able to promote buoyancy driven flows and mixing.

Figure 3.10 shows the comparative temperature contour plots for the three different cases at 1200 s. Since the bottom placed recombiner case recombines maximum amount of hydrogen in the domain, the temperatures are higher in most parts of the domain due to more exothermic heat liberated during the recombination reaction. As seen in the contour plots of hydrogen concentration, there is no significant planar distribution of concentration at any horizontal plane inside the domain. Hence the trace point data for five trace points on any particular X-Y plane show almost the same value. Therefore, H_2 concentration profiles are plotted on single trace point in each X-Y plane. Data on trace point 1 which is on the axis of the vessel has been plotted at elevations such as bottom of the catalyst plates, top of the plates, top of the recombiner box, top of the vessel and bottom of the vessel. Such plots are made for all three cases having top, middle and bottom recombiner positions.

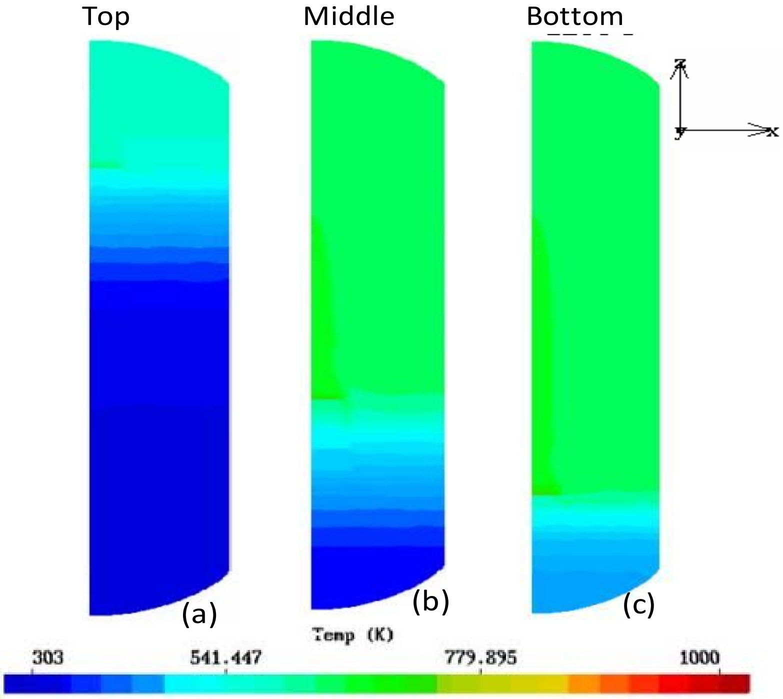

Fig. 3.10: Temperature Contours at 1200s on ZX-Symmetry plane for (a) top, (b) middle and (c) bottom recombiner positions in dry cases

Figures 3.11 and 3.12, show hydrogen and steam concentrations respectively at various elevations for top, middle and bottom recombiner positions. Concentration of hydrogen inside the entire domain is 8% at initial time and starts decreasing over time due to surface reaction. The reduction of hydrogen concentration at elevations above catalyst plates and above recombiner box is more rapid for all three cases. This is because hot product gases of recombination which are lean in hydrogen, rise upwards causing sharp decrease in hydrogen concentration at these locations. The hydrogen concentration at trace points near the top of the vessel has a gradual drop as compared to trace points near plate top and box top. This is because the upward moving product gases of recombination have more distance to cover and hence have more hydrogen to displace during their travel up to the vessel top.

At trace points near the bottom of the vessel, the drop in hydrogen concentration is slowest. This is because the hot product gases leaving the recombiner box rise upwards and accumulate at the top by displacing the hydrogen present there towards the lower elevations. This effect takes maximum time to reach the bottom of the vessel. For the bottom recombiner case, since there is very little gas volume present below the box, the hydrogen present there is affected by this process more rapidly as compared to the middle and top recombiner positions. The steam concentration at all trace points rise proportionally in accordance with fall in hydrogen concentration. This is evident from Figure 3.11 and 3.12.

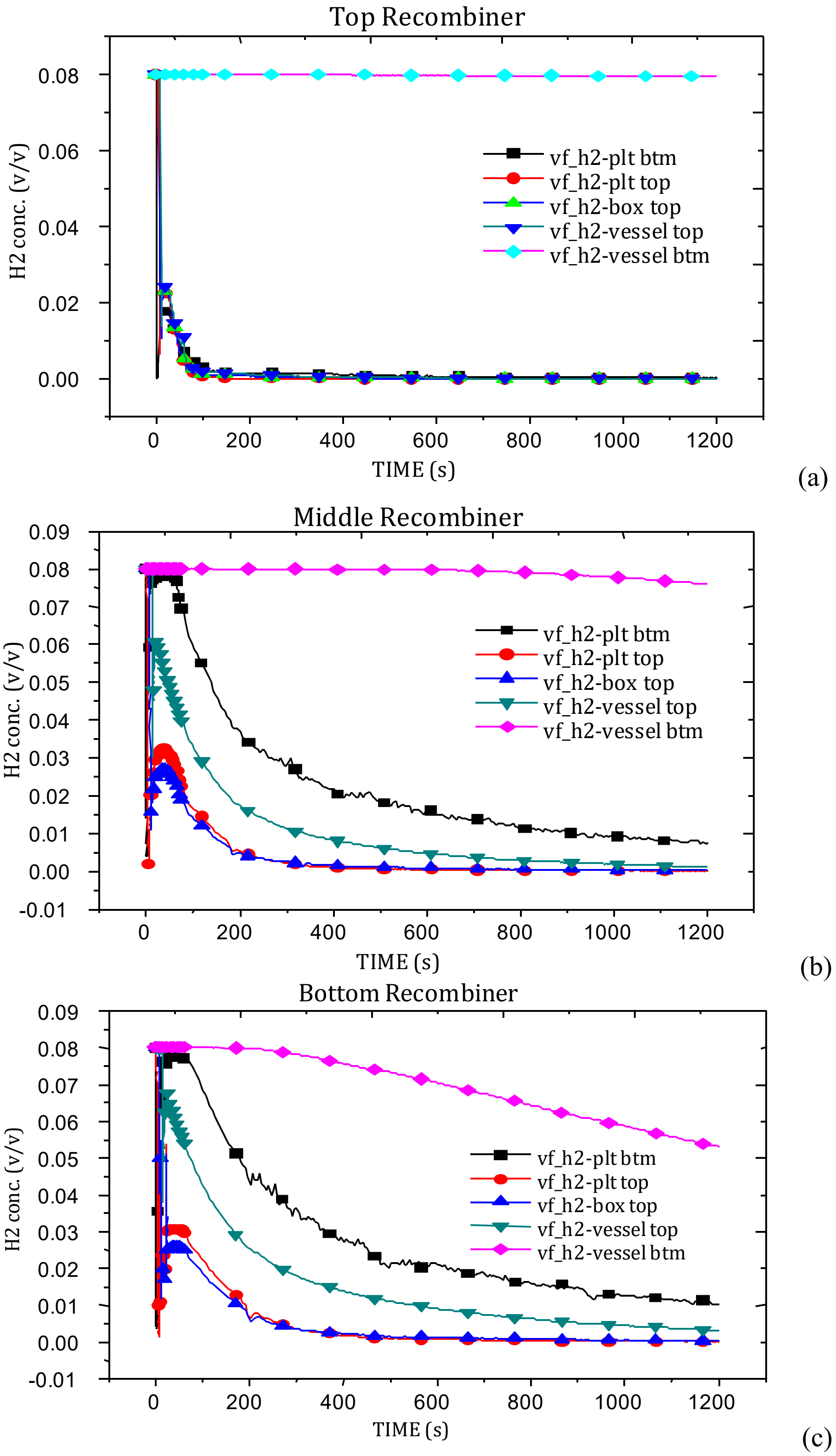

Fig. 3.11: History plots for hydrogen concentration (v/v) at various elevations (a) top, (b) middle and (c) bottom recombiner positions in dry cases

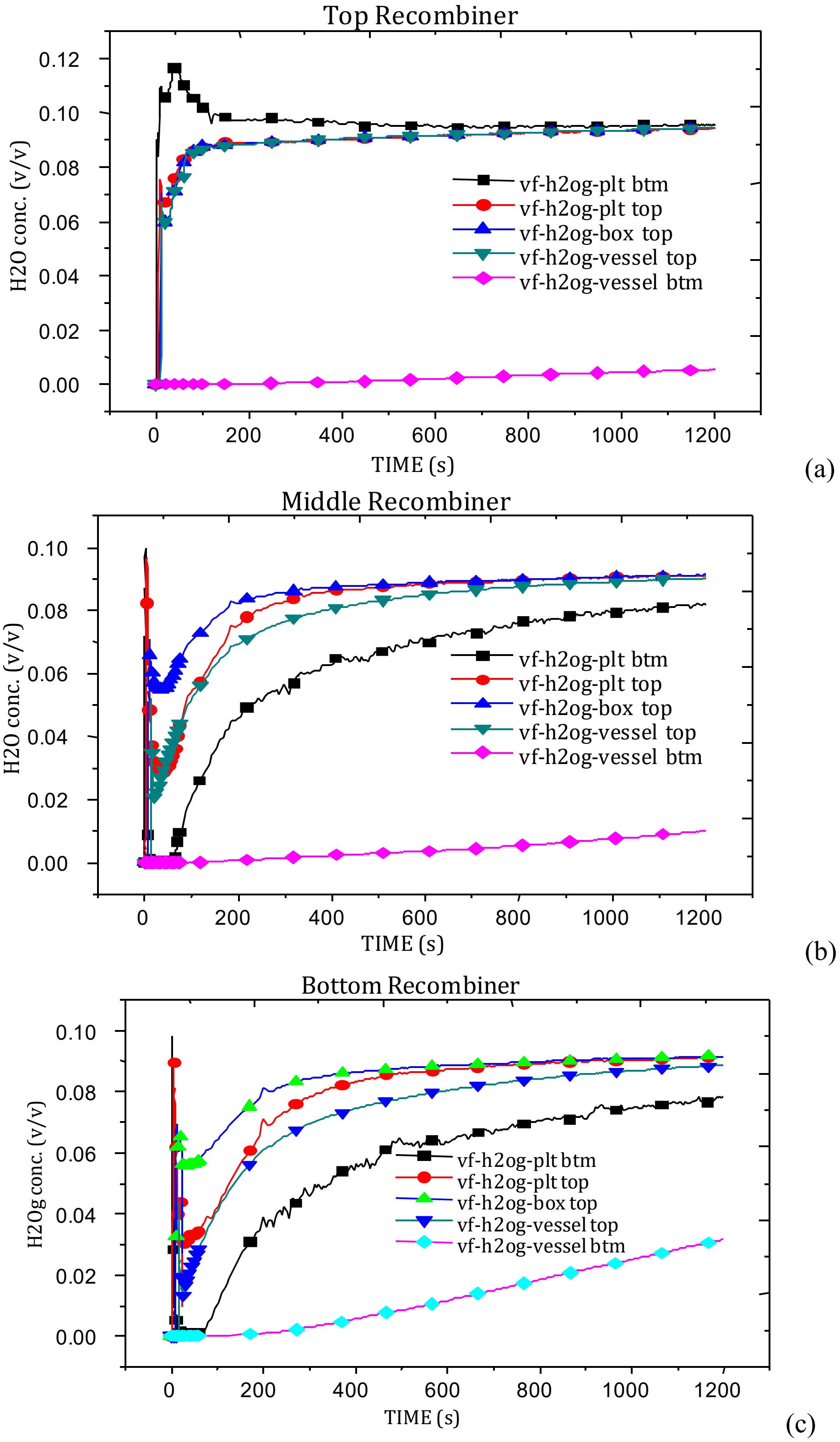

Fig. 3.12: History plots for steam concentration (v/v) at various elevations (a) top, (b) middle and (c) bottom recombiner positions in dry cases

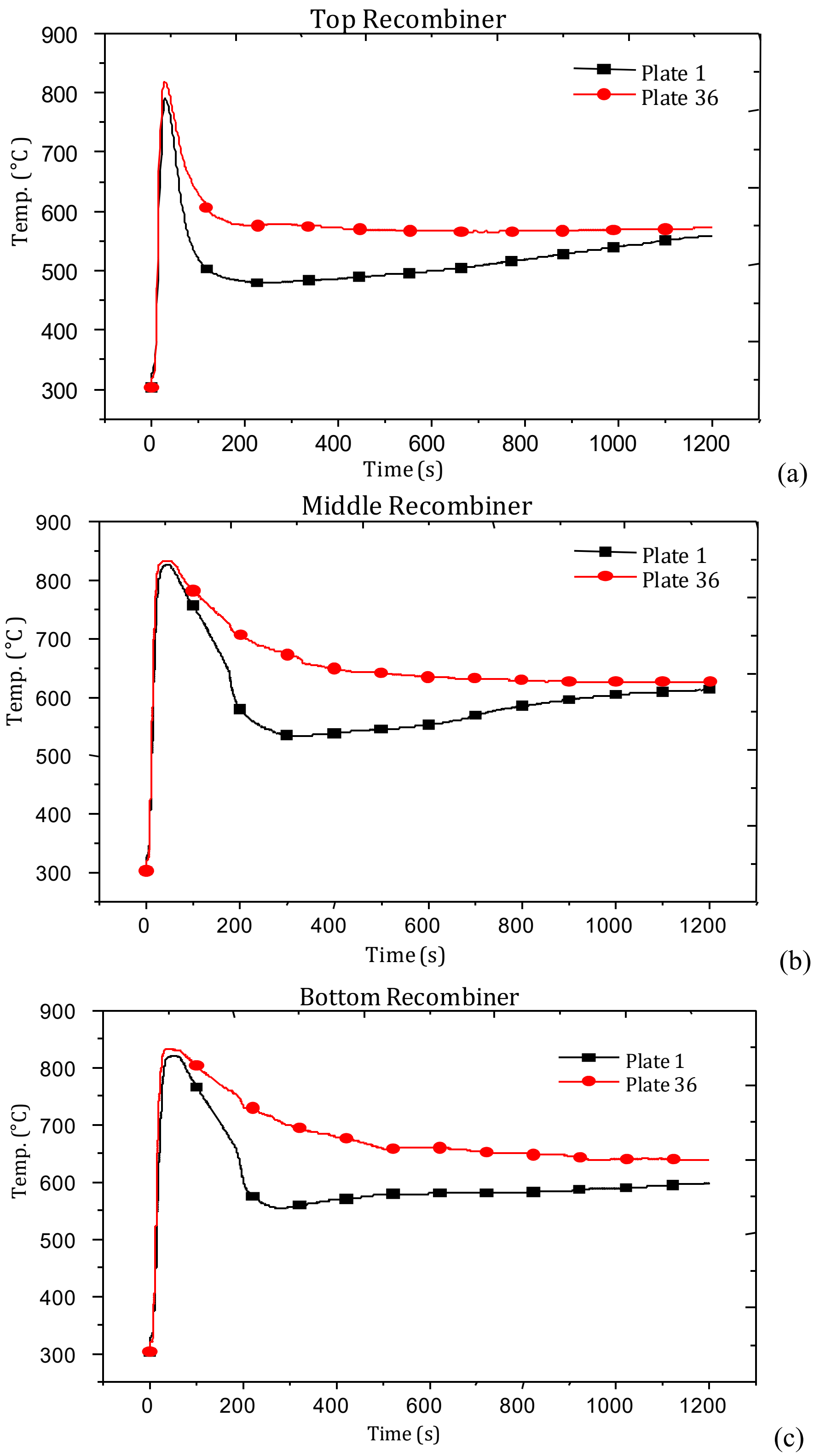

Fig. 3.13: History plots of catalyst temperature at plate centre for plate 1 and plate 36 (a) top, (b) middle and (c) bottom recombiner positions in dry cases

Figure 3.13 shows the time history plot of catalyst plate temperature at the centre of the plate for plate – 1 and plate – 36 for top, middle and bottom recombiner positions. The maximum temperature observed at centre of both plates is around 850K with the trace points placed at same positions on both plates behaving similarly. It is worth noting that the maximum plate temperature is observed at the bottom of the plate as it sees maximum hydrogen concentration. The maximum temperature value at plate bottom for all the cases is around 950 K.

The temperatures of both the plates fall most rapidly for the top recombiner position while the fall is gradual for middle and bottom recombiner positions due to the constant flow of hydrogen into the recombiner box due to buoyancy induced flows driven by hot gases coming out of the recombiner box. The trace points on plate – 36 had at higher temperatures, since the availability of hydrogen is more at center plates than at end plates of the box due to recirculation of the flow while entering into the recombiner box.

3.6.2 Cases for Wet condition with Premixed Hydrogen

Cases with steam laden conditions were analyzed in same manner as the dry cases with respect to the recombiner position, the location of trace points and other parameters to be analyzed in the results. Figures 3.14 and 3.15 show the comparative contour plots for concentration of hydrogen and steam respectively after 1200 seconds for these three cases having different recombiner positions. These figures show that cases where recombiner is located at the bottom inside the facility consumed the maximum hydrogen during 1200s for wet cases as was in the case of dry cases.

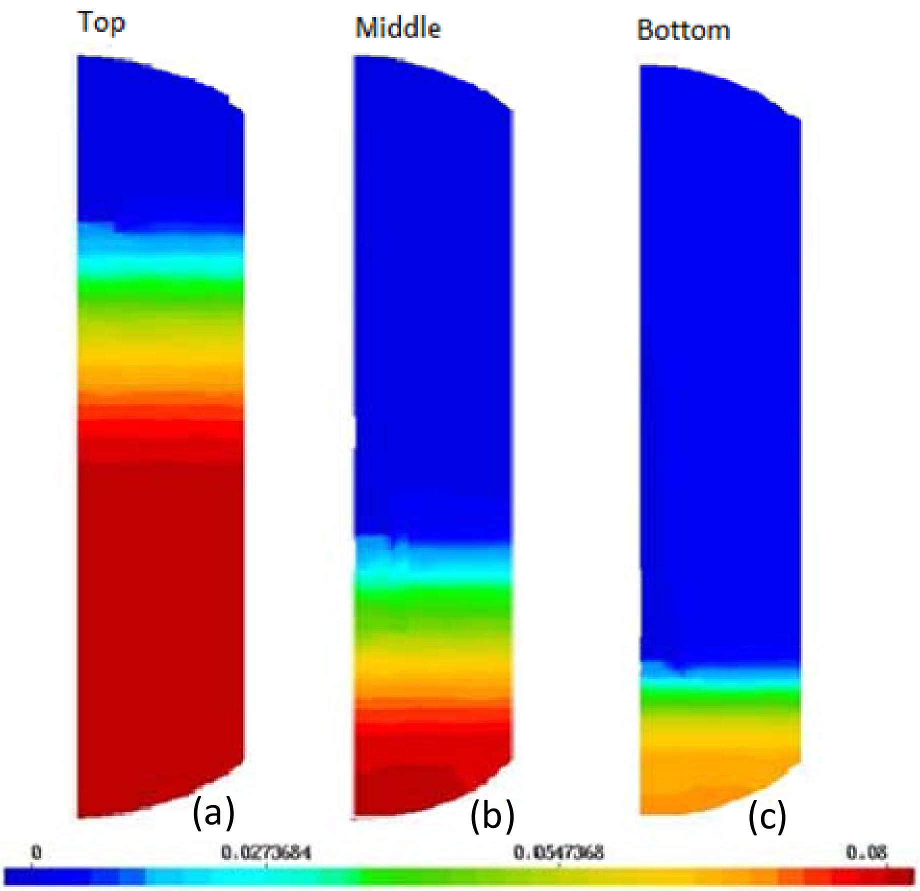

Fig. 3.14: H_2 concentration (v/v) Contours at 1200s on ZX-Symmetry plane (a) top, (b) middle and (c) bottom recombiner positions in wet cases

The maximum concentration of hydrogen in the facility in top and middle positioned recombiner by the end of 1200s is similar to the initial concentration of hydrogen (8% v/v), where as in bottom positioned recombiner, its maximum concentration in the domain reduced to around 6% v/v for these wet cases. This is primarily due to the hot gases coming out of recombiner box moving upwards and promoting better buoyancy driven flows for lower recombiner positions. The effect is not prominent for the case having recombiner box at top location as the hot gases coming out from the box are already near the top of vessel and hence are not able to promote buoyancy driven flows and mixing.

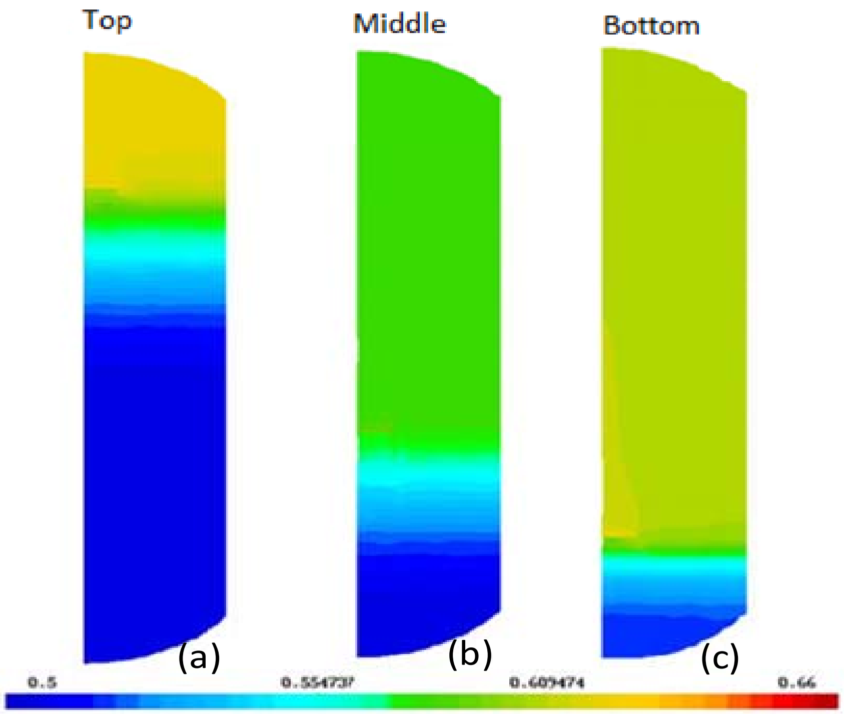

Fig. 3.15: Steam concentration (v/v) Contours at 1200s on ZX-Symmetry plane (a) top, (b) middle and (c) bottom recombiner positions in wet cases

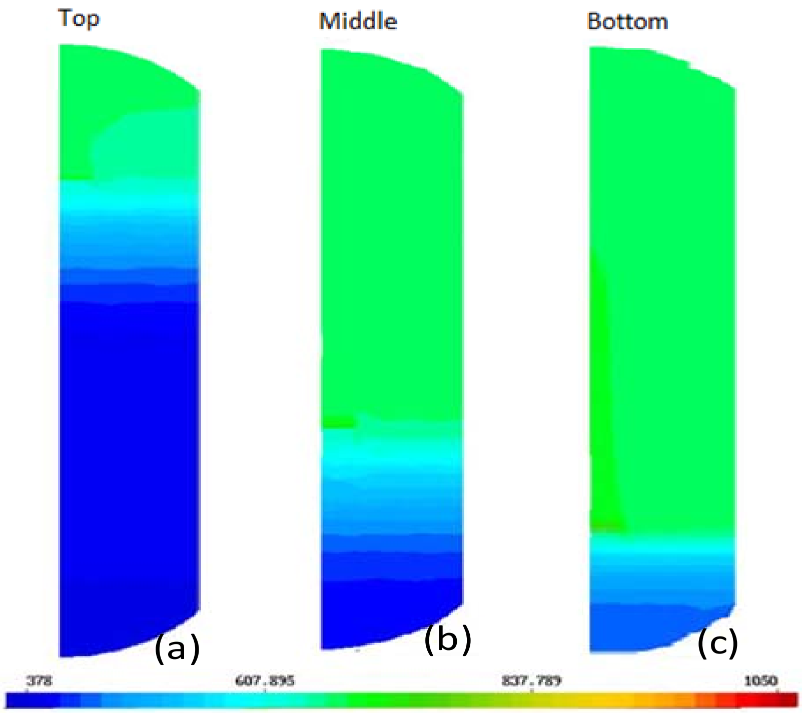

Fig. 3.16: Temperature Contours at 1200s on ZX-Symmetry plane (a) top, (b) middle and (c) bottom recombiner positions in wet cases

Figure 3.16 shows the comparative temperature contour plots for the three different cases at 1200 s. Since the bottom placed recombiner case recombines maximum amount of hydrogen, the temperatures in this case are higher in most part of the domain due to more exothermic heat liberated during the recombination reaction.

Since there was no significant difference between trace point data for five trace points on any particular plane as seen in contour plots, H_2 concentration profiles were plotted on trace point 1 i.e. on the axis of the vessel at various elevations such as bottom of the catalyst plates, top of the plates, top of the recombiner box, top of the vessel and bottom of the vessel. Such plots were made for all three different cases having top, middle and bottom recombiner positions. Figure 3.17 shows hydrogen concentration at various elevations for top, middle and bottom recombiner positions. All these plots reveal that hydrogen concentration falls sharply above the catalyst plates and near the top of recombiner box for all the cases. This is because of the exothermic recombination reaction taking place at the plates resulting in hot gases rising upwards and replacing the hydrogen present there. For all these cases, the hydrogen concentration near the bottom of the catalyst plates falls gradually. This is because of the natural convection flow developed around the recombiner box resulting in fresh supply of hydrogen at the box inlet (bottom) from other locations in the vessel.

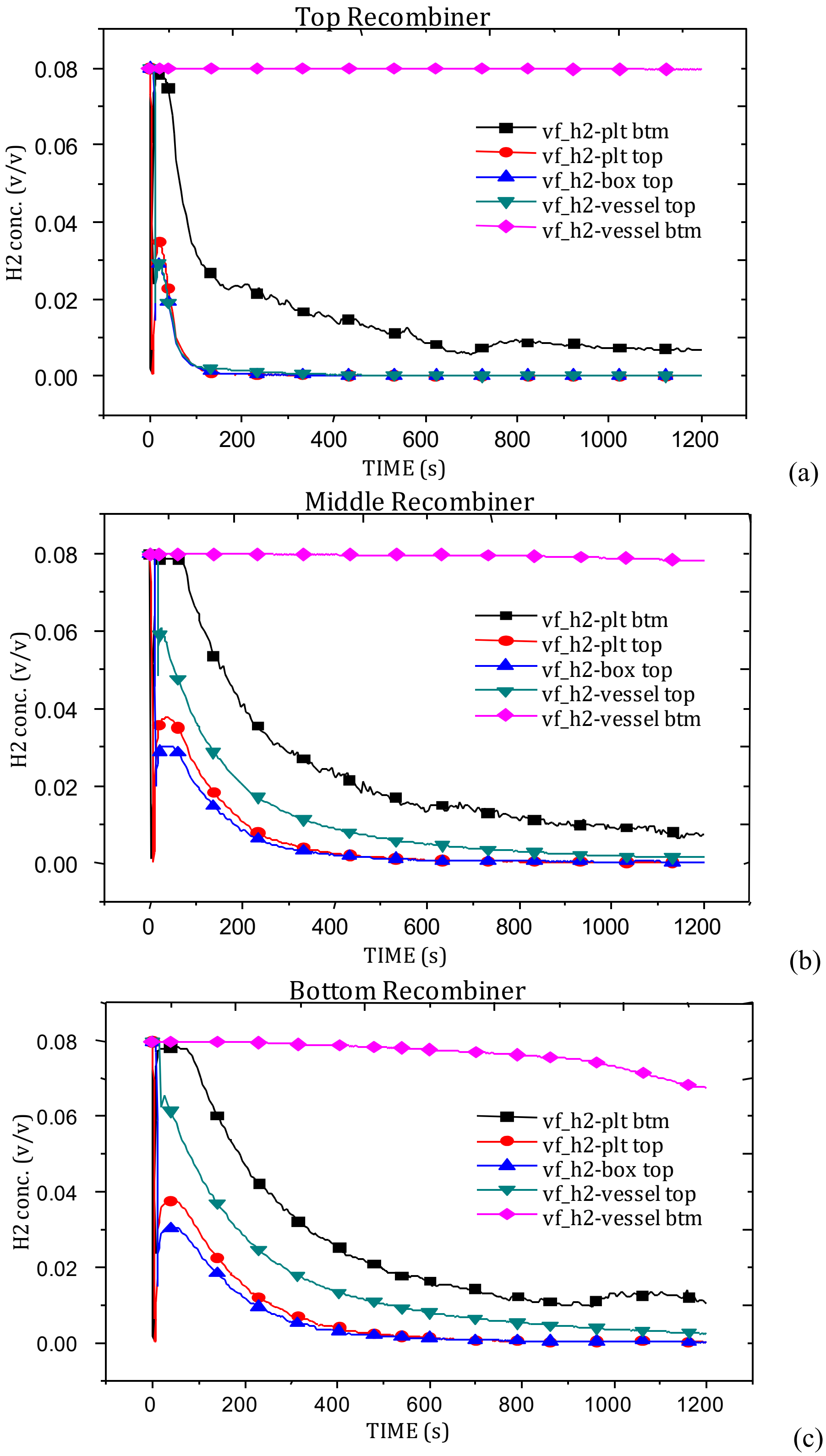

Fig. 3.17: History plots for hydrogen concentration (v/v) 1 at various elevations (a) top, (b) middle and (c) bottom recombiner positions in wet cases

The hydrogen concentration at the top of vessel falls fastest for the top recombiner position to reach zero value at around 500 s. The H_2 concentration for the middle and bottom recombiner positions also fall to almost zero value near the end of simulation. However, the hydrogen present near the bottom of the vessel takes maximum time to decrease and remains almost constant for top and middle recombiner positions where as for the bottom recombiner position it starts to fall at around 300 s and reaches to around 7% (v/v) at the end of simulation.

Figure 3.18 shows the profiles of steam concentration on the central trace points at various elevations such as bottom of the catalyst plates, top of the plates, top of the recombiner box, top of the vessel and bottom of the vessel for top, middle and bottom recombiner positions. Steam concentration rises with respect to time in accordance with the fall of H_2 concentration as seen from these plots.

There is a rapid rise in steam concentration at elevations above catalyst plates and above recombiner box for all three cases. This is because hot product gases of recombination containing steam, rise upwards causing sharp rise in steam concentration at these locations. The steam concentration at trace point near the top of the vessel has a gradual rise as compared to trace points near plate top and box top. This is because the upward moving product gases of recombination have more distance to cover and hence have more volume to disperse during their travel up to the vessel top. At trace point near the bottom of the vessel, the rise in steam concentration is slowest. This is because hot product gases leaving the recombiner box rise upwards and accumulate at the top. This effect takes maximum time to reach the bottom of the vessel. For top recombiner position case, the steam concentration rises steeply at all elevations except near the bottom of the vessel. The rise in steam concentration is relatively gradual for the bottom recombiner position due most prominent natural convection effect when recombiner is placed near the bottom of the vessel. This is because of maximum travel height for hot gases coming out from recombiner. The same causes mixing and homogenization in the vessel hence the steam concentrations rise gradually in this case.

Figure 3.19 shows the time history variation of catalyst plate temperature at the centre of the plate for plate – 1 and plate – 36 for top, middle and bottom recombiner positions. The maximum plate temperature is observed at the bottom of the plate as it sees maximum hydrogen concentration which decreases along the plate height. The maximum temperature value at plate bottom for all the cases is around 1050 K. As the central trace point is located away from the plate bottom, the maximum value observed at plate centre as seen in figure 3.18 is around 870 K.

The temperatures of both the plates fall rapidly for the top recombiner position while the fall is gradual for middle and bottom recombiner positions. This is due to constant hydrogen flow into box due to buoyancy induced flows driven by hot gases coming out of the recombiner box.

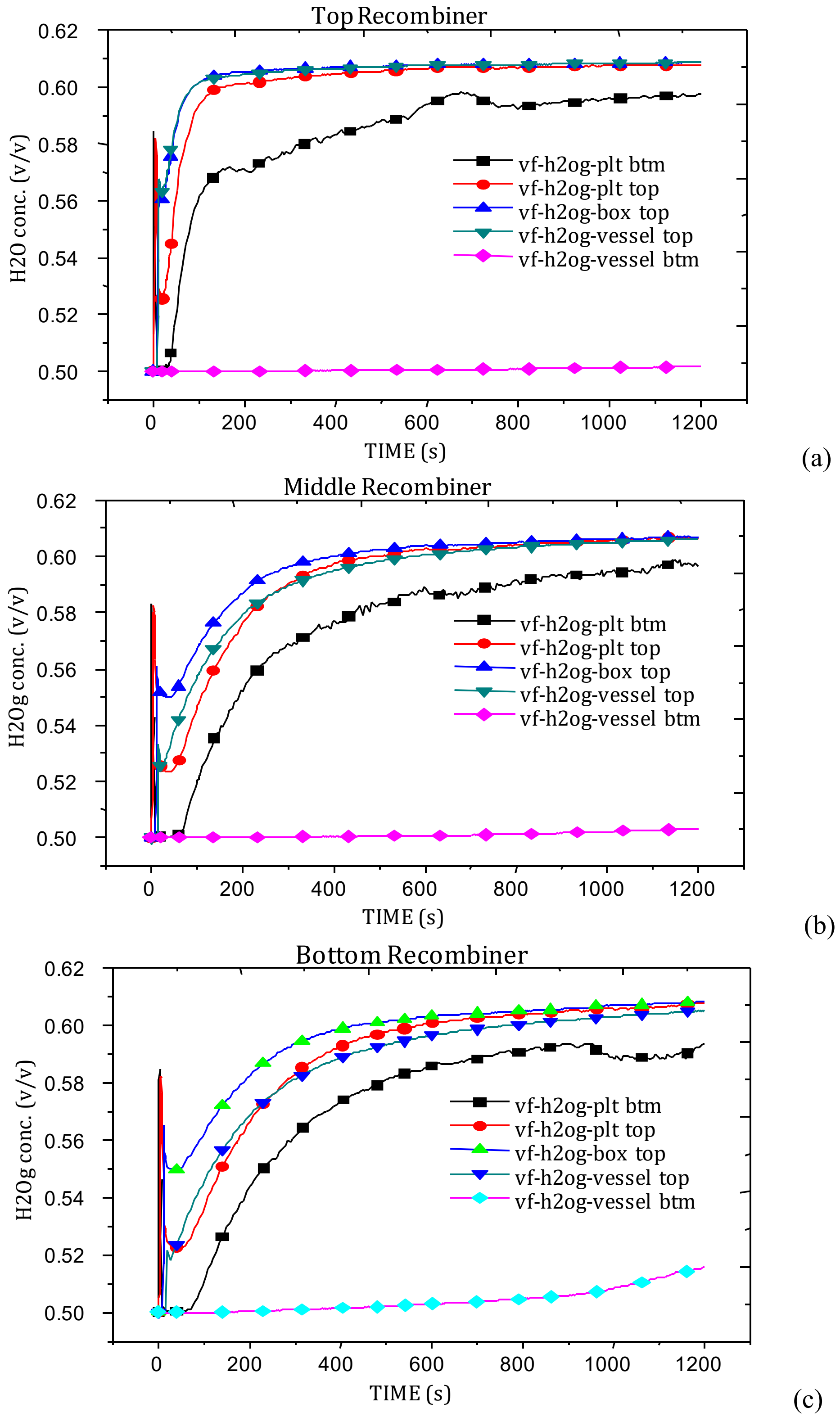

Fig. 3.18: History plots for steam concentration (v/v) at various elevations (a) top, (b) middle and (c) bottom recombiner positions in wet cases

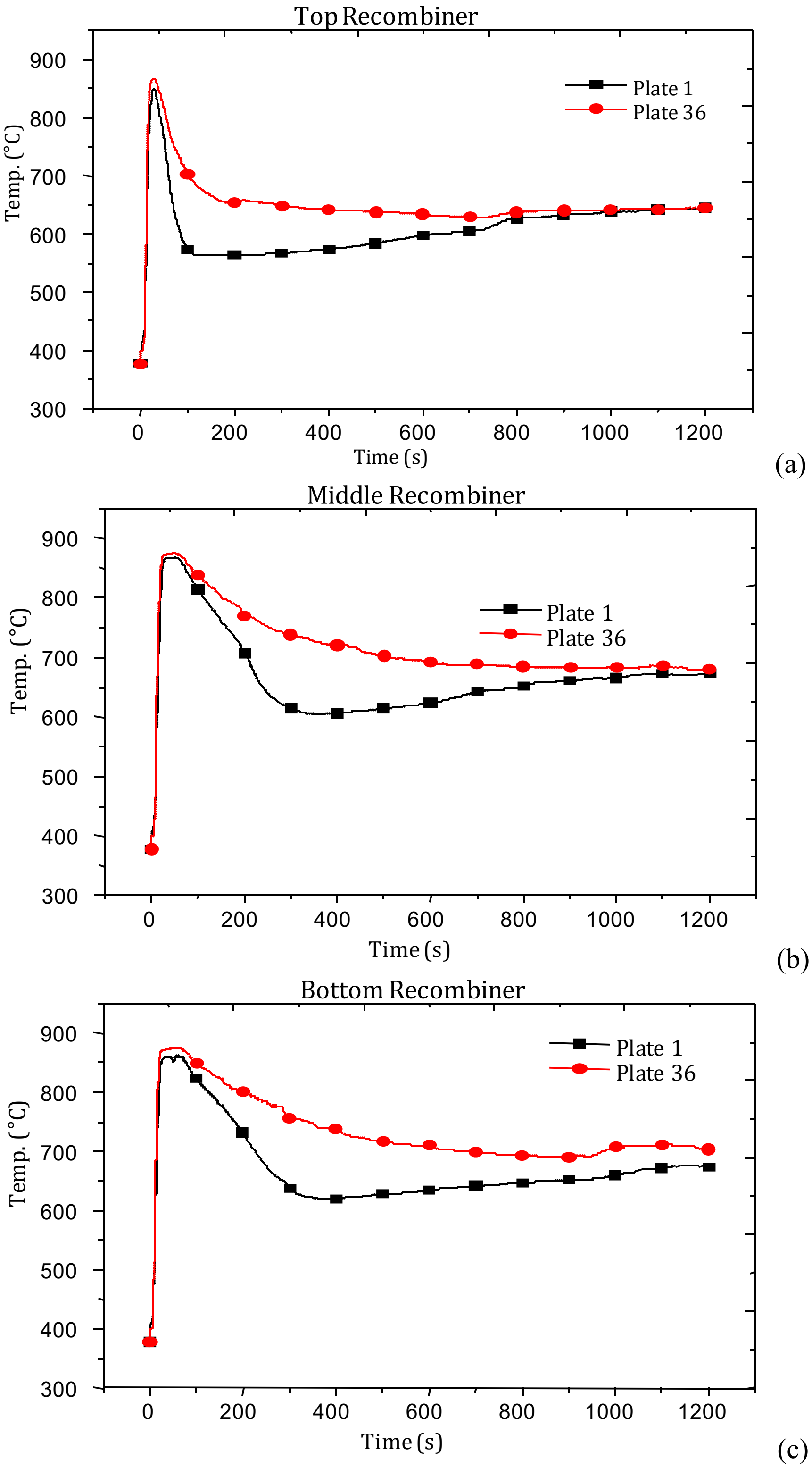

Fig. 3.19: History plots of catalyst temperature at plate centre for plate 1 and plate 36 (a) top, (b) middle and (c) bottom recombiner positions in wet cases

3.7 Conclusions

Numerical model has been developed and validated for PCRD using commercial CFD software FLUIDYN. The model has been validated against experimental data available in open literature. The same is then implemented to investigate the recombiner performance by placing the recombiner box at different locations inside a closed vessel. This is performed for different conditions (i.e. dry and steam) with premixed hydrogen environment. The conclusions of all these studies are as listed below.

- The exothermic recombination on catalyst plates placed in parallel inside PCRD causes natural convection & promotes mixing. The effectiveness of this natural convection to homogenize the gas mixture depends on PCRD location as demonstrated by the parametric study.
- For Dry cases, the temperature observed on catalyst plates in all the cases is similar and it is around 950K. This is because the initial hydrogen concentration is same for all three cases.
- The nature of transient in cases having wet condition is almost similar to the dry cases. In spite of the higher initial temperature in wet cases, the overall temperature rise and performance of catalyst plates does not increase much as compared to the dry cases. This is because of the high heat capacity of steam present in the domain.
- The maximum concentration of hydrogen in the facility in top and middle positioned recombiner during the analysis is close to the initial concentration of hydrogen (8% v/v). Whereas in bottom positioned recombiner, it decreases with time and is around 5% v/v for dry and 6% v/v for wet cases at the end.

- The findings reveal that the bottom positioned recombiner in the vessel consumed maximum hydrogen during the simulation time for dry as well as wet cases. This signifies the fact that effectiveness of recombiner box is more when it is placed near the bottom of the vessel.
- Models for condensation in bulk as well as at the walls have been used in the simulation owing to the steam formed during recombination reaction and also the steam already present in wet cases. However due to the exothermic reaction, the water vapor formed during recombination gets heated up and does not condense in any of the cases presented.
- The investigation establishes that PCRD location plays important role in its effectiveness to curtail hydrogen stratification inside closed geometry.

CHAPTER 4

Experimental Evaluation of Reaction Kinetics

4.1 Introduction

The chemical kinetics of the catalyst deployed used plays significant role in the performance and efficiency of any recombiner. Hence, there is a need to the generate reaction kinetics data for the in-house catalyst developed for our Passive Catalytic Recombiner Devices (PCRDs). The same is required to fine tune the developed CFD model for accurate prediction of the PCRD behavior. This chapter focuses on experimental evaluation of reaction kinetics associated with hydrogen-oxygen recombination on the surface of the developed PCRD catalyst. Catalyst preparation and its characterisation will be discussed. Details of the experimental setup and the methodology used to perform various experiments are also presented in this chapter. Reaction kinetics of the hydrogen recombination reaction on the surface will be evaluated for the SS wire mesh substrate-based Pt - Pd catalyst. Behaviour of catalyst plates stacked in parallel inside PCRD is also aimed to be evaluated.

As mentioned in section 2.2 earlier, different catalyst types have been developed and evaluated in the past for use in our PCRDs. The first type of catalyst device developed in India was based on a chemically coated polyester curtain (Belapurkar, 2000), which would roll down in the event of an accident. However, due to the low melting temperature of polyester cloth, this device could not perform beyond 150°C. One of the important developments in this field is the catalyst (Sanap et al., 2011) having Pt + Pd simultaneously deposited over stainless steel wire gauze substrate.

Similarly, a novel breed of catalysts based on cordierite supported Pt nano-particles has been prepared by (Sanap et al., 2014) using chemical reduction route. From the different catalysts developed, the catalyst based on stainless steel wire gauze substrate has been selected for characterisation and use in PCRD based on the comparative property evaluation. Hence the same has been used for carrying out experiments for evaluation of reaction kinetics related to H_2-O_2 recombination taking place on its surface.

4.2 Catalyst Preparation

The Pt - Pd catalyst on stainless steel wire gauze substrate has been prepared by electroless deposition method Sanap (2011). This method involves chemical deposition of noble metals (Platinum and Palladium) over the stainless-steel wire gauze in presence of a reducing agent. Used SS-304 wire gauze has 0.125 mm wire diameter and 80 mesh size. The precursors used for Pt and Pd are Chloroplatinic acid (39.8% Pt) and palladium chloride (59.96% Pd). The reducing agent used is formaldehyde (Thomas Baker, 37-41%). The coating process employed is based on the following reactions with anodic oxidation of formaldehyde and cathodic reduction of noble metal taking place at the metal support surface, which has been pre-activated by acid etching (Barker, 1981).

$$HCHO + H_2O \rightarrow HCOOH + 2H^+ + 2e^-; E = 0.057\ V \qquad (4.1)$$

$$Pd^{2+} \text{ or } Pt^{2+} + 2e^- \rightarrow Pd(0) \text{ or } Pt(0)\ ; E = 0.915\ V\ (Pd),\ 0.726\ V\ (Pt) \qquad (4.2)$$

Though reduction of noble metal is reported to take place at enhanced rate at higher pH, it also requires presence of complexing agents like EDTA to prevent precipitation of metal in solution itself. Considering these effects of pH, the electroless deposition is carried out at pH 2-4. The rate of coating is found to be moderate but it result in amorphous black noble metal coating with good adherence. The method of preparation of catalysts is described in detail Sanap (2011).

4.3 Catalyst Characterization

The final catalyst used for deployment in PCRD is shown in Figure 4.1. Based on its characteristics, the same can be summarised as 80 mesh SS wire gauze based catalyst having noble metal loading of 0.8 wt% with a Pt-Pd ratio of 2:1 and having rough spherical particles of size 0.1 - 1 micron.

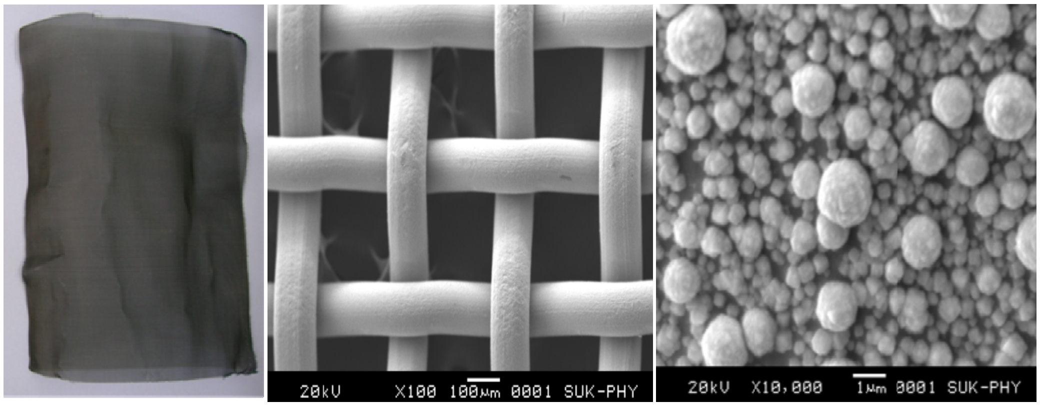

(a) (b) (c)

Fig. 4.1: Pt-Pd / Stainless steel wire gauze catalyst; (a) Optical photograph, Scanning electron micrographs at (b) 100x and (c) 10000x magnification

Powder X-ray Diffraction has been used to assess the crystalline phase purity of deposited noble metals over the wire gauze surface. The XRD patterns were recorded with Philips analytical instrument with Ni filtered Cu-K-α radiation in the scanning range of 10-70° two theta value. Surface morphology and particle size of deposited noble metal nano-particles has been studied using Scanning Electron Microscopy (JEOLJSM-6360).

4.3.1 X-ray Diffraction

Figure 4.2 shows the XRD pattern of wire gauze as well as the catalyst. The XRD pattern of the catalyst when compared to the SS wire gauze have additional peaks at ~40°, ~46° and ~67°, 2Θ values. These peaks correspond to Platinum (JCPDS No.04-0802) and palladium (JCPDS 46-1043). The average crystallite size of noble metal particles determined by Scherrer equation using 40° peak and it is found to be around 21 nm.

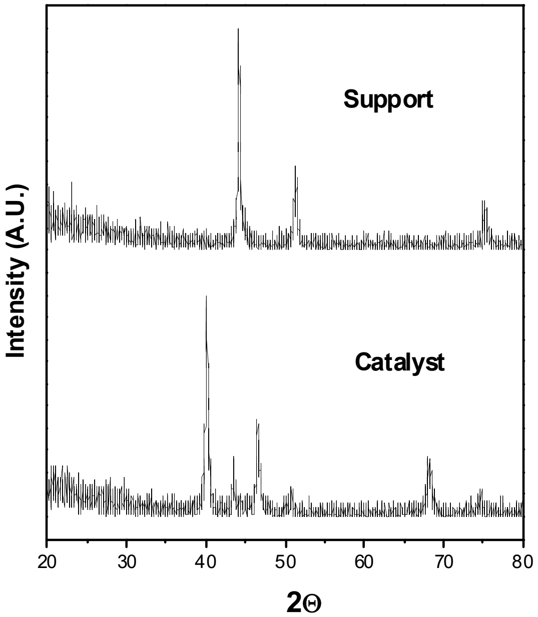

Fig. 4.2: XRD pattern of SS wire gauze support and Pt-Pt catalyst

4.3.2 Scanning Electron Microscopy

Scanning electron microscopy is used to evaluate the effect of the deposition on morphology of the wire gauze surface along with morphological study of Pt-Pd nano-particles over the wire gauze surface. Figure 4.3 (a) and 4.3 (b) shows the SEM images of pristine wire gauze and HCl etched wire gauze. The pristine wire gauze exhibits smooth surface and HCl etched wire gauze also shows similar morphology. The surface morphology of the catalyst sample is shown in Figure 4.3 (c). It shows near spherical agglomerates with size ranging from few tens of nm to 1 micron.

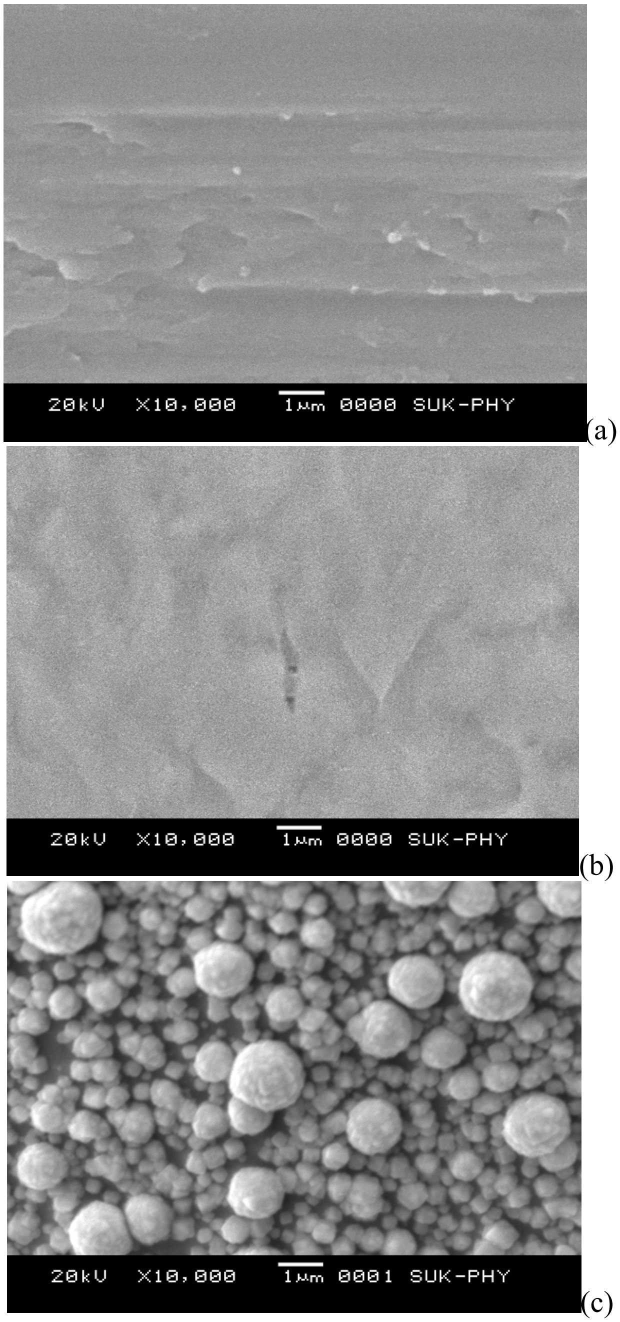

Fig. 4.3: Scanning electron micrographs of (a) stainless steel Wire gauze, (b) stainless steel Wire gauze after HCl etching and (c) Pt-Pd catalyst over wire gauze

4.4 Catalytic Activity Evaluation

For generation of kinetics data for the prepared catalyst, the H_2 and O_2 recombination reaction is performed under static air condition at room temperature in a 40 L stainless steel reactor as shown in Figure 4.4. Hydrogen is supplied through stainless steel tubing connected to a hydrogen cylinder having a pressure regulating valve mounted on it. This line feeds hydrogen to a 250 ml injector, having needle type isolation valves at its inlet and outlet. The injector can be pressurized up to 1200 kPa and hence can be used to inject up to 6% v/v hydrogen into the reactor vessel in a single shot when isolated from the hydrogen cylinder. The catalyst is hung inside the cylindrical reactor through a hook connected to the top flanged cover. The hydrogen concentration inside reactor is monitored using thermal conductivity detector (TCD) based online hydrogen monitor. The reaction being exothermic, the temperature rise on the catalyst surface is recorded with the help of K-type thermocouples placed on the catalyst.

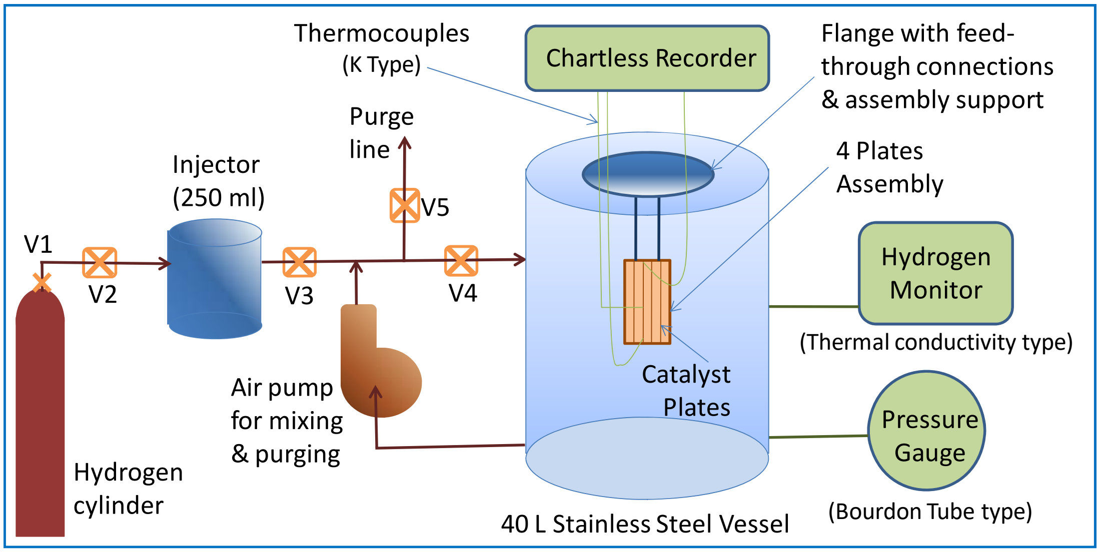

Fig. 4.4: Schematic of Experimental Setup for study of kinetics

Before the beginning of each experiment, the reactor vessel is sufficiently flushed with fresh air with the help of an air pump. After this, fixed volume injector is flushed with hydrogen to make sure that pure hydrogen is present inside it. The injector is then pressurized with pure hydrogen and isolated from the cylinder. During the start of each experiment, the cylinder is initially pressurized with air to 10.13 kPa above atmosphere and then with hydrogen to a pre-calculated value above the initial pressure to attain the desired initial molar hydrogen concentration for various experiments (~0.8-4.5%). The change in concentration of hydrogen and the catalyst surface temperature are recorded as functions of time. After the completion of each experiment, the residual hydrogen and water vapor present inside the reactor vessel are flushed out by operating the air pump.

The rate of H_2 and O_2 recombination reaction has been found to depend on various factors like initial hydrogen concentration, catalyst geometric area and the temperature of the catalyst surface. All these parameters are also found to be interlinked. The recombination reaction of hydrogen and oxygen is:

$$H_2 + \frac{1}{2} O_2 \leftrightarrow H_2O \quad \Delta H_0 = -242 \text{ kJ/mol} \tag{4.3}$$

The rate of the reaction at any instant in time can be described by Eq. (4.4).

$$Rate = -\frac{d[H_2]}{dt} = k_T.[H_2]^x.[O_2]^y \tag{4.4}$$

where, k_T is the rate constant at temperature T (Kelvin) and x and y are the orders of the reaction with respect to H_2 and O_2 respectively. The expected operating range of PCRD involves hydrogen lean gas mixtures (< ~8% v/v of hydrogen). For such gas compositions, the oxygen becomes an excess reactant and the rate of reaction gets dictated only by the concentration of hydrogen. Hence, for the operating range of the PCRD, the recombination process is essentially a first order reaction. This has also been corroborated by various other researchers such as Morfin et al. (2004), Acres (1966), Kim et al. (2001). Additionally, it has been reported that hydrogen has a high adsorption probability even on the catalyst surface preoccupied by adsorbed oxygen. Such scenarios are more likely in case of PCRDs, as the catalyst generally has long exposure to oxygen from ambient air before encountering hydrogen during postulated accidents. For such scenarios also, the order of reaction has been reported to be one Warnatz et al. (1994) and Hellsing et al. (1991). Hence for estimating the kinetics of the recombination reaction in the PCRD, the reaction is assumed to be first order for hydrogen concentration and independent of oxygen concentration. Therefore, the value of ‘x’ in Eq. (4.4) is taken as 1 and value of ‘y’ is taken as 0 to arrive at Eq. (4.5). For the performed experiments also, the range of initial hydrogen concentration in the hydrogen-air mixture of the experimental reactor is around 4% v/v and consequently, oxygen still acts as an excess reactant justifying the assumption of a first order reaction kinetics.

$$-\frac{d[H_2]}{dt} = k_T \, . \, [H_2] \qquad (4.5)$$

This equation is rearranged to get Eq. (4.6)

$$k_T = \frac{-1}{[H_2]} . \frac{d[H_2]}{dt} \qquad (4.6)$$

For a constant value of k_T, applicable for a fixed temperature, the reaction rate is given as per Eq. (4.5). But for the present case, since the reaction is highly exothermic, the catalyst temperature is expected to vary widely leading to variation of the rate constant k_T. Hence there is a need to represent k_T as a function of temperature. As per Arrhenius law, rate constant k_T is written as a temperature function given by Eq. (4.7):

$$k_T = Ae^{-E/RT} \tag{4.7}$$

where, A is the pre-exponential factor, E is the activation energy, R is the universal gas constant and T is the temperature. Eq. (4.7) can be modified on a logarithmic scale to get the equation of a straight line:

$$\ln(k_T) = \ln A + \frac{-E}{RT} \tag{4.8}$$

During the experiments, change in concentration of hydrogen and the catalyst surface temperature are recorded as functions of time. Data points pertaining to variation of hydrogen concentration and temperature with time are generated from a series of experiments involving different initial hydrogen concentrations. The derivative plot of $[H_2]$ vs. time provides for $d[H_2]/dt$ data for time 't', at temperature 'T'. Substituting the values of $[H_2]$ and $d[H_2]/dt$ in Eq. (4.6), k_T is calculated for the respective temperature T.

For different experiments with initial hydrogen concentrations ranging from 2.5 to 4 % in air, Figure 4.5 depicts the obtained data which is used for reaction kinetics and activation energy calculations. The scatter plots in Figure 4.5 (a) represents change in hydrogen concentration in mol/l and Figure 4.5 (b) depicts the change in temperature with respect to time. The derivative plot $-d[H_2]/dt$ in mol/l/s corresponding to rate of reaction, with time t is depicted in Figure 4.5 (c).

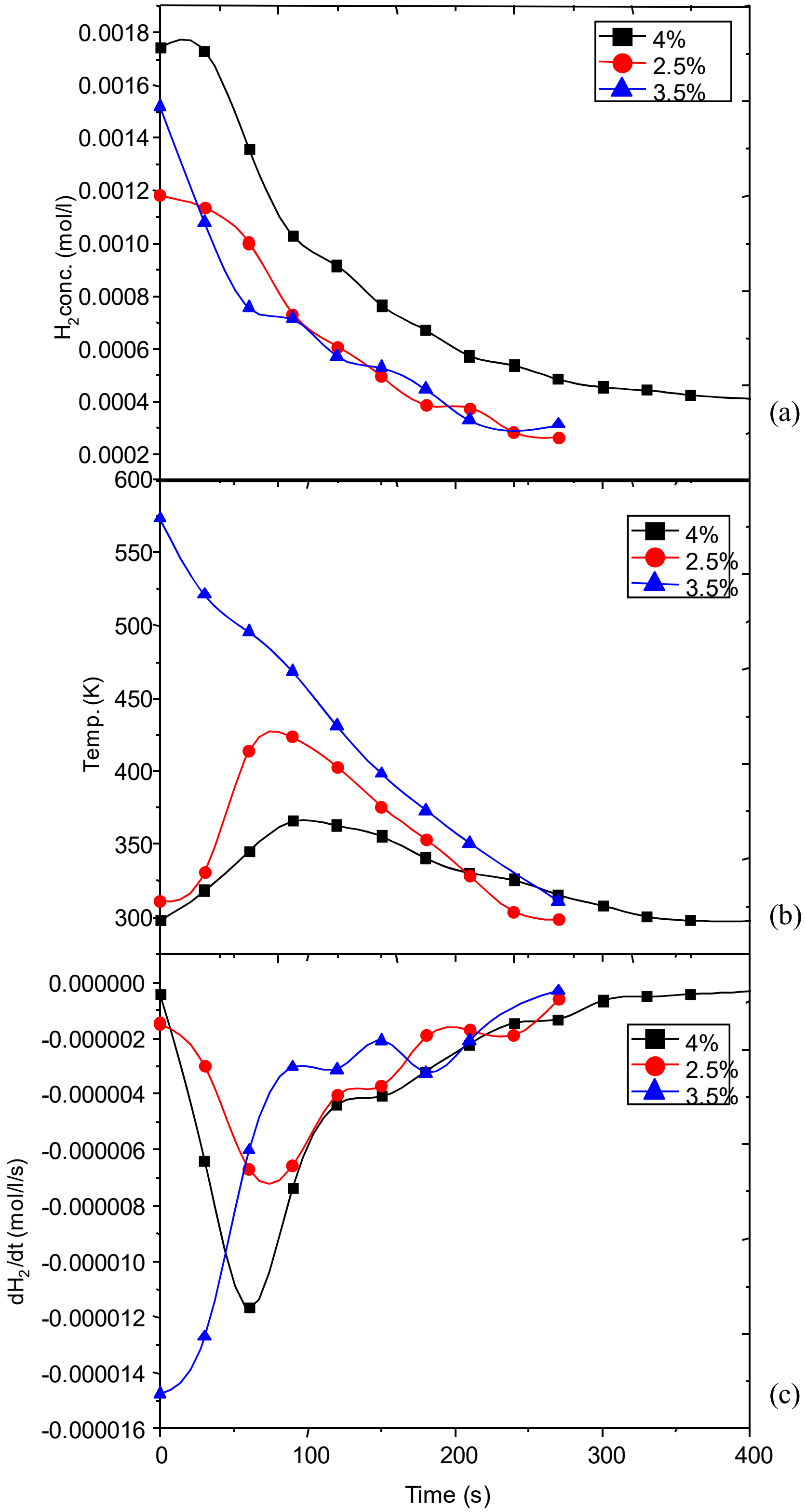

Fig. 4.5: (a) Hydrogen concentration, (b) Catalyst temperature and (c) Derivative plot of $[H_2]$ with respect to time

One aspect observed is that the rate of reaction is strongly dependent on initial concentration of hydrogen. As hydrogen is injected into the reactor, it starts spontaneously reacting with oxygen on the catalyst surface. The exothermicity of the reaction leads to a sharp rise in temperature on the catalyst surface, which in turn enhances the reaction rate further. During the complete process the gas mixture and reactor wall temperature are found to remain close to ambient conditions. The catalyst temperature also comes down fast as the reaction rate subsides with decreasing hydrogen concentration in the reactor vessel. This clearly indicates the usefulness of stainless steel wire gauze support in terms of effective dissipation of generated reaction heat.

From Eq. (4.8) it can be seen that, when ln (k_T) values are plotted against 1/T values, the slope of the straight line can be used to get the value of activation energy while the intercept can be used to obtain the pre exponential factor. ln (k_T) vs 1/T data obtained from various set of experiments is plotted in Figure 4.6. The activation energy obtained from the above experiments is found be in the range of 18.1 kJ/mol, while the intercept signifying pre-exponential factor is 2.14.

This value of activation energy for the recombination reaction taking place on the catalyst surface is significantly lower than the activation energy for the gas phase oxidation process which is in the range of 109 -150 kJ/mol Seshadri et al. (1994). This lower activation energy barrier highlights the ability of the catalyst to initiate and promote the hydrogen-oxygen recombination even at room temperatures.

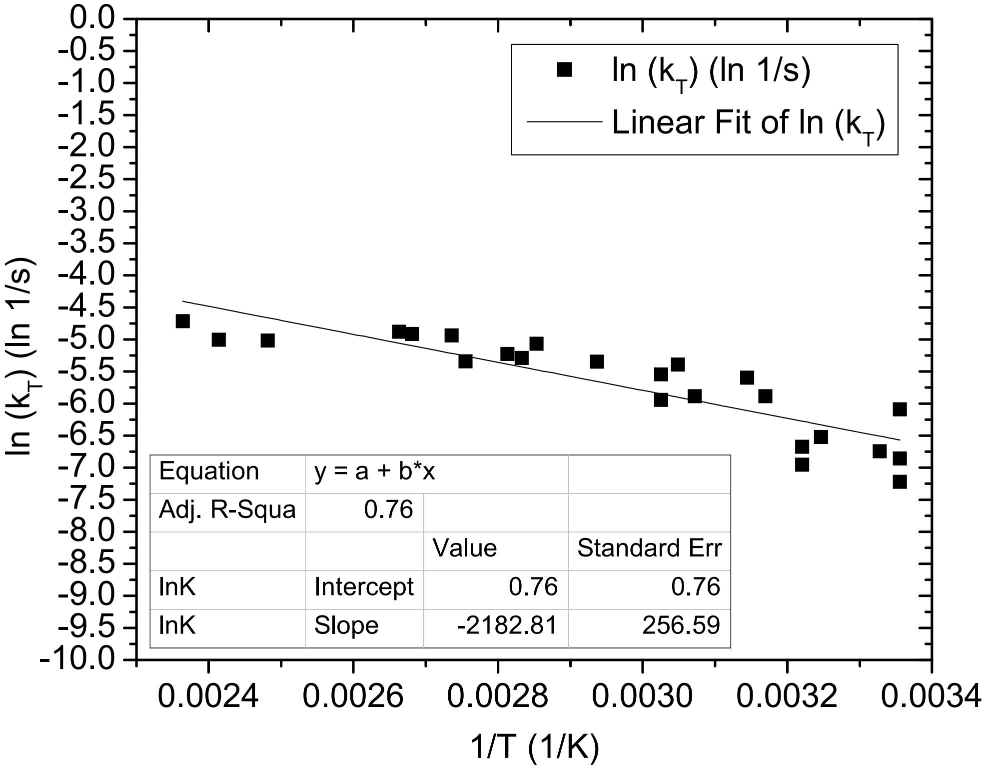

Equation	y = a + b*x		
Adj. R-Squa	0.76		
		Value	Standard Err
lnK	Intercept	0.76	0.76
lnK	Slope	-2182.81	256.59

Fig. 4.6: ln (k_T) vs 1/T plot for the single plate of catalyst

Two prominent approaches have been reported in literature to explain the nature of heterogeneous reaction occurring at the catalyst surface. The first mechanism as discussed by Clyne et al. (1961) involves reaction between adsorbed oxygen and the gaseous hydrogen in two steps based on $[O] + H_2 \leftrightarrow OH + H$ and $H_2 + OH \leftrightarrow H_2O + H$. For this type of mechanism, the activation energy requirement is around 25 kJ/mol. Since this value exceeds the activation energy data obtained from our experiments by large margin, this approach is not suitable to explain the recombination reaction occurring on our catalyst. Compared with this, the second mechanism, Clyne et al. (1961), involves reaction of adsorbed oxygen with the dissociated hydrogen atom. This mechanism exhibits activation energy for various reaction steps in the range of 11.5 and 17.5 kJ/mol. As the value obtained during our experiments is quite close to this value, it implies that dissociative adsorption of both hydrogen and oxygen, followed by combination of the adsorbed species on the catalysts surface is a suitable explanation of the recombination reaction occurring on the developed catalyst.

4.5 Study of Channel effect on the kinetics

After evaluation of the reaction kinetics for the catalyst used in PCRD, the next step is to investigate the behaviour of the PCRD as a whole. The same is important to understand the effect of parallel channels on the kinetics of the recombination reaction. Here it is worth noting that the final surface reaction taking place on the catalyst surface is one of the many steps preceding and succeeding the same. The phenomena of hydrogen and oxygen transport towards the catalyst surface and the product water vapour away from the catalyst surface by the virtue of diffusion and convection is different for a bare catalyst as compared to a stack of parallel channels of these catalyst plates. The estimation of overall reaction kinetics for the device as a whole has been approximated by the single step Arrhenius equation.

For generation of reaction kinetics data of parallel channels of catalyst plates, the set up shown in Figure 4.4 has been modified. In place of the hook for hanging a single catalyst plate, new catalyst holder is designed and fabricated to accommodate four catalyst plates of the dimensions 50 mm x 160 mm. The schematic of stainless-steel assembly made for the same is shown in Figure 4.7. It has four parallel slots with a pitch of 10 mm to accommodate SS wire gauze catalyst plates. The plates are inserted from the top and rest on the bottom plate in respective slots. Arrangement is provided to attach the thermocouples for temperature monitoring of the catalyst surface. The assembly loaded with four plates and thermocouples attached on them is shown in

Figure 4.8. The top flange of the reactor is also changed to have feed through connections for four thermocouples. These four thermocouples are used for recording the temperature at different heights of one of the two central catalyst plates.

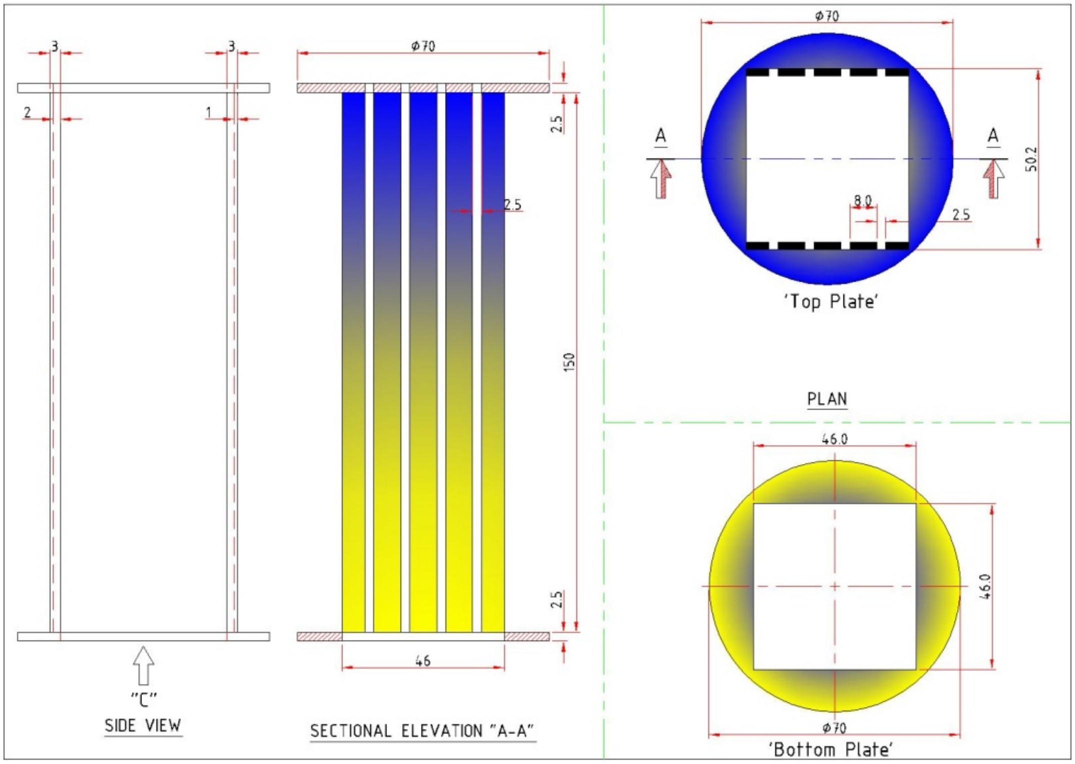

Fig. 4.7: Schematic of Assembly for supporting four catalyst plates

Fig. 4.8: Photograph of the Four Plate assembly with thermocouples

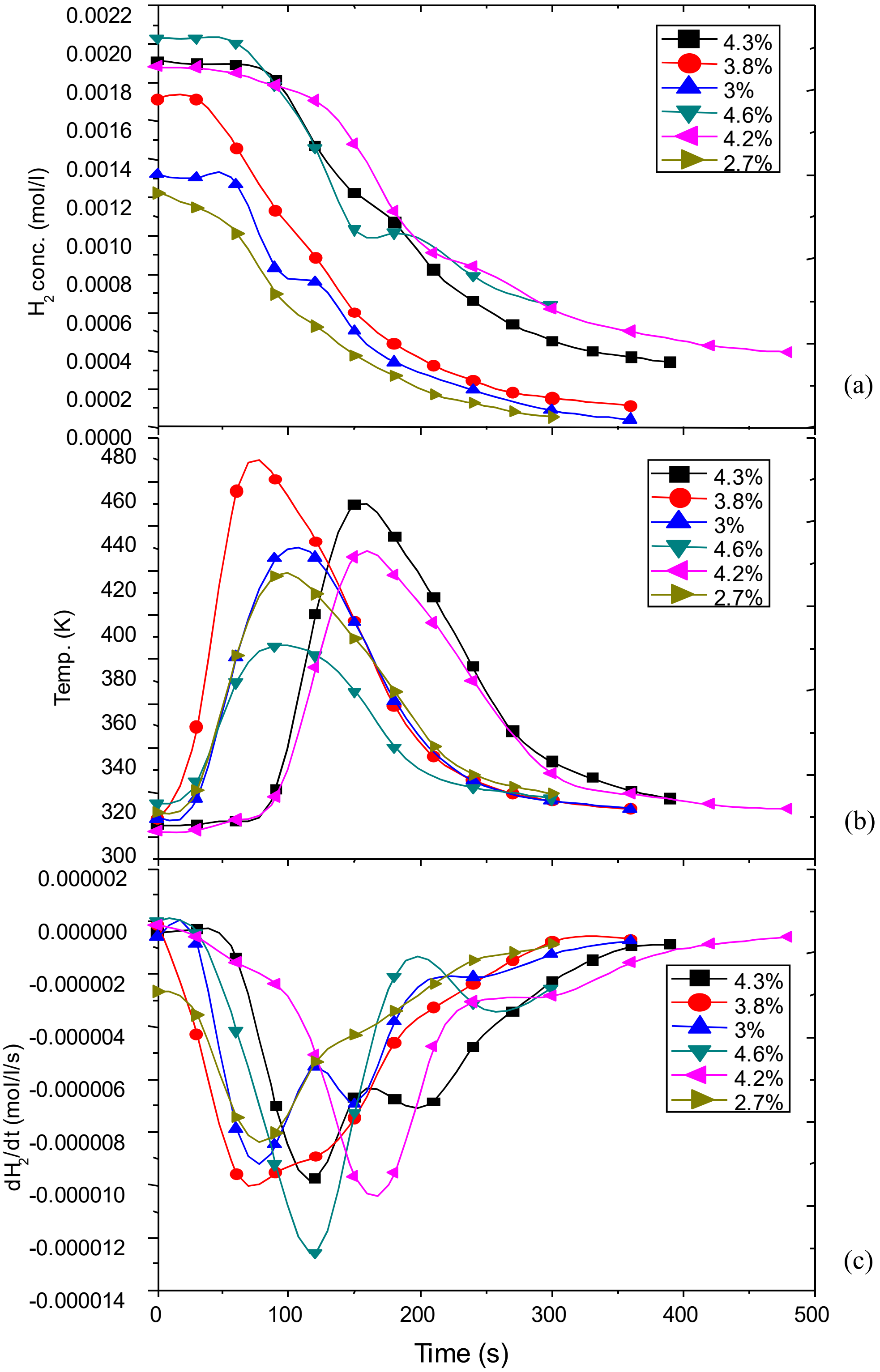

Fig. 4.9: (a) Hydrogen concentration, (b) Catalyst temperature and (c) Derivative plot of $[H_2]$ with respect to time for four plate arrangement

Similar to single plate experiments, data points have been generated for a series of experiments involving different initial hydrogen concentrations. Figure 4.9 shows catalytic activity data obtained for catalyst for initial hydrogen concentration ranging from around 2.0 to 4.5 % in air. The temperatures at different heights of central channel were averaged suitably to get the temperature value resulting from the recombination reaction. The derivative plot of [H_2] vs. time provides for d[H_2]/dt data for time 't' and at temperature 'T'. Substituting the values of [H_2] and d[H_2]/dt in Eq. (4.6), k_T is calculated for the respective temperature T. ln (k_T) vs. 1/T values obtained from various set of experiments are plotted in Figure 4.10. The activation energy for the parallel channels arrangement obtained from the above experiments is found be in the range 18.7 kJ/mol, while the intercept signifying pre-exponential factor is 2.2.

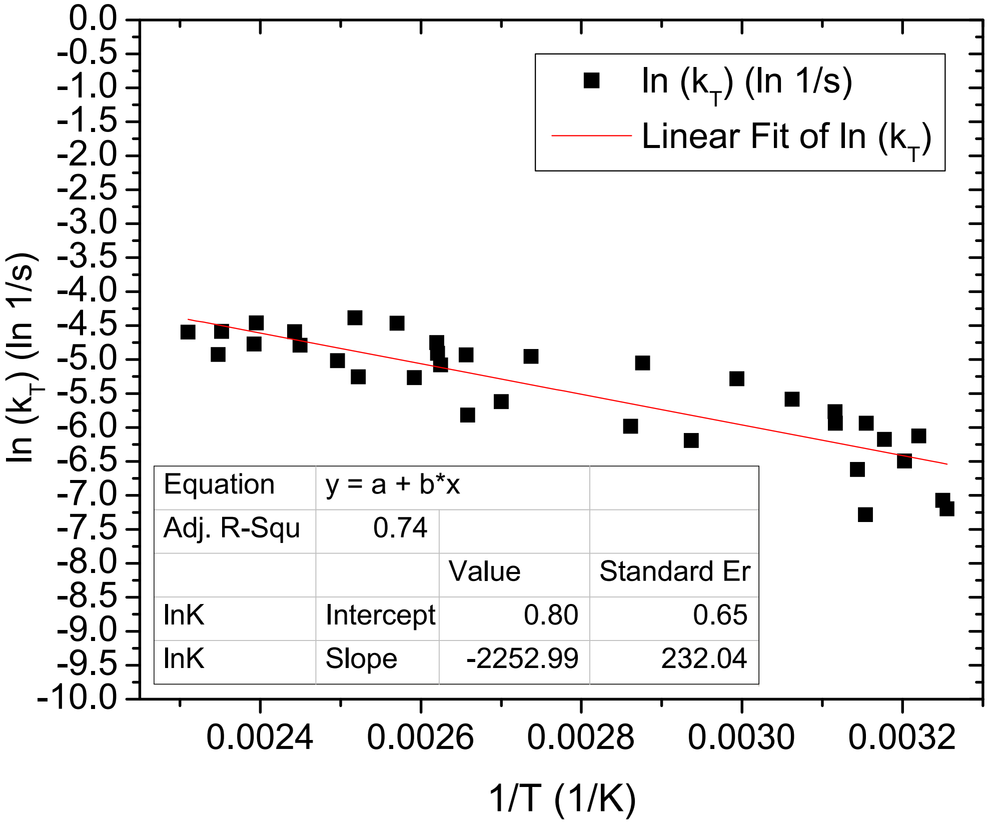

Fig. 4.10: ln (k_T) vs 1/T plot for parallel channels arrangement between four plates

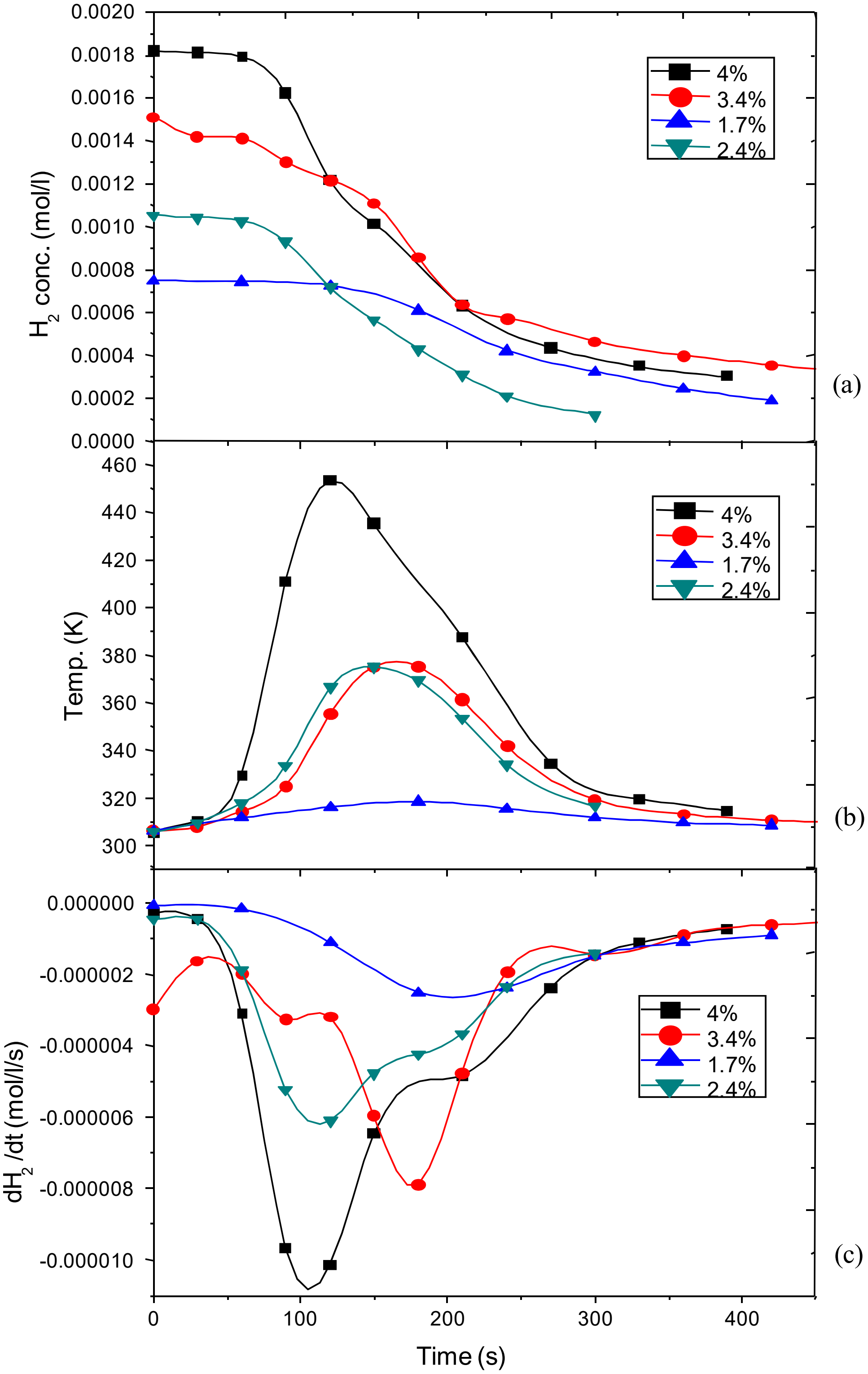

Fig. 4.11: (a) Hydrogen concentration, (b) Catalyst temperature and (c) Derivative plot of [H_2] with respect to time for four plates with side plates blocked from outside

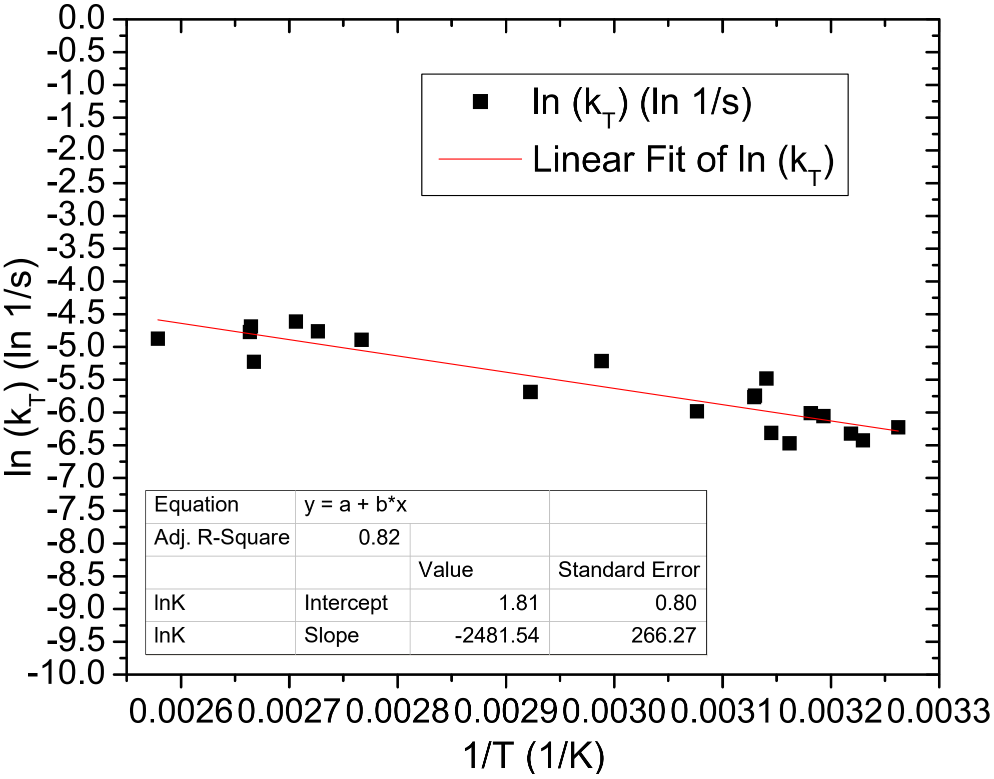

Equation	y = a + b*x		
Adj. R-Square	0.82		
		Value	Standard Error
lnK	Intercept	1.81	0.80
lnK	Slope	-2481.54	266.27

Fig. 4.12: ln (k$_T$) vs 1/T plot for parallel channels arrangement between four plates with side plates blocked from outside

One set of experiments has also been carried out by blocking the outer surface of the two side plates with aluminium foil to restrict the lateral diffusion of hydrogen from the sides, thus forcing all the hydrogen movement towards the catalyst surface from the bottom of the channels. Figure 4.11 shows data obtained for these experiments for initial hydrogen concentration ranging from 1.5 to 4.0 % in air. The temperature averaging is done similar to the earlier case to get the temperature value resulting from the recombination reaction. The derivative plot of [H_2] is also plotted similarly.

Similar to the above procedure, the values of [H_2] and dH_2/dt were substituted in Eq. (4.6), to calculate the k$_T$ respective temperature T. Figure 4.12 shows the ln (k$_T$) vs 1/T values obtained from various set of experiments. The activation energy for the parallel channels arrangement by blocking the outer surface of the two side plates with aluminium foil is found out to be 20.6kJ/mol, while the intercept signifying pre-exponential factor is 6.1.

4.6 Conclusions

Reaction kinetics for the catalyst developed for PCRDs to be deployed in NPPs has been studied by carrying out various lab scale experiments on the same. The behaviour of these catalyst plates, when stacked in parallel inside the recombiner box, has also been evaluated by carrying out experiments involving parallel catalytic plates. The activation energy calculated for the recombination reaction on the standalone catalyst plate is found to be in range 18.1 kJ/mol. This value is in accordance with the values reported for similar catalyst in open literature. The intercept signifying pre-exponential factor is found to be 2.14 for this case.

For the parallel channel arrangement having outer surface of the two corner plates, blocked, the lateral diffusion of hydrogen from the sides is prohibited. This leads to inflow of hydrogen towards the central channels from the bottom only. Thus, a natural convection flow gets developed inside the channels between the catalyst plates. This flow leads to ease of adsorption of reactants and desorption of the product at the catalyst surface. Hence, in this case the activation energy is found out to be 20.6 kJ/mol, while the pre-exponential factor is 6.1. The higher value of pre exponential factor in comparison for the standalone catalyst signifies higher natural convection effect as explained above.

CHAPTER 5

Incorporation of Reaction Kinetics Model into CFD Code & Validation Studies

5.1 Introduction

The use of specific reaction kinetics of a catalyst is highly significant for modeling of a recombiner in CFD. This is required to ensure the accuracy of the theoretical model in predicting the performance of the recombiner. Hence, researchers aim to validate their theoretical models against experimental data based on known reaction kinetics of the catalyst involve. For instance, Mimouni et al. (2011) published CFD based recombiner modeling and its validation on the H2-Par and Kali-H2 experiments (from Reinecke, 2010). Similarly, Rożeń (2018) used CFD to study the dynamic behavior of a plate-type Areva FR-380 recombiner in a quiescent environment. Thus, there is the need of an accurate CFD model based on actual reaction kinetics for predicting the behavior of our Passive Catalyst Recombiner Devices (PCRDs) also.

This chapter aims to approximate the reaction kinetics obtained for the developed catalyst plates stacked in parallel, as a single step reaction model. This single step equation will represent the combined effect of multiple processes such as adsorption of gaseous reactants on the catalyst surface, heterogeneous chemical reaction between the adsorbed species and desorption of the reaction products from the catalyst surface. The equation will be incorporated into the detailed CFD model described in Chapter 3. Thus, the in-house CFD model for recombiner can be fine-tuned for the specific

PCRD catalyst. It is also planned to validate the updated CFD model against data from the in-house experiments which were performed with four catalyst plates placed in parallel. This model will be capable to accurately simulate multiple simultaneous phenomena such as the heterogeneous chemical reaction occurring at the fluid solid interface, conjugate heat transfer between solid catalyst and the surrounding fluid region owing to the exothermic heat of the reaction, radiation heat transfer between catalyst plates and fluid due to the high temperatures involved, buoyancy induced gas transport etc. Such a detailed CFD model, capable of accurate quantitative prediction for PCRD performance is vital to understand the behavior of recombiner under varying hydrogen concentrations inside closed geometries like the nuclear reactor containment. The ability to predict the local temperatures of individual catalytic plates in a PCRD is important, as at sufficiently high temperatures, the catalyst plate can become a source of auto-ignition for the surrounding hydrogen-air-steam mixture.

5.2 Fine Tuning of the recombiner model

From the experimental studies presented in the previous chapter, the overall reaction kinetics evaluated for the catalyst plates stacked in parallel can be written in the form of a single step Arrhenius equation as given by Eq. (5.1).

$$k_T=6.1\ \exp\left\{\frac{-20.6\times10^6}{R\,T}\right\} \tag{5.1}$$

where, k_T is the temperature dependent reaction rate constant, T (Kelvin) is the temperature and R is the universal gas constant. For purpose of comparison, the rate constant given by Eq. (5.1) for the in-house catalyst is plotted against the rate constant from Eq. (3.10) given by Schefer (1982) which has been used in the original

CFD model. Their values have been plotted vs. various temperatures in Figure 5.1. It is evident that though the profile of variation of the rate constant vs. temperature is same, the rate constant for present catalyst is comparatively lower at every temperature. This may be due to the fact that there is a significant difference in the fluid dynamic behaviour of the in-house set-up against the set-up of Schefer where there is forced flow along single flat plate. The single step reaction kinetics given by Eq. (5.1) represents the overall performance of parallel catalyst plates which have more resistance for mass transfer towards the surface as compared to a bare catalyst plate as the reactants are allowed to enter only from the bottom of the channels rather than freely diffusing laterally on the surface. Moreover, the reaction kinetics is also highly dependent on the substrate type and manufacturing process of the catalyst and hence can be significantly different for different catalysts as is evident in this case.

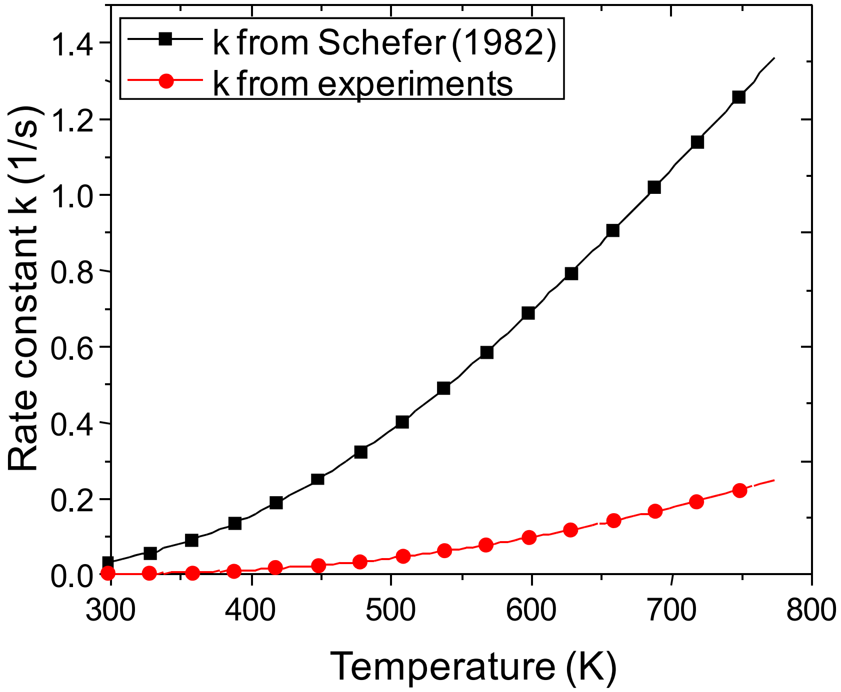

Fig. 5.1: Comparison of reaction kinetics of developed catalyst with the one used in original recombiner model

As a next step for achieving the envisaged objectives, the kinetics used in the earlier developed recombiner model represented by Eq. (3.10) has been replaced with the parameters from Eq. (5.1) to fine tune the recombiner model as per the kinetics of the developed PCRD catalyst.

5.3 Validation of Updated CFD Model Against Experiments

The updated recombiner model has been used to carry out simulation of the experiments described in the last section of Chapter 4. This has been performed to assess the accuracy of the CFD model for predicting the performance of specific PCRDs. The details of the CFD simulations carried out are presented in this section.

5.3.1 Geometry

As described earlier, a 40 L cylindrical reactor as shown in Figure 4.4 has been used for the experiments. The reactor made of stainless steel has a diameter of 300 mm and height of 570 mm. Four Pt-Pd coated catalyst plates made of stainless-steel wire mesh having dimensions 50 mm x 160 mm and thickness of 0.15 mm are placed at a pitch of 10 mm near the centre of the cylinder. These plate dimensions are selected so that the height of 160 mm is same as that of the actual PCRD plate together with the channel gap between them. This makes sure the hydraulic resistance inside the parallel channels is same as that of the actual PCRD. Hence the overall effect of transport phenomena on the reaction kinetics of PCRD catalyst can be captured more accurately by the single step Arrhenius equation used in the recombiner model developed using CFD. The bottom of the plates is kept 240 mm from the bottom of the cylinder. Figure 5.2 describes the model geometry with plan and elevation view of the same.

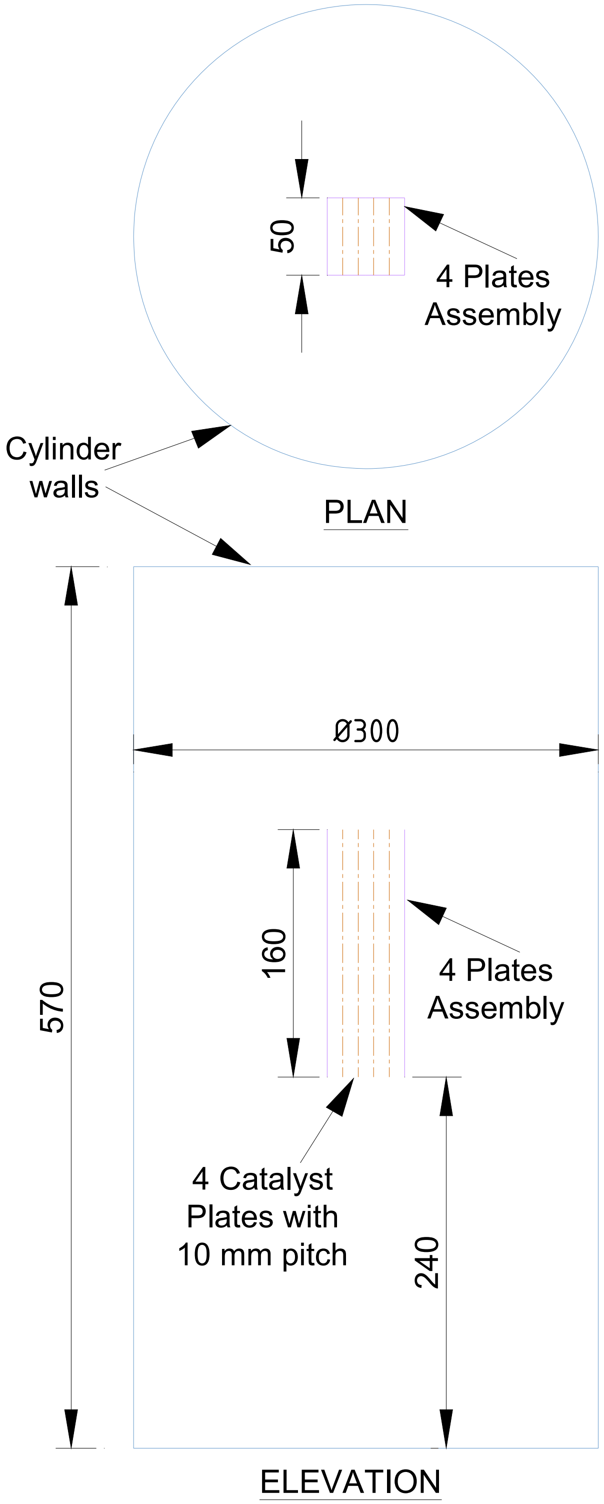

Fig. 5.2: Plan and elevation view of the simulation geometry

5.3.2 Mesh

Completely structured mesh, with all hexahedral elements, is used for modeling fluid as well as structural domain. The mesh for the region near thin catalyst plates is selected based on grid sensitivity study performed during validation of the recombiner model described in Chapter 3. Fine mesh is used in the regions where gradients are expected to be large. Other than these regions, relatively coarse mesh is used to reduce computational time. Figure 5.3 shows the mesh near the catalyst plates region where a power law approach has been used to ensure fine mesh near the surface and progressively coarse mesh towards channel centre. As fine mesh is not required in all regions of the domain, a non-conformal mesh was considered surrounding the central region having the catalyst plates to maintain sufficient fine mesh inside the channels and coarse mesh away from this region. This is done to reduce the total number of elements in the domain without compromising on the accuracy of the results. The 40 liter reactor having four catalyst plates was modeled using 37184 hexahedral elements and 46343 nodes.

5.3.3 Volume Conditions

Based on the experience from earlier simulations described in Chapter 3, the fluid region has been assigned with a compressible gas mixture comprising of hydrogen, nitrogen, oxygen, and water vapour. For calculations related to buoyancy induced flows owing to the low density of hydrogen Buoyancy Gravity model with a reference density of 1.2341 kg/m^{3}has been used in the fluid domain. Chen-Kim turbulence model from the k-ε familyhas been used for the simulation based on previous experience.

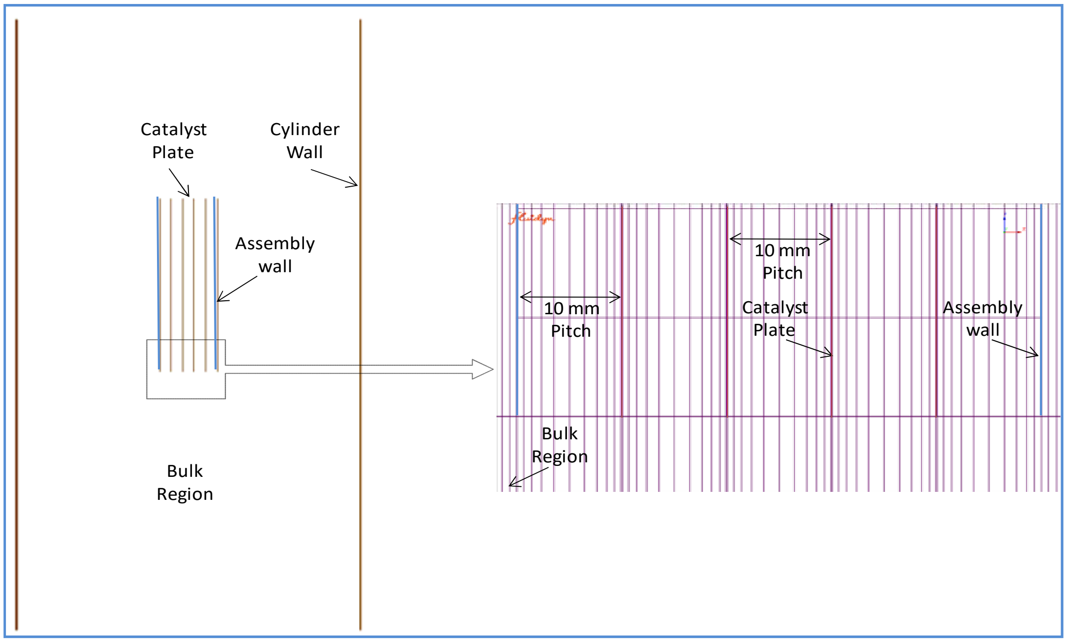

Fig. 5.3: Power law-based structure mesh near catalyst plates

5.3.4 Initial Conditions

As mentioned earlier, the experiments involving H_2 and O_2 recombination reaction were performed under static air conditions at room temperature and the cylinder was pressurized to 10.13 kPa (gauge) with air during the start of each experiment. Hence for carrying out the simulation, fluid and structure node temperature of 305 K as recorder during the experiments and pressure of 111.43 kPa was used as initial conditions. The initial gas mixture concentration used in the fluid domain for two cases is presented in Table 5.1.

Table 5.1: Initial Gas mixture concentrations for various cases

Variable	**2% H_2 Case**	**4% H_2 Case**
Mass. fr. of H_2	0.0014133	0.0028812
Mass. fr. of N_2	0.76590633	0.76478045
Mass. fr. of O_2	0.2326804	0.2323384
Mass. fr. of H_2O	0	0

5.3.5 Boundary Conditions

From the experiments, it is observed that during complete process the gas mixture and reactor wall temperatures are found to remain close to ambient conditions. Moreover, since the stainless-steel reactor is not insulated and its walls are good heat conductor, the cylinder walls are considered as isothermal no-slip wall condition in the CFD simulation. Since the surface reaction is modelled in fluid domain, the interface of the catalyst plates and surrounded fluid domain has been applied with surface reaction and the total energy released due to exothermic reaction is applied on to the catalyst plate.

Since the outer surface of the two side plates are covered during the experiments, and the catalyst holder restricts the flow from the other two vertical sides also, the same has been modelled in the simulation by a thin isothermal wall with no slip boundary condition which surrounds the 4 plate assembly and hence flow is only allowed from top and bottom of the channels. This can be easily understood from Figure 5.2. For the solution of thermal radiation using DOM, an emissivity of 0.8 has been assigned to the surfaces.

5.3.6 Method of solution

These transient simulations have been performed using pressure based 1st order Euler Implicit solver (i.e. MP-NSNT) in order to solve the set of non-dimensional governing equations. Semi-Implicit Method for Pressure Linked Equations-Consistent (SIMPLEC) has been used for pressure-velocity coupling while Upwind Differencing Scheme (UDS) has been used as convection scheme for all the simulations. The solver parameters for different flow variables are taken based on Table 3.6 from Chapter 3.

5.4 Results & Discussion

As the central channel formed between plate number two and three out of the four plates, has a neighbouring channel on its either side, the same has been chosen for monitoring the reaction kinetics. This has been done to get an accurate idea of the effect of transport phenomena (channel effect) on the overall single step equation describing the reaction kinetics of the PCRD catalyst. The trace points to get the time history of temperature on catalyst plate are considered at bottom, middle and top of the inner plate in such a way that locations are same as that of the thermocouple positions during the experiments.

For the 2 % v/v initial hydrogen concentration case, Figure 5.4 shows the comparison between time history variation of temperature at top, middle and bottom of the central plate monitored during the experiment and predicted by the simulation. Lines with solid symbols are used to depict the experimental values whereas lines without symbols are used to represent the simulation results.

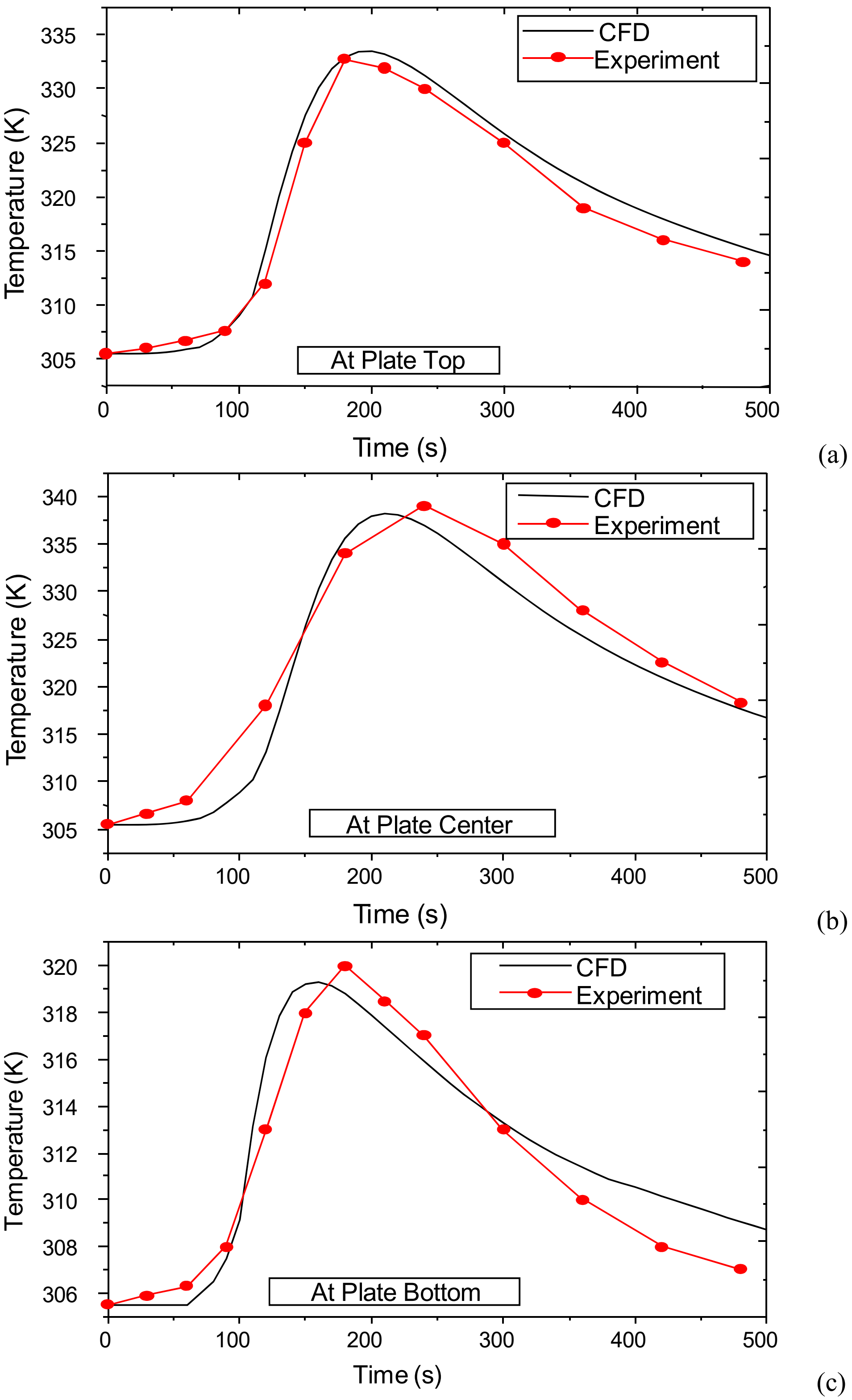

Fig. 5.4: Comparison of catalyst plate temperature at (a) top, (b) middle and (c) bottom for 2 % initial H_2 case

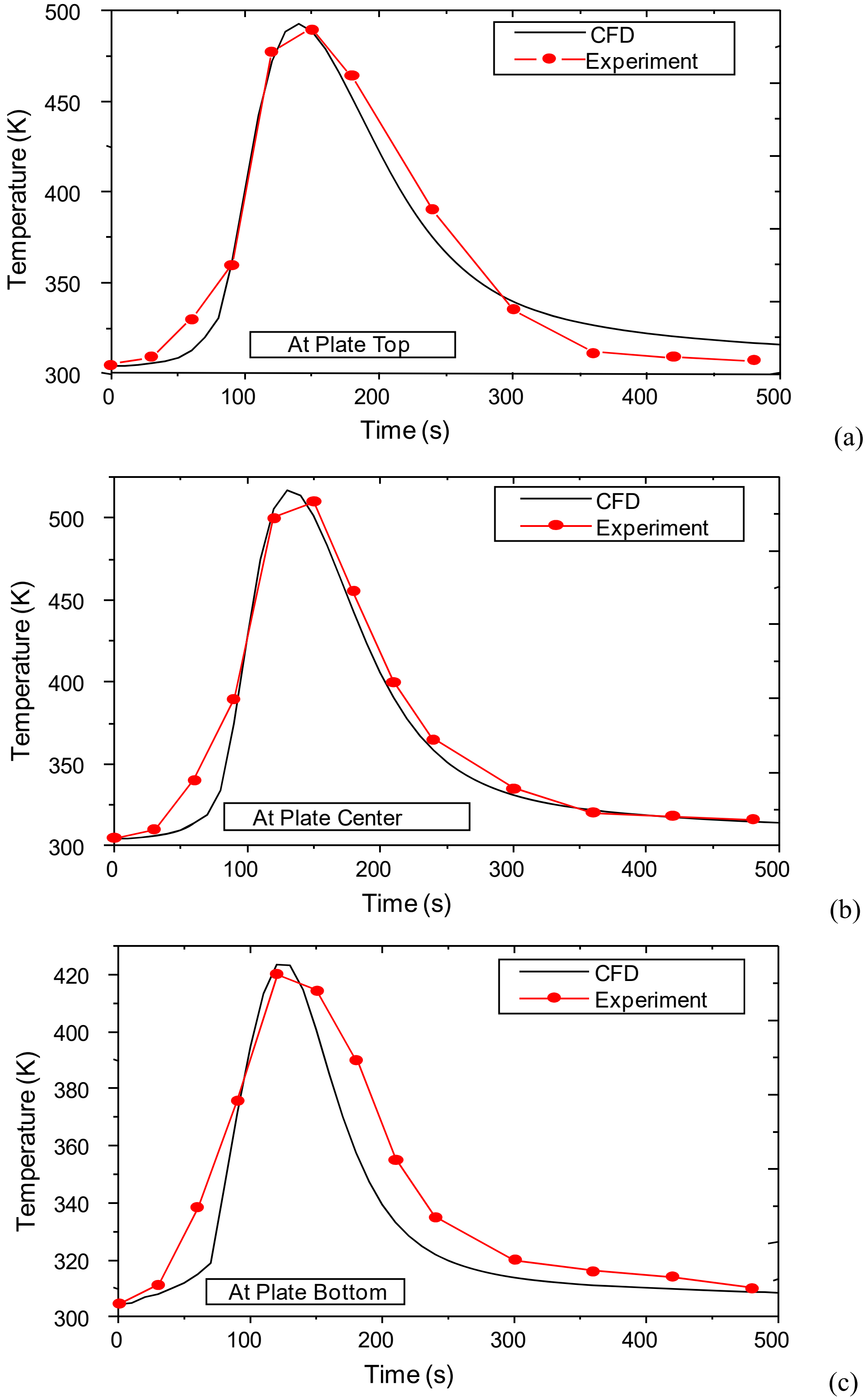

Fig. 5.5: Comparison of catalyst plate temperature at (a) top, (b) middle and (c) bottom for 4 % initial H_2 case

Similarly Figure 5.5 shows the comparison between time history variation of temperature at bottom, centre and top of the central plate monitored during the experiment and predicted by the simulation for the 4 % v/v initial hydrogen concentration case. Temperatures in this case are higher as compared to the 2 % v/v initial H_2 case due to higher recombination reaction causing higher exothermic heat of reaction.

From both these figures, it is evident that the temperatures predicted by the simulation at different locations of the catalyst plate closely match with the experimental values throughout the process time. This shows that results predicted by the CFD simulation are in close agreement with that of the actual experiment.

Figure 5.6 (a) shows the hydrogen concentration prolife along the centre-line of the middle channel at different times during the transient simulation having 4% v/v initial concentration of hydrogen. It can be observed that although the simulation case has a static gas mixture of well mixed hydrogen at the start, a gradient of hydrogen concentration tends to develop along the channel height as the transient progresses. This happens due to the establishment of natural convection flow inside the channel between catalyst plates caused by the heating from exothermic recombination reaction at the catalyst surface. This flow causes the product gas mixture, depleted in hydrogen, to rise upwards causing drop in the hydrogen concentration inside the channel. From the figure, it is clear that the gradient also changes as the simulation progresses and is highest between 100 s and 150 s. This is because during the progress of the process, the catalyst temperature rises, causing improvement in reaction kinetics but later-on the overall hydrogen concentration itself comes down causing decrease in the reaction rate and hence the gradient along channel height. This is evident from decrease in gradient of profiles corresponding to 300 s and 500 s.

Similar trends are observed for the simulation with 2% v/v initial concentration of hydrogen as seen in Figure 5.6 (b). The gradients developed in this case are not as sharp due to less temperature rise and hence weaker natural convection flows in view of less availability of hydrogen. The corresponding temperature profiles along the centre of the middle channel at different times during the transient simulations having initial hydrogen concentration of 4 % v/v and 2 % v/v are presented in Figures 5.7 (a) and 5.7 (b) respectively.

From the figures, it is evident that for 4% v/v initial H_2 case, the maximum value of gas temperature reached at the top end of the channel centre is around 420 K between 100 s and 150 s as seen in Figure 5.7 (a). Compared to this, the temperature rise is slow for the 2% v/v initial hydrogen case which attains the maximum value of around 350 K at the top end of the channel centre at around 200 s as seen in Figure 5.7 (b). From these plots it is evident that initial hydrogen concentration has a strong bearing on the overall process.

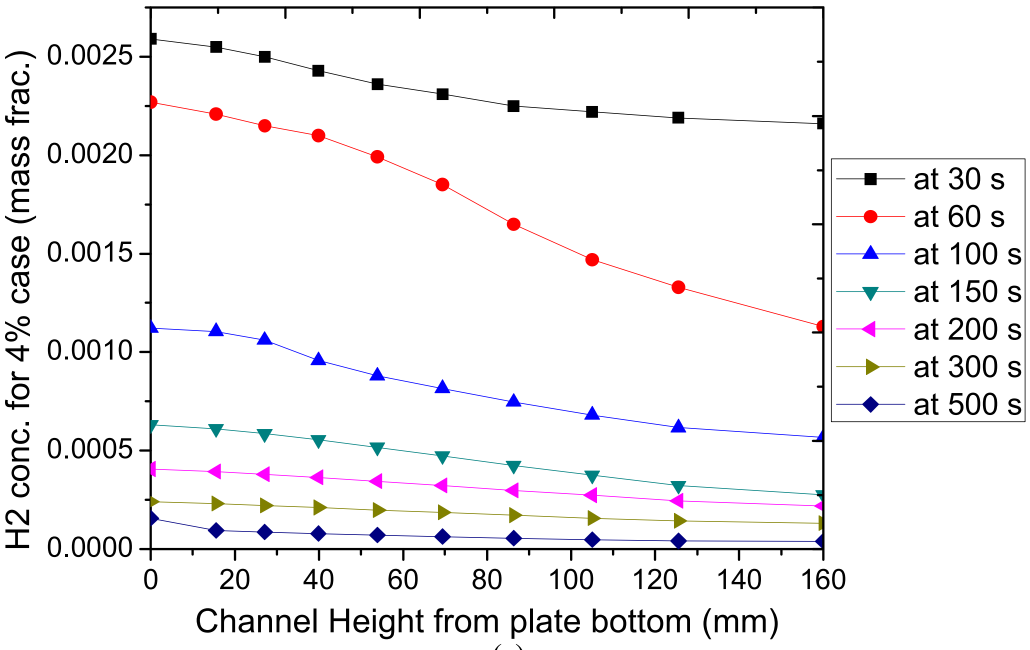

(a)

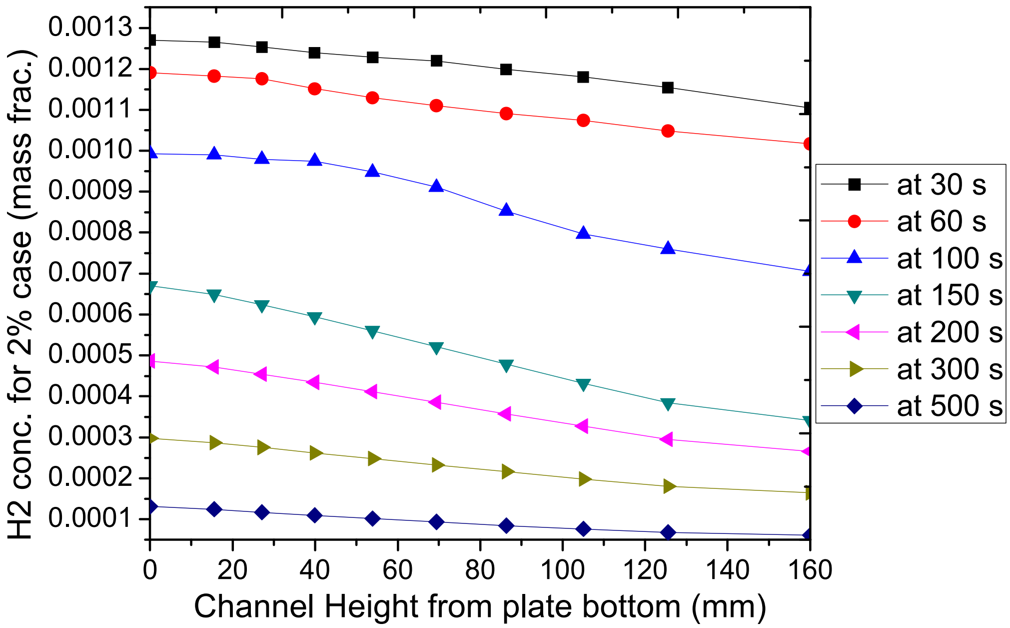

(b)

Figure 5.6: H_2 concentration profile along canter of the middle channel at different times for (a) 4 % v/v initial H_2 case & (b) 2% v/v initial H_2 case

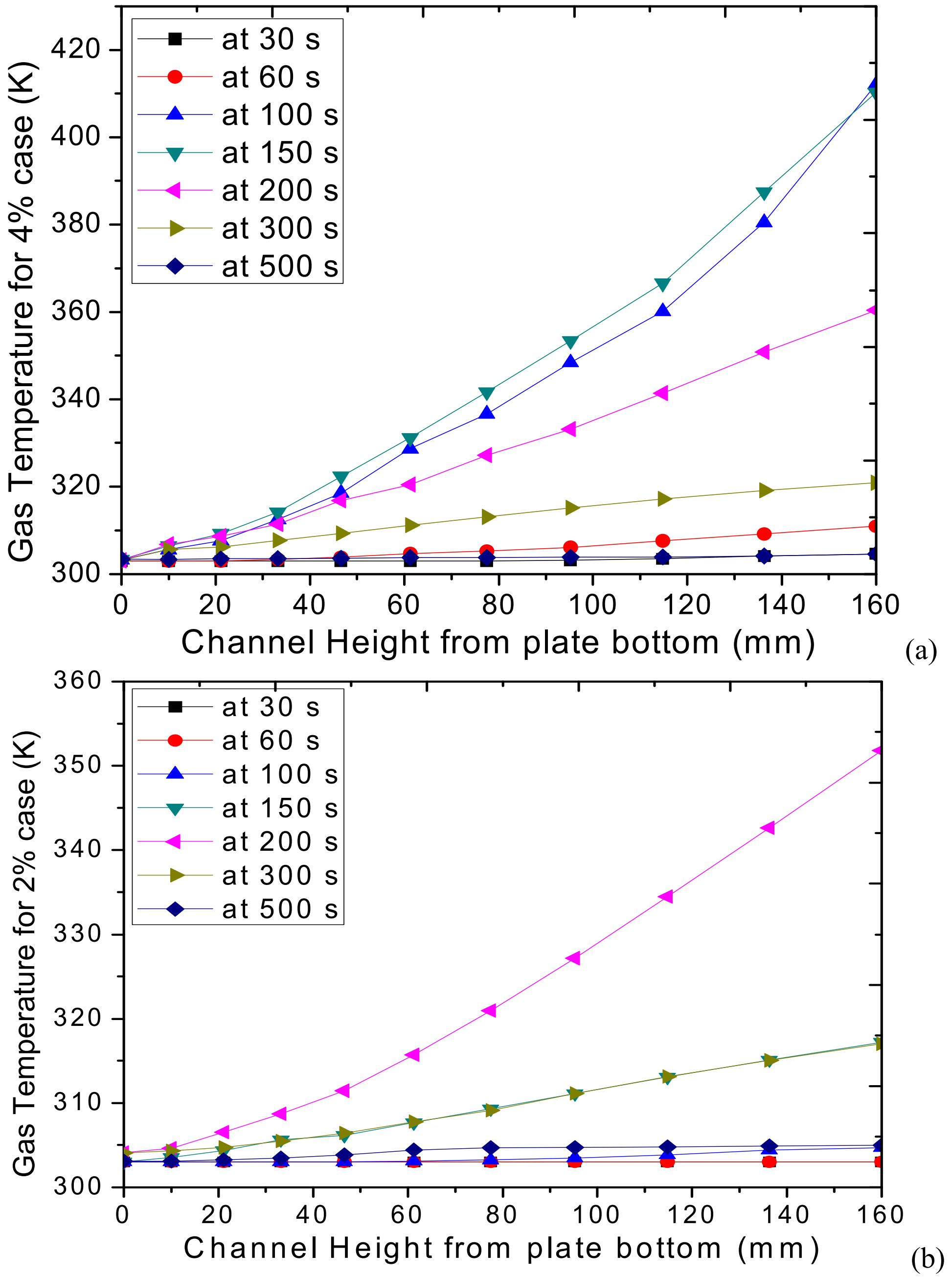

Figure 5.7: Gas temperature profile along canter of the middle channel at different times for (a) 4 % v/v initial H_2 case & (b) 2 % v/v initial H_2 case

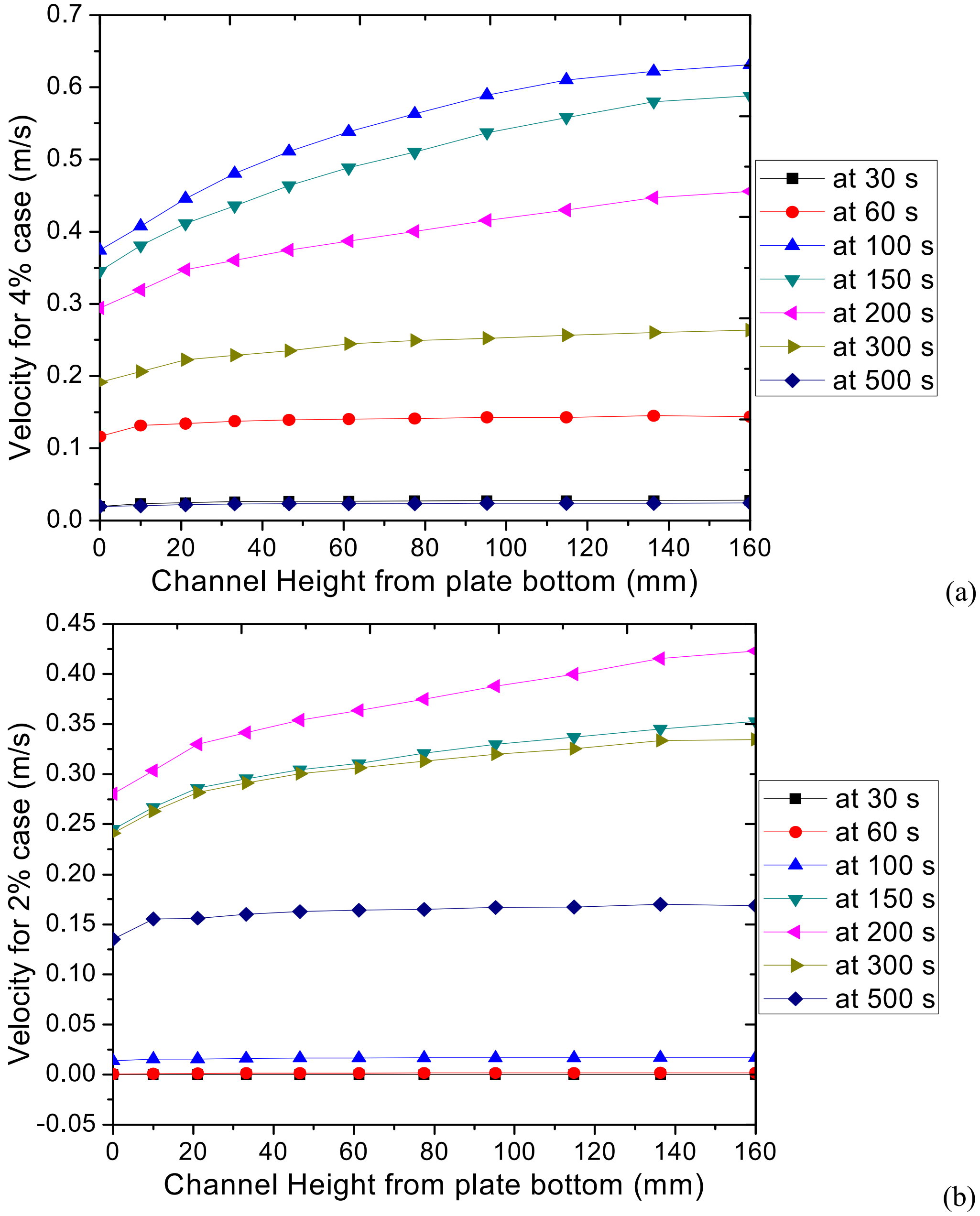

Figure 5.8: Gas velocity profile along canter of the middle channel at different times for (a) 4 % v/v initial H_2case& (b) 2% v/v initial H_2case

The velocity attained due to natural convection caused by heating inside the channel increases along the channel height, as evident from Figure 5.8. For the case with 4 % v/v initial hydrogen concentration shown in Figure 5.8 (a), maximum velocity of around 0.6 m/s is attained between 100 s and 150 s. On the other hand, the maximum velocity of 0.42 m/s is attained between 150 s and 300 s for the case with 2% v/v initial hydrogen as shown in Figure 5.8 (b). As evident from the figures, comparatively less initial hydrogen concentration in the 2% v/v initial hydrogen case develops slower reaction rate causing the overall process to be delayed compared to the 4% v/v initial H_2 case.

The above comparison of overall process, for the two cases, with respect to time can be summarised in Figure 5.9. Figure 5.9 (a) shows the history plots of maximum cell temperature in the fluid domain and Figure 5.9 (b) depicts the history plots of maximum velocity magnitude inside the domain for the two cases having initial hydrogen concentration of 4% and 2 % v/v basis respectively.

For the case with 2 % v/v initial hydrogen concentration, the maximum cell temperature in the fluid domain reaches a value of 384 K after 209 seconds from start of the simulation. The velocity attained due to natural convection rises to a maximum value of 0.44 m/s in almost the same time from start of the simulation. While for the 4 % v/v initial hydrogen concentration case, the maximum cell temperature in the fluid domain rises to a value of 509 K in around 128 seconds from start of the simulation and causing a maximum cell velocity of 0.67 m/s during almost the same time in the fluid domain for this case. As evident from earlier discussion also, the percentage drop in maximum fluid cell temperature as well as peak fluid velocity is rapid for the 4 %v/v initial hydrogen concentration case. While for the 2 %v/v initial H_2 case, slow reaction rate causes availability of hydrogen for comparatively longer duration. Hence the percentage drop in maximum cell temperature as well as velocity is also less.

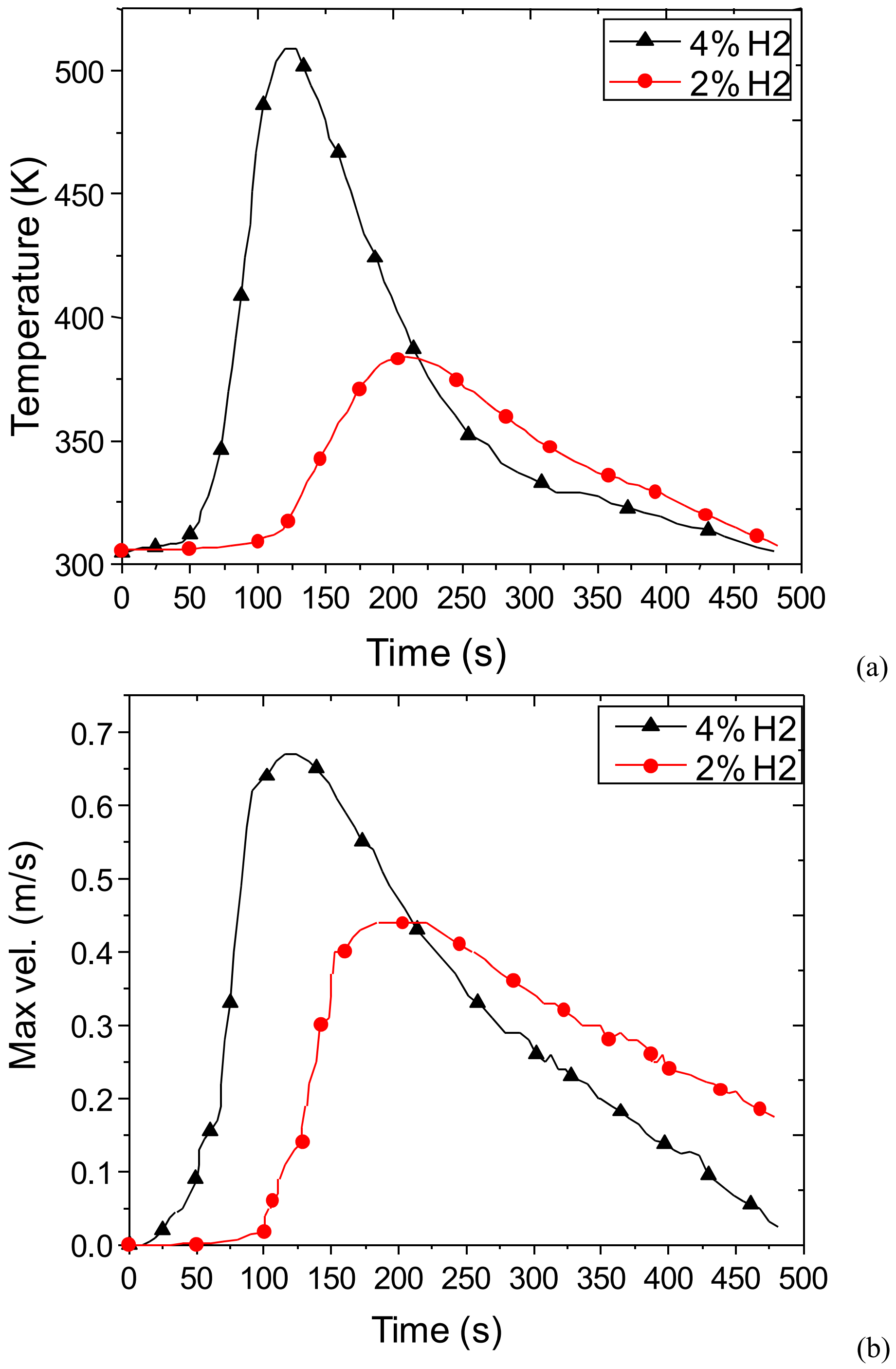

(a)

(b)

Fig. 5.9: (a) Maximum fluid cell temperature & (b) Maximum velocity inside domain for 4% and 2 % v/v initial H_2 cases

Here, it may be noted that the maximum cell fluid temperatures are corresponding the fluid cell adjacent to the fluid-solid interface hence the values of temperature are largely different from the temperature at the centre of the channel seen in Figure 5.7 earlier. This is due to that due to the natural convection flow developed in the upward direction, causing a sharp gradient along the direction perpendicular to the plate surface (along the channel width).

Typical contour plots have been plotted on a vertical plane that cuts the four plates from the centre. For the simulation, having 4 % v/v initial hydrogen concentration, Figures 5.10 (a), (b) and (c) present the hydrogen concentration, gas temperature and vertical velocity respectively near the plate region inside the fluid domain at 128 seconds from the start. These contour plots correspond to the YZ plane which is normal to the catalyst plate surfaces and passes through the centre of the reactor.

It is evident from the figure that the product gases after getting heated up, rise upward towards the top of the cylindrical reactor. From the vertical velocity contour plot shown in Figure 5.10 (c), it is evident that the gases accelerate only inside the three channels between four catalyst plates due to channel effect. This is despite the fact that reaction takes place on both inner and outer surfaces of the plates causing temperature rise on both sides of each catalyst plate as seen in Figure 5.10 (b). The acceleration continues slightly above the channels also as the three velocity streams merge after leaving the parallel channels. Figure 5.10 (b) also reveals that while the gas temperature along the channel length increases with a gradual and smooth gradient, the gradient along the direction away from the plate surface along channel width is very sharp. This is due to the direction of gas flow in the upward direction along the channel height.

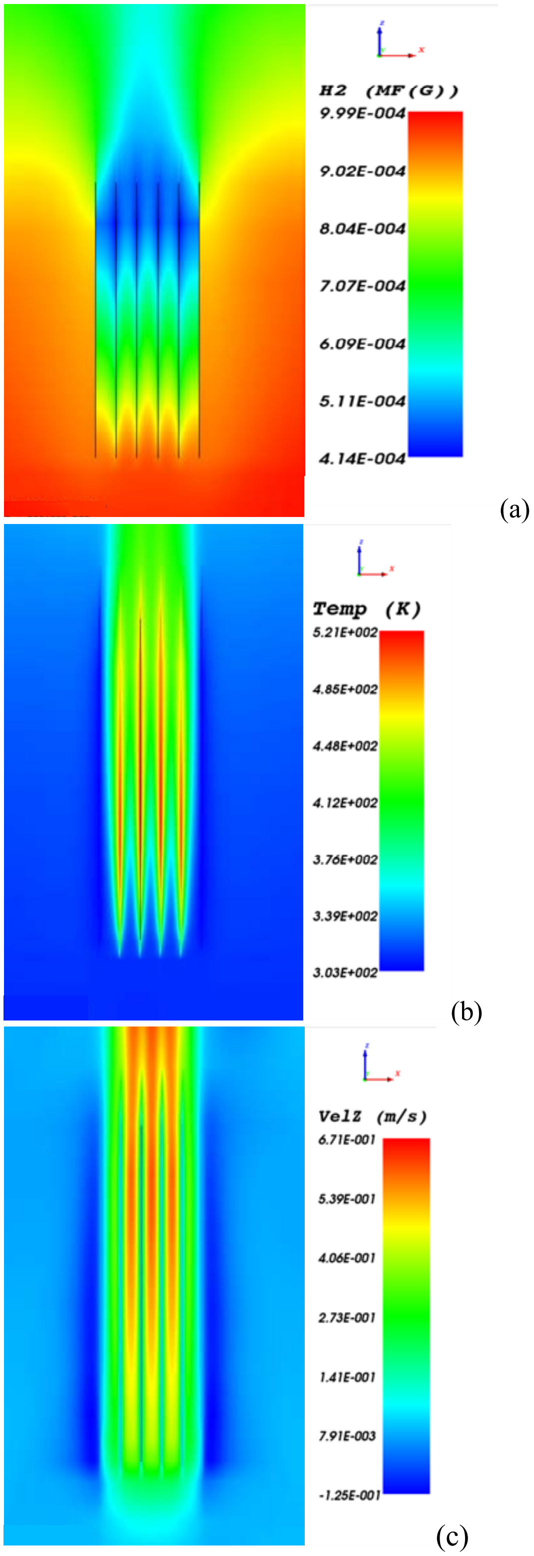

Fig. 5.10: Contour Plot for (a) H_2 concentration, (b) gas temperature and (c) vertical velocity at 128 seconds for 4% initial H_2 case

From the results and above discussion, it is evident that the recombiner model with updated reaction kinetics is accurate and capable of predicting the behavioral details of PCRDs. The same can be confidently employed for obtaining quantitatively accurate performance of the recombiners in future studies. This will be very useful for hydrogen mitigation studies for nuclear reactors during severe accidents.

5.5 Conclusions

The kinetics obtained for the developed PCRD catalyst plates stacked in-parallel is used to fine-tune the CFD model. The updated recombiner model has then been validated by simulating the experiments performed for generation of kinetics data. This is done to assess the accuracy of the CFD model for predicting the performance of specific PCRDs. From the study involving different initial hydrogen concentrations, it is evident that the same has a strong bearing on the overall process. Higher initial hydrogen concentration accelerates the overall process of recombination. This happens due to higher release of exothermic heat for more initial hydrogen concentration, leading to temperature rise and in turn improved kinetics. The results of these simulations are in good agreement with the experimental results and hence establish the ability of updated CFD model to accurately predict the behaviour of the developed PCRDs. Hence this model becomes a vital tool for characterising PCRDs to assist further experimental and analytical studies related to hydrogen recombination inside reactor containment.

CHAPTER 6

Parametric Studies & Development of Empirical Model for Hydrogen Recombiner

6.1 Introduction

Detailed containment analysis needs to be carried out for optimizing the choice between using a greater number of recombiners of smaller size and using fewer ones of relatively larger size to cater to the amount of hydrogen released inside a reactor containment. However, using full scale three dimensional recombiner model such as the one presented in Chapter 3, for simulating Passive Catalytic Recombiner (PCRD) performance in large reactor containment is computationally extensive. This is because the catalyst plates used in PCRD are very thin, having thickness of the order of sub-millimeter while the geometries where PCRDs need to be placed are very large having volume in thousands of cubic meter. The mesh requirement for catalyst plate is of the order of less than 1 mm while the mesh in containment domain is of the order of 100 mm. Thus, achieving the desired results in a fixed time frame is a challenging endeavor. Hence, the use of a lumped model for the PCRD, while modelling rest of the geometry using detailed CFD is more practical approach. Use of such a lumped (empirical) model obviates the need of using fine mesh for modelling the PCRD.

Researchers such as Gera et al. (2011 b, c), Kudriakov et al. (2008) have used empirical correlations for specific PCRDs provided by different PCRD manufacturers for carrying out analysis based on varying assumptions and solution mechanisms. Hence it is contemplated that there is a need to develop such an empirical model for our developed PCRD also. This chapter aims to develop these empirical correlations for the performance of PCRD. For this purpose, a parametric study will be carried out using the updated and validated CFD model developed in Chapter 5. A data matrix will be formulated to derive the correlation for hydrogen conversion across the PCRD as well as other outlet variables as functions of inlet variables.

6.2 Coupled Approach for Recombiner Modeling

Three different methodologies for modelling the PCRDs using a lumped approach have been in use. In the first approach, the containment is meshed as per the dimensions and shape of its geometry. The cells present at the locations of PCRD are assigned the volumetric sink terms of hydrogen, oxygen and source terms of energy and water vapor. The PCRD reaction zone is considered as porous media with porosity assigned from the PCRD geometric data. The sink term for hydrogen is based on correlation for hydrogen conversion in the particular PCRD as supplied by its manufacturer. The conversion formula of the PCRD manufacturer is applied to the hydrogen concentration present in those cells to obtain the desired sink term at every time step. The corresponding sink term for oxygen and source term for water vapor is simply obtained based on the stoichiometry of the hydrogen oxygen recombination reaction as per Eq. 4.3.

Similarly, the energy source term is derived based of the calculated hydrogen sink term multiplied to the enthalpy of recombination reaction as per Eq. 4.3. Gera et al. (2011 b) used this approach to model PCRD in PARIS 1 benchmark geometry. Due to porous zone at catalytic section the heat released during recombination reaction is partly added to the solid mass of the catalyst plates and partly transferred to the surrounding fluid.

In the second approach, PCRD is modeled as a box with a single plate. Here all the catalyst plates inside a PCRD are lumped into one single solid plate having the same mass as that of the combined number of catalyst plates inside PCRD. Thus, the mesh required is not very fine as in the case of modeling every single catalyst plate. The volumetric sink and source terms for hydrogen, oxygen and water vapor respectively are applied in a similar way as that of the previous method. This approach takes care of the energy distribution between solid and fluid and hence more accurately predicts the fluid temperatures. The momentum change inside actual PCRD is taken care by an artificial pressure resistance term along the length of the box that is equivalent to the resistance of the total number of catalyst plates inside PCRD. Gera et al. (2011 c) used this approach to model PCRD in PARIS 1 benchmark geometry. This approach needs an artificial pressure resistance term in addition to the hydrogen conversion correlation for the particular PCRD.

In the third method, while the containment fluid volume as well as the inlet and the outlet of the PCRD are meshed, the PCRD volume is taken as a void with no mesh inside it. The recombiner model is applied with space-averaged boundary conditions with the variables at the outlet of PCRD being derived as a function of the variables at its inlet. A schematic of this methodology of coupled approach for modelling of PCRD in CFD is illustrated in Figure 6.1.

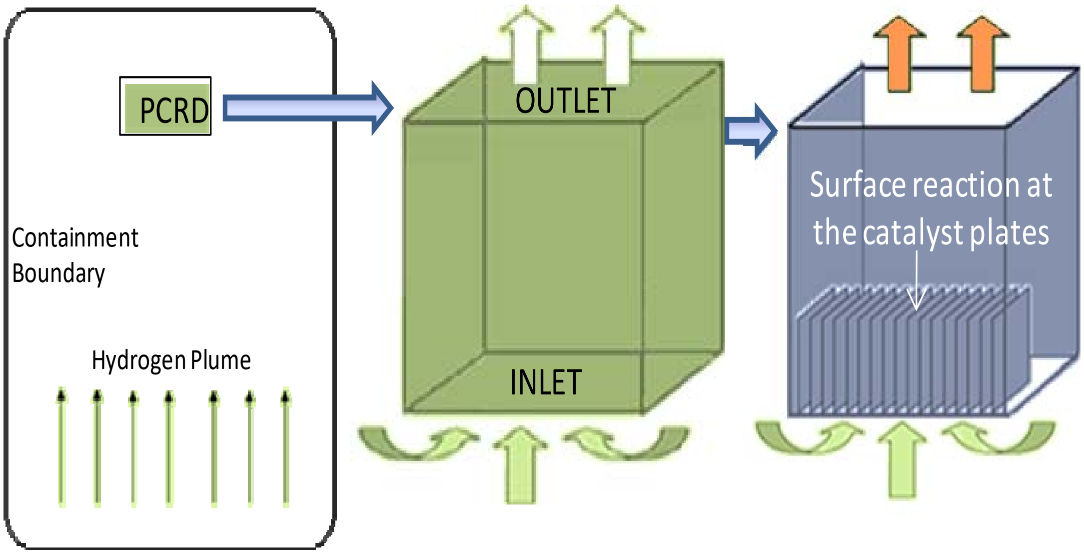

Fig. 6.1: Representation of the coupled approach for PCRD modelling

The hydrogen conversion rate due to the catalytic reaction is calculated using a manufacturer correlation as in the two earlier approaches. The corresponding sink and source terms for oxygen and water vapor are calculated based on their relative stoichiometry as per recombination reaction. The exothermic heat energy is assumed to be completely applied to the solid mass. This heat then gets transferred from solid to the fluid on the basis of the total surface area of the catalyst plates, the total fluid mass entering the inlet of PCRD and its average inlet temperature. Based on this, the fluid temperature at the outlet of PCRD is calculated. The momentum change inside actual PCRD is calculated based on the total free cross-sectional area for the fluid inside the PCRD and the path length. All these calculations are carried out as a separate program at each time step and the variables obtained as a result are applied to the outlet face of PCRD in the CFD simulation. Kudriakov et al. (2008) used the TONUS code for carrying out hydrogen mitigation calculations in EPR containment using a similar approach.

6.3 Parametric study using updated CFD model for PCRD.

All three approaches described in the above section, require a hydrogen conversion correlation specific to the PCRD being modeled. The studies reported in literature are based on correlations supplied by respective PCRD manufacturers. Hence there is a need to develop such correlations for hydrogen conversion and outlet variables as functions of inlet variables for Indian PCRDs also. Large amount of data related to PCRD performance for various inlet parameters such as hydrogen concentration, steam concentration, inlet velocity, inlet temperature etc. need to be generated. This data can then be processed to derive the correlation between various inlet and outlet variables. In order to generate this data, the fine tuned and validated CFD model from Chapter 5 has been used.

6.4 CFD simulation for generation of data matrix.

6.4.1 Geometry & Mesh

The updated CFD based recombiner model has been used for generating the data matrix required for mapping the PCRD performance. For this purpose, geometry was selected such that it accurately captures all the processes such as surface reaction, heat transfer, buoyancy etc. taking place inside the actual PCRD. A typical Indian PCRD consists of more than seventy identical catalyst plates stacked in parallel. In the present geometry, four catalyst plates having same dimensions as those of the actual PCRD were used. These plates having a length of 0.36 m, height of 0.16 m and a thickness of 0.15 mm are kept at a pitch of 10 mm. They are placed inside an enclosure of rectangular cross section that is open from the top and bottom. This box is 360 mm long, 50 mm wide and has a height of 1 m. The plates are placed vertically along their height near the middle of the box meaning that the bottom of the plates is 420 mm above the inlet of the box. Figure 6.2 shows the geometry details.

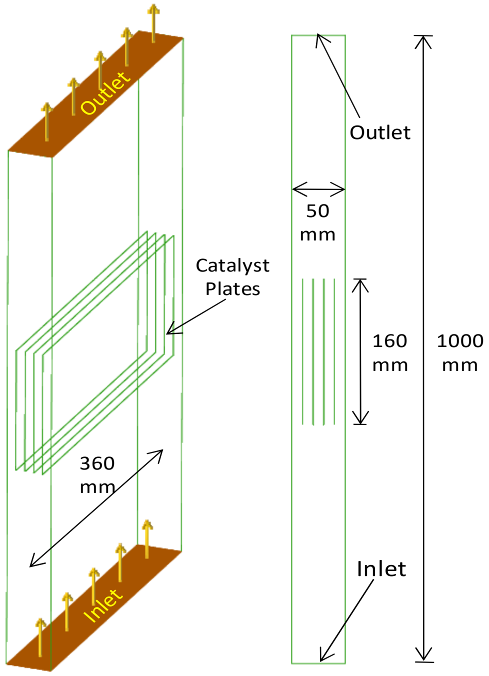

Fig. 6.2: Geometry with four plate arrangement

Out of the three parallel channels between these four plates, the middle channel is an exact replica of a typical channel inside actual PCRD. This is because it has in its neighbourhood, an identical channel on either side similar to the PCRD. Thus all the processes inside this channel such as mass transfer by diffusion and convection, conjugate heat transfer coupled with radiation, surface reaction taking place on catalyst plates, buoyancy effect etc are same as those occurring inside actual PCRD. This geometry is considered to reduce the meshing requirement, as many cases are to be simulated for generation of the desired data matrix. Meshing for fluid as well as structural domain has been done using structured mesh approach. Mesh near wall region is fine compared to the bulk region. The same is used for capturing the ‘no slip’ wall effect on the fluid velocity and the surface reaction at fluid-solid interface near catalyst plates. The cell size near the walls is 0.15 mm and progressively increases as per power law in the direction perpendicular to the walls. The region above and below the catalyst plates has also been meshed using similar elements as in the plates region to avoid any non conformal mesh in the domain. The mesh parameters (the smallest cell size, the power law used and the nature of grid) are selected based on grid sensitivity study performed during the validation exercise of the recombiner model against literature data, presented in Chapter 3. These parameters are valid for the present case as hydrogen recombination is a surface reaction and hence remain unchanged for slight variation in geometrical parameters such as plate height and pitch between plates etc as is the scenario in this case. Total 23900 hexahedral fluid cells and 1452 structural nodes were used to model the geometry. Figure 6.3 shows the meshing scheme used for modelling the geometry.

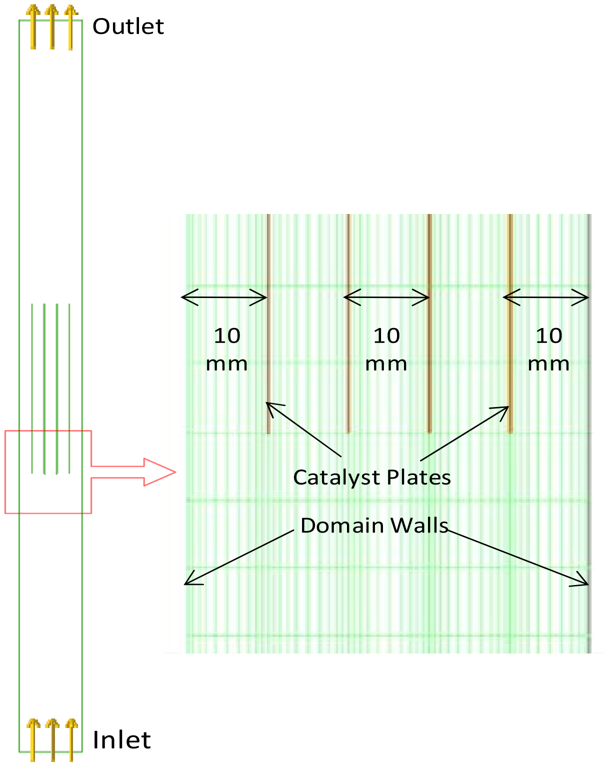

Fig. 6.3: Mesh near the catalyst plates region

6.4.2 Volume conditions

Similar to the recombiner model described in previous chapters, the solution domain has been divided into fluid and solid portion. Four catalyst plates have been modeled as solid domain and the rest of the geometry has been considered as fluid. The walls of the box have been treated as fluid boundary. The fluid region has been considered as a compressible mixture of four ideal gases namely hydrogen, nitrogen, oxygen and water vapor. Buoyancy Gravity model, with a reference density based on initial conditions in each case, has been considered to account for the density difference between these gases.

6.4.3 Initial Conditions

The fluid domain is considered to be initially free of any hydrogen and completely filled with either dry air or a mixture of air and water vapour of known proportion based on the case being simulated. The pressure in the fluid domain has been considered as 101.3 kPa and temperature has been taken as 298 K for dry cases and 378 K for wet cases respectively. Similarly the initial node temperature for solid mesh has been taken as 298 K for dry cases and 378 K for wet cases respectively.

6.4.4 Boundary Conditions

The purpose of the present study is to simulate the steady state performance of the typical gas flow channels between catalyst plates. In the actual PCRD, there are a large number of catalyst plates placed parallel to each other with a small pitch, because of which almost all the plates will be at similar temperatures. For the channels between these plates, there will effectively be no heat loss in the lateral direction perpendicular to the flow. Hence, the walls of the enclosure have been considered as no slip adiabatic walls. Surface reaction has been applied at the interface of the catalyst plates and surrounding fluid. The fluid-solid boundary at the plate surface is taken as a no slip isothermal wall. It may be noted here that isothermal here means specific boundary condition for the surface reaction at the interface to take care of the thermal equilibrium between solid and fluid at the interface and is not the general isothermal condition. This has been done to take care of the temperature rise of the plate as well as the fluid due to exothermic heat released during the reaction. At each time step heat is added because of the exothermic reaction, and hence the plate temperature rises. Due to the isothermal boundary condition, heat flux is added at the surface to the fluid based on the temperature difference between fluid and solid cell. The bottom boundary face of the geometry has been assigned as inlet while the top boundary face has been taken as outlet. While ‘pressure static’ boundary condition has been applied at the outlet, velocity inflow boundary condition has been considered at the inlet. Since the problem involves compressible gas mixture subjected to density change, the pressure static boundary condition effects a net flow in or out of the boundary based on the difference between the actual pressure at each time step and the pressure specified in the boundary condition. As the box is assumed to be kept at atmospheric pressure (or the pressure mentioned for the initial condition), the pressure value defined at the outlet boundary face is taken as the same value. For defining the ‘velocity inflow’ boundary condition in such problems involving energy equation as well as compressible flow, temperature and pressure values are also required along with the velocity magnitude and direction. Hence values same as the initial conditions are used at the inlet. The velocity, temperature and gas mixture composition at the inlet is varied for different cases to generate a data matrix from the parametric studies.

6.4.5 Method of solution

Steady state simulations have been carried out for various inlet conditions. 3-D mass, momentum, energy, conservation equation for hydrogen, oxygen, water vapor and turbulent quantities are solved. In order to solve the set of governing equations, pressure based 1st order collocated Euler Implicit solver is used to evaluate Cartesian velocity components (MP-NSNT solver of FLUIDYN). Semi-Implicit Method for Pressure Linked Equations-Consistent (SIMPLEC) was used for pressure-velocity coupling. Convection fluxes are computed by blending of pure upwind scheme and higher order schemes. The time integration is performed using an Euler implicit scheme. Chen-Kim turbulence model from the k-ε family has been used for the simulation based on previous experience. To calculate radiation between catalyst plates, box and fluid, Radiative Transfer equation (RTE) is solved by the Discrete Ordinates Method. The solver parameters for different flow variables are taken based on Table 3.6 from Chapter 3.

Based on this model, various simulations have been carried out with different inlet conditions. These conditions have been selected based on the expected ranges of velocity, temperature, hydrogen and steam concentration expected in the reactor containment during severe accident scenarios. Table 6.1 presents the variables and their values that have been used as inlet boundary condition to carry out the parametric study.

Table 6.1: Inlet variables and their values used for parametric study

Inlet Parameter	**Unit**	**Values Taken for Parametric Study**
Gas mixture velocity	m/s	0.25, 0.5, 1.0
H_2 concentration in gas mixture	v/v %	1, 2, 4, 8
H_2O concentration in gas mixture	v/v %	0, 20, 40, 60
Temperature of gas mixture	K	298, 350, 378, 400, 450, 500, 550

The range of hydrogen concentrations for the parametric study has been decided based on the fact that expected safe recombiner operation is generally considered till around 8 % v/v as the gas mixtures can become detonable beyond this value. Moreover, similar concentration ranges have also been observed from the hydrogen distribution studies for reactor containments. On the other end, these recombiners are considered better if they can initiate operation at lower hydrogen concentrations. Hence a lower value of 1 % has been used for the hydrogen concentration. Similarly, the steam concentration range has been selected based on the fact that for steam concentrations beyond 60%, the hydrogen-air-steam mixture becomes inert. The velocity range for the parametric study is based on the expected values inside recombiners which are below 1 m/s. The temperature range for parametric study is actually taken higher than the expected values considering the fact that a recombiner placed near to the break point of the coolant or steam pipe can see such higher temperatures.

Table 6.2 describes the various cases that have been simulated with their respective inlet boundary conditions for the generation of PCRD data matrix.

Table 6.2: Various cases simulated and their respective inlet boundary conditions

Case No.	**Reference Name**	**Inlet Conditions for Different Cases**			
		Velocity m/s	**Temperature** K	**H_2** Vol. %	**H_2O** Vol. %
1	0.25.1	0.25	298	1	0
2	0.25.2	0.25	298	2	0
3	0.25.4	0.25	298	4	0
4	0.25.8	0.25	298	8	0
5	0.5.1	0.5	298	1	0
6	0.5.2	0.5	298	2	0
7	0.5.4	0.5	298	4	0
8	0.5.8	0.5	298	8	0
9	1.0.1	1	298	1	0
10	1.0.2	1	298	2	0
11	1.0.4	1	298	4	0
12	1.0.8	1	298	8	0
13	20.0.25.1	0.25	378	1	20
14	20.0.25.4	0.25	378	4	20
15	20.0.25.8	0.25	378	8	20
16	20.0.5.1	0.5	378	1	20
17	20.0.5.4	0.5	378	4	20
18	20.0.5.8	0.5	378	8	20
19	20.1.0.1	1	378	1	20
20	20.1.0.4	1	378	4	20
21	20.1.0.8	1	378	8	20
22	40.0.25.1	0.25	378	1	40
23	40.0.25.4	0.25	378	4	40
24	40.0.25.8	0.25	378	8	40
25	40.0.5.1	0.5	378	1	40
26	40.0.5.4	0.5	378	4	40
27	40.0.5.8	0.5	378	8	40
28	40.1.0.1	1	378	1	40
29	40.1.0.4	1	378	4	40
30	40.1.0.8	1	378	8	40
31	60.0.25.1	0.25	378	1	60
32	60.0.25.4	0.25	378	4	60
33	60.0.25.8	0.25	378	8	60

Case No.	Reference Name	Inlet Conditions for Different Cases			
		Velocity m/s	Temperature K	H_2 Vol. %	H_2O Vol. %
34	60.0.5.1	0.5	378	1	60
35	60.0.5.4	0.5	378	4	60
36	60.0.5.8	0.5	378	8	60
37	60.1.0.1	1	378	1	60
38	60.1.0.4	1	378	4	60
39	60.1.0.8	1	378	8	60
40	0.5.1.350	0.5	350	1	0
41	0.5.1.400	0.5	400	1	0
42	0.5.1.450	0.5	450	1	0
43	0.5.1.500	0.5	500	1	0
44	40.1.0.8.400	1	400	8	40
45	40.1.0.8.450	1	450	8	40
46	40.1.0.8.500	1	500	8	40
47	40.1.0.8.550	1	550	8	40

6.5 Results and Discussions

Steady state simulations were carried out for all the 47 cases with mass convergence criteria of 1E-10 to ensure sufficient convergence. CPU time for each simulation was around 2 hours. Trace point was selected at the center of the outlet boundary face as it geometrically lies above the middle of the central channel between catalyst plates. This way, the values of various variables can be considered to represent the performance of the typical PCRD. Output from these simulations was the velocity, temperature, hydrogen concentration, water vapor concentration etc. The results of a typical case having steam concentration of 40 % v/v and hydrogen concentration 8 % v/v at inlet with an inlet velocity of 1 m/s are presented in the form of contour plots. Since the case has water vapor, i.e. it is wet case; the temperature at inlet is 105 ^{0}C as mentioned earlier.

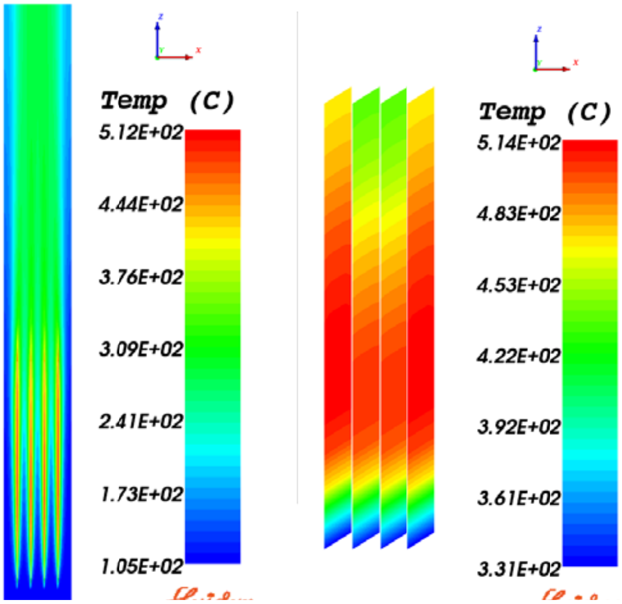

(a) (b)

Fig. 6.4: Contour plots for (a) fluid temperature and (b) plate temperature

From Figure 6.4 (a) it is observed that as the fluid coming from the inlet having 8% v/v hydrogen reaches the catalyst channels, the temperature starts to increase. The fluid temperature keeps on rising along the channel length due to exothermic heat of reaction. After the channel region, the fluid temperature averages out as it reaches the outlet. Figure 6.4 (b) represents catalyst plate temperature. In this plot, it is seen that temperature for the two middle plates forming the central channel falls more quickly along their length as compared to the two corner plates. This is because the fluid in central channel is encountered by catalyst plates on both sides. Thus, the hydrogen here gets consumed earlier than the corner plate region where the fluid has a catalyst plate only on one side.

Figure 6.5 shows the density and velocity contours for this case. Here it is seen that the fluid density decreases along the channel length. There are two competing factors along the plate length, (i) Density decreases with increasing temperature and (ii) With decrease in hydrogen concentration, water vapor concentration increases along the plate length. Because of this, the average molecular weight and hence the density of gas mixture increases. The rise in fluid temperature due to exothermic reaction is seen to dominate the effects due to hydrogen depletion and there is an overall drop in the fluid density along the channel length. This drop in the density increases the buoyancy, because of which the fluid velocity increases along the channel length. This can be seen in Figure 6.5 (b). The inlet velocity of 1 m/s reaches a value of 1.94 m/s at the outlet due to this effect.

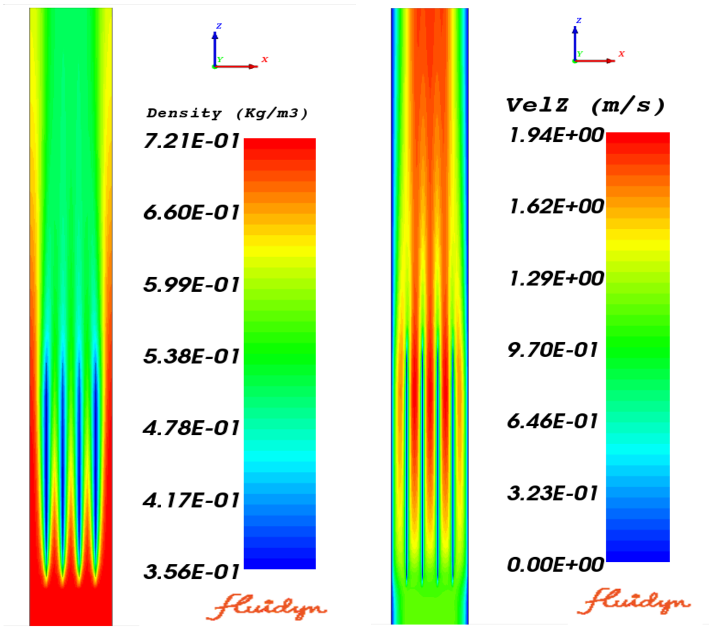

(a) (b)

Fig. 6.5: Contour plots for (a) fluid density and (b) vertical velocity

Figures 6.6 (a), 6.6 (b) and 6.6 (c) represent the contour plots for hydrogen, water vapor and oxygen in terms of their respective mass fractions along the channel length. From these plots it is observed that, along the length of catalyst plates, the hydrogen concentration decreases due to recombination reaction on catalyst surface. This causes proportionate increase in water vapor concentration along the channel length.

The concentration of oxygen also decreases along the plate length due to consumption in the recombination reaction. Since the walls have been considered as adiabatic, they reach the same temperature as that of the inlet fluid at steady state. The catalyst plates being at a much higher temperature, condensation of water vapour does not occur in any of the simulated cases. In actual containment scenario also, since the PCRD and its internals will be at a higher temperature as compared to the surrounding fluid, condensation is not expected during the progression of the recombination reaction.

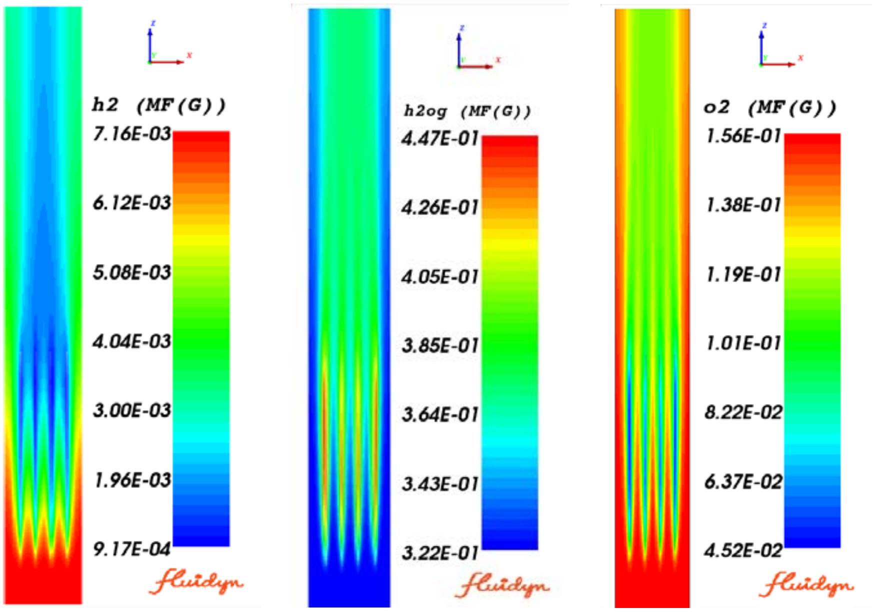

(a) (b) (c)

Fig. 6.6: Contour plots for (a) hydrogen, (b) water vapor and (c) oxygen in terms of their respective mass fractions

Such detailed analysis was carried out for each of the 47 steady state simulations and their results were compiled in a tabulated form to represent values of inlet variables and outlet variables as a data matrix. The inlet gas mixture influence on the performance of the recombiner depending on hydrogen concentration, steam concentration, gas velocity and gas temperature, has been evaluated by plotting hydrogen conversion efficiency of the recombiner against these parameters.

Conversion efficiency of PCRD can be defined in terms of the mass fraction of hydrogen in the gas mixture at the inlet and outlet of the recombiner given by Eq. (6.1).

$$\%\ \text{Efficiency} = 100 \times \frac{\text{H2 mass fraction at inlet} - \text{H2 mass fraction at outlet}}{\text{H2 mass fraction at inlet}} \qquad (6.1)$$

The efficiency of hydrogen conversion inside PCRD has been calculated as function of various inlet parameters for all the cases simulated in the parametric study. Figure 6.7 represents efficiency vs. inlet water vapour concentrations plots for different hydrogen concentrations at 1 m/s inlet velocity. Here it can be seen that the conversion efficiency remains almost the same with change in inlet steam concentration. Similar trends are observed for other inlet gas mixture velocities also. Hence to avoid repetition, further conversion efficiency plots against other inlet parameters have been presented here for the case with 40% steam concentration. Figure 6.8 represents efficiency vs. inlet gas hydrogen concentration plots at 40% v/v steam for various inlet velocities. It can be observed that hydrogen concentration at inlet significantly affects conversion efficiency of PCRD. This effect is due to the fact that higher hydrogen concentration causes higher rate of recombination reaction. This leads to higher catalyst plate temperatures owing to exothermic nature of the reaction. High temperatures give higher rates of reaction as per the Arrhenius law described earlier. This higher reaction rate leads to higher conversion efficiency of PCRD. This dependence of conversion efficiency on temperature can be seen from Figure 6.9 which represents efficiency vs. inlet gas temperature plot for a typical case having 40 % v/v steam, 8% v/v hydrogen in the gas mixture with an inlet velocity of 1 m/s.

Here it can be seen that the conversion efficiency increases with inlet fluid temperature.

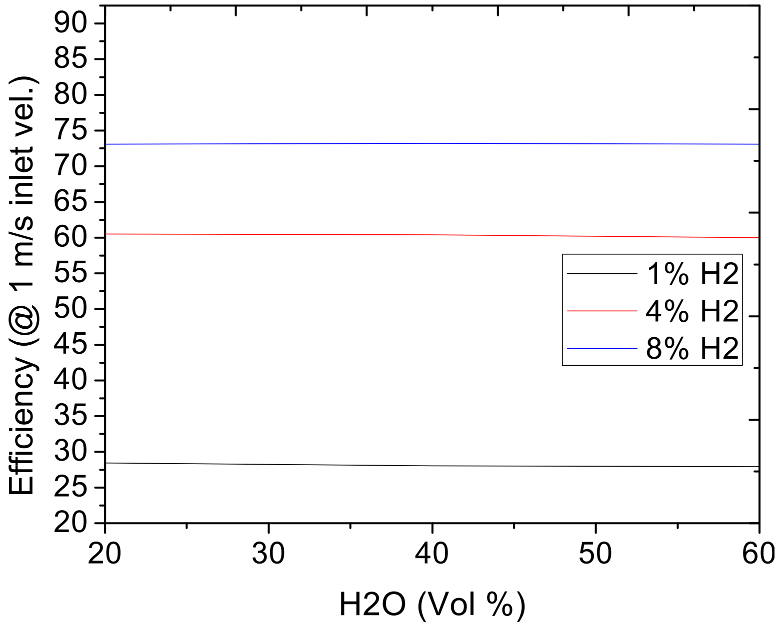

Fig. 6.7: Conversion efficiency vs. inlet steam concentration for 1 m/s inlet velocity

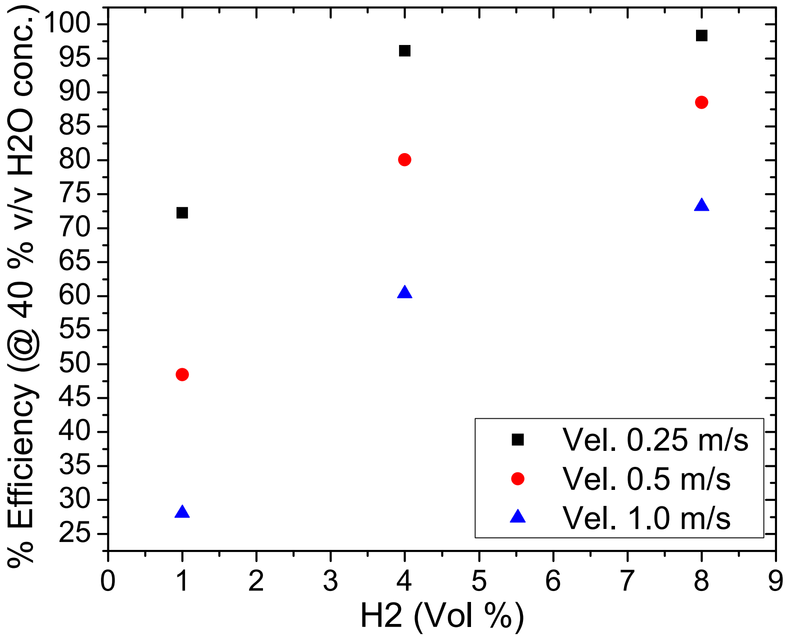

Fig. 6.8: Conversion efficiency vs. inlet hydrogen concentration for 40% v/v steam

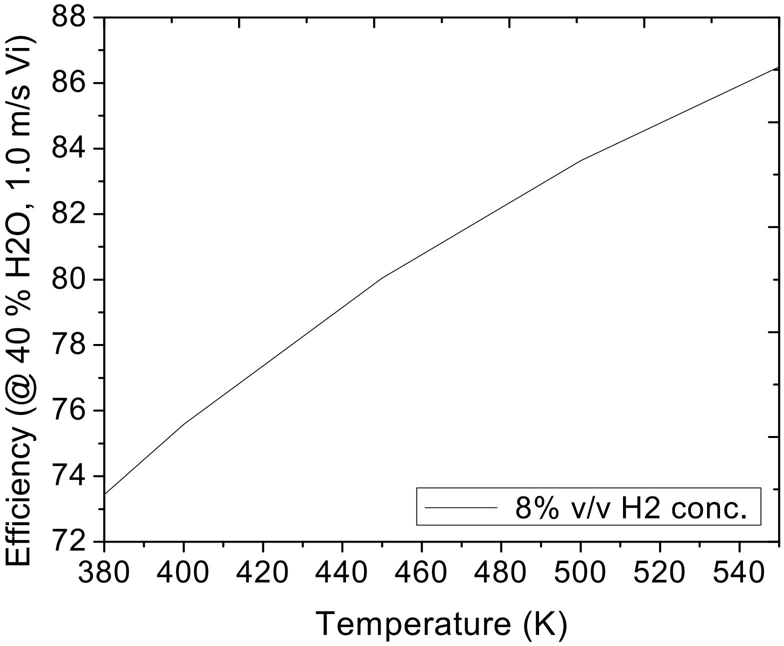

Fig. 6.9: Conversion efficiency vs. inlet fluid temperature for 40% v/v steam & 8% v/v hydrogen

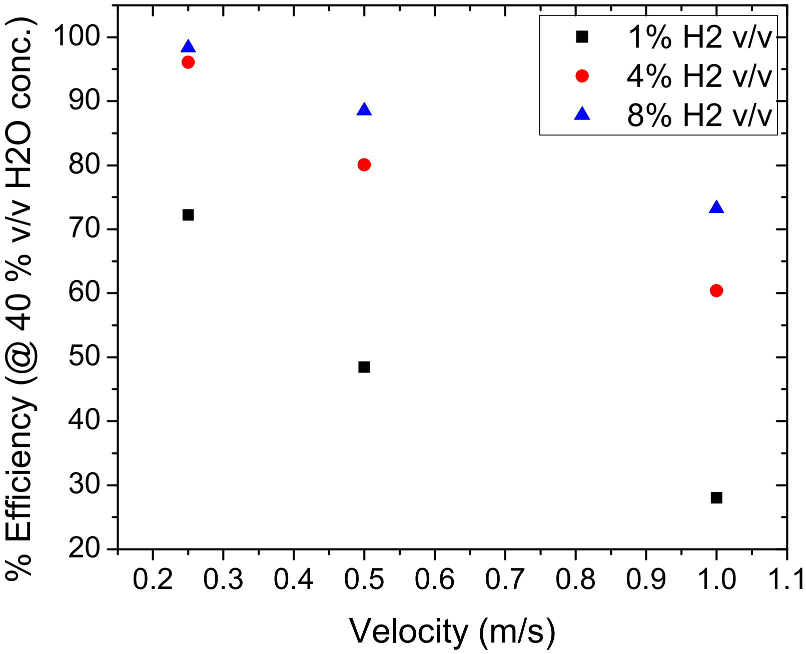

Fig. 6.10: Conversion efficiency vs. inlet velocity for 40% v/v steam

Figure 6.10 represents conversion efficiency vs. inlet gas velocity plots for different hydrogen concentrations having 40 % v/v steam concentration. It reveals the fact that increase in inlet gas velocity causes decrease in conversion efficiency. This phenomenon can be explained by the fact that as gas velocity increases, the time for the gas mixture to get adsorbed on the catalyst surface and undergo recombination reaction decreases. Thus, recombination rate decreases with increase with gas velocity. From the figure, it can be seen that this effect is more prominent for gas mixtures having less hydrogen concentration. This is due to the reason that for leaner gas mixtures, fall in residence time gives even lesser chance for hydrogen to get adsorbed and undergo recombination reaction causing un-reacted hydrogen at outlet.

6.6 Empirical Correlation for PCRD

The results of all the cases indicated in Table 6.2 were analyzed in detail in order to generate a correlation between inlet and outlet variables. Various combinations of inlet variables were evaluated for multi-linear regression analysis so that hydrogen conversation efficiency can be represented as a suitable function of inlet variables. Out of these combinations, the best fit expressions have been selected based on R-square values and standard error. Similar analysis was carried out for representing other outlet variables as a function of suitable combination of inlet variables. Unlike other approaches as reported in literature, instead of calculating the fluid temperature at the outlet based on conversion efficiency, or taking the mass of all the catalyst plates in PCRD as a lumped solid mass for heat balance calculation, the outlet temperature has been directly represented as a function of the inlet variables. Thus the present methodology for the CFD analysis is a better representative of the thermal hydraulic phenomena associated with the working of a PCRD. As the mass of fluid entering the PCRD at inlet is same as that leaving at the outlet and is proportional to the area, the change in fluid velocity is only due to the density change in the fluid along the channel length. In the other approaches mentioned earlier, solution of the momentum equation requires the evaluation of a representative resistance coefficient. However, in the present approach, by evaluating the outlet velocity as a suitable function of the inlet variables, we can avoid the solution of the momentum equation and thus override the uncertainties in assumed values for the resistance coefficient. The empirical correlation thus developed to represent the PCRD is described below.

Variables at PCRD Inlet

Mass fractions of Species: $Y^i_{H_2}$ $Y^i_{H_{H_2O}}$ $Y^i_{O_2}$ $Y^i_{N_2}$

Inlet temperature: T^i; Inlet Density: ρ^i; Inlet velocity: v^i

Variables at PCRD Outlet

Mass fractions of Species: $Y^o_{H_2}$ $Y^o_{H_{H_2O}}$ $Y^o_{O_2}$ $Y^o_{N_2}$

Outlet temperature: T^o ; Outlet Density: ρ^o ; Outlet velocity: v^o

Difference between inlet and outlet variables is taken such that the value is positive during normal functioning of the recombiner. This has been done for better and easy explanation of the physics involved. For example hydrogen concentration decreases inside PCRD so its change is taken as ‘in’ minus ‘out’, while temperature increases in the recombiner so its change is taken as ‘out’ minus ‘in’. The equations have been written accordingly to take care of positive or negative sign of these differences.

$$Y^o_{H_2} = Y^i_{H_2} - Y^r_{H_2} \tag{6.2}$$

Where, $Y^r{}_{H2}$ is the net mass fraction of hydrogen consumed in recombination reaction inside PCRD at each time step. Mass fractions of oxygen and water vapor are calculated using Eq. (6.3) and (6.4) based on the stoichiometry of the reaction given by Eq. (4.3)

$$Y^{o}_{O_2} = Y^{i}_{O_2} - \frac{\nu_{O_2} M_{O_2}}{\nu_{H_2} M_{H_2}} Y^{r}_{H_2} \tag{6.3}$$

$$Y^{o}_{H_2O} = Y^{i}_{H_2O} + \frac{\nu_{H_2O} M_{H_2O}}{\nu_{H_2} M_{H_2}} Y^{r}_{H_2} \tag{6.4}$$

where, $\nu_{H_2} = 2$, $\nu_{O_2} = 1$, $\nu_{H_2O} = 2$, $M_{H_2} = 2$, $M_{O_2} = 32$, $M_{H_2O} = 18$ as per Eq. (4.3).

$$v^{o} = v^{i} + dv \tag{6.5}$$

$$T^{o} = T^{i} + dT \tag{6.6}$$

$$Y^{r}_{H_2} = a_{H_2} + b_{H_2} Y^{i}_{H_2} + c_{H_2} Y^{i}_{O_2} + d_{H_2} Y^{i}_{H_2O} + e_{H_2} v^{i} + f_{H_2} T^{i} \tag{6.7}$$

where, $Y^{r}_{H_2} = Y^{i}_{H_2} - Y^{o}_{H_2}$

$$dv = a_{v} + b_{v} Y^{i}_{H_2} + c_{v} Y^{i}_{O_2} + d_{v} Y^{i}_{H_2O} + e_{v} v^{i} + f_{v} T^{i} \tag{6.8}$$

where, $dv = v^{o} - v^{i}$

$$dT = a_{T} + b_{T} Y^{i}_{H_2} + c_{T} Y^{i}_{O_2} + d_{T} Y^{i}_{H_2O} + e_{T} v^{i} + f_{T} T^{i} \tag{6.9}$$

where, $dT = T^{o} - T^{i}$

The values of various coefficients in the above equations as obtained by multi linear regression analysis are listed in Table 6.3 below.

Table 6.3: Values of variable function coefficients obtained using multi linear regression analysis

Sr. No.	Coefficient	Value	Coefficient	Value	Coefficient	Value
1	a_{H_2}	-7.53E-4	a_v	1.215	a_T	28.8
2	b_{H_2}	0.925	b_v	127.577	b_T	23014.4
3	c_{H_2}	0	c_v	0	c_T	0
4	d_{H_2}	0	d_v	0	d_T	–61.9315
5	e_{H_2}	– 1.44E-3	e_v	- 0.31525	e_T	0
6	f_{H_2}	3.1E-6	f_v	- 2.28E-3	f_T	0

By using the values from Table 6.3, the Eq. (6.7) can be rewritten as:

$$Y^r_{H_2} = -7.53E\text{-}4 + 0.925\ Y^i_{H_2} - 1.44E\text{-}3\ v^i + 3.1E\text{-}6\ T^i \qquad (6.10)$$

The correlation given by Eq. (6.10) has R square value for is 0.9893 and overall standard error of 0.000267. The positive coefficient of inlet hydrogen concentration in equation 10 signifies that the amount of hydrogen recombined inside PCRD increases with increase in inlet hydrogen concentration. However the conversion efficiency is independent of water vapour concentration at the inlet as is also evident in Figure 6.7 above. The conversion however decreases with fluid velocity at inlet as is apparent with the negative coefficient of velocity in the Eq. 6.10. The positive coefficient of inlet temperature in the equation indicates improvement in conversion with inlet fluid temperature due to faster reaction kinetics at higher temperatures. Similarly by using the values from Table 6.3, the equation (6.8) can be rewritten as:

$$dv = 1.215 + 127.577\ Y^i_{H_2} - 0.31525\ v^i - 2.28E\text{-}3\ T^i \qquad (6.11)$$

Eq. (6.11) has R square value for is 0.6312 and overall standard error of 0.2688. The negative coefficient of inlet velocity means lesser conversion as explained above which leads to smaller change in fluid velocity. The negative coefficient of inlet fluid temperature signifies that for the same velocity and hydrogen concentration at inlet, if the fluid temperature is more, the effect of exothermic heat addition on fluid density and hence on buoyancy is relatively less.

By using the values from Table 6.3, the Eq. (6.9) can be rewritten as:

$$dT = 28.8 + 23014.4Y^{i}_{H_2} - 61.9315\ Y^{i}_{H_2O} \quad (6.12)$$

Eq. (6.12) has R square value for is 0.8212 and overall standard error of 27.88. The change in fluid temperature inside PCRD has a positive coefficient for inlet hydrogen concentration due to the reasons explained earlier. On the other hand, the negative coefficient of water vapour concentration signifies that higher water vapour content at the inlet causes higher specific heat of the gas mixture entering PCRD. This higher specific heat causes lesser rise in fluid temperature for the same amount of heat added due to recombination reaction.

After the development of the empirical correlations for different variables at the PCRD outlet, their accuracy has been examined. This has been done by comparing the predictions made by these correlations against CFD simulation results for the set of inlet parameters used in the cases described in Table 6.2. The comparison results are presented in Figures 6.11 to 6.13. The calculations made by detailed CFD model are compared against the calculations from empirical model for hydrogen consumption between the inlet and outlet of PCRD in Figure 6.11.

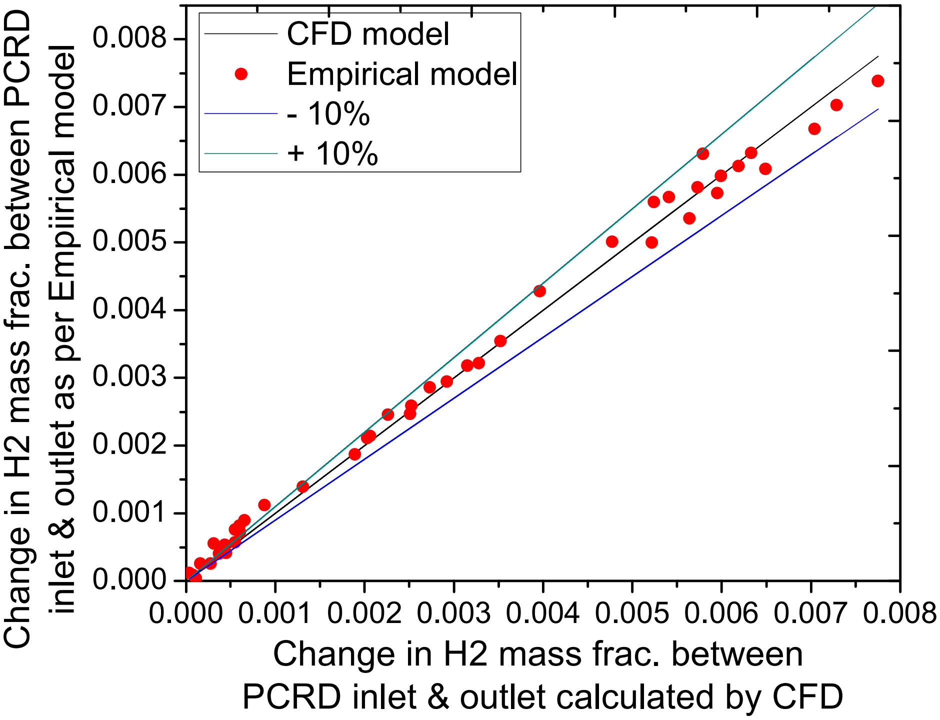

Fig. 6.11: Comparison of prediction made by CFD model and Empirical model for change in H_2 concentration across the recombiner

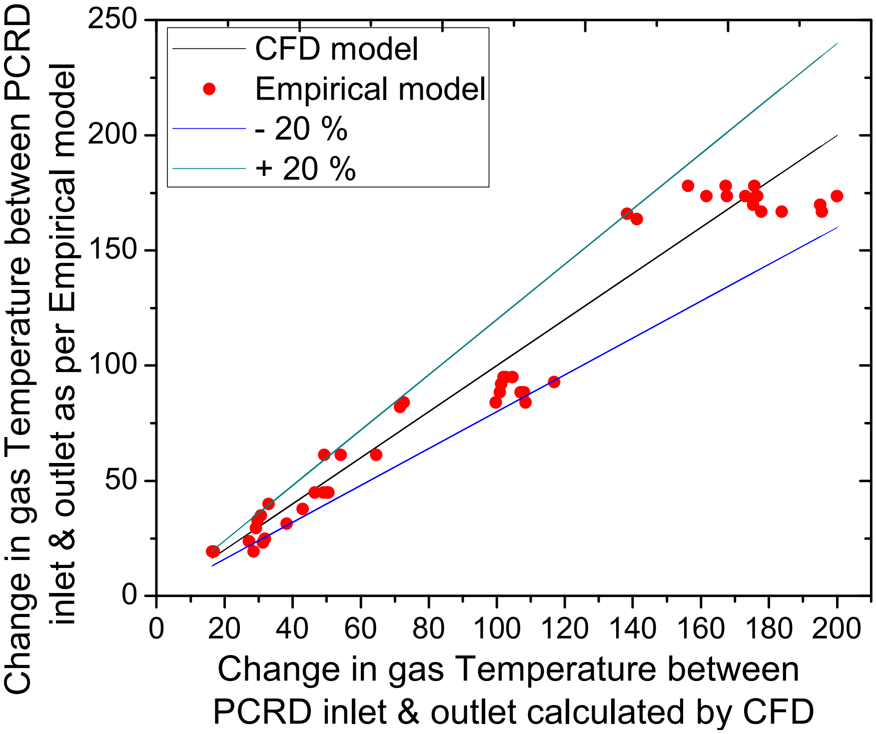

Fig. 6.12: Comparison of prediction made by CFD model and Empirical model for change in gas temperature across the recombiner

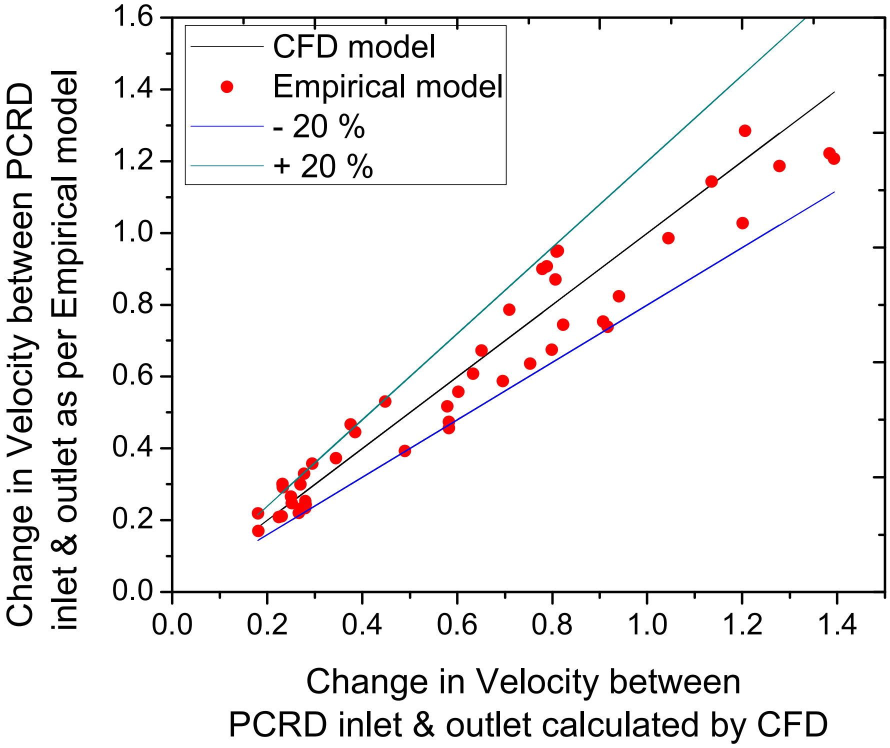

Fig. 6.13: Comparison of prediction made by CFD model and Empirical model for change in velocity across the recombiner

Similar comparison has been made for gas temperature change and velocity change across the PCRD in Figure 6.12 and Figure 6.13 respectively. From these figures, it is evident that, the predictions from the empirical model developed above are in good agreement with the simulation results of the detailed CFD model. Thus, the empirical model can be confidently applied to predict the performance behavior of our specific PCRDs.

The empirical model can be easily plugged into CFD based simulations of PCRDs in nuclear containments. It is generic and can be used even when the number of catalyst plates is different inside a PCRD as long as the plate dimensions and the pitch between them remains the same. The same is a design feature and hence is expected to remain the same for all the PCRDs used in Indian NPPs. Thus this, correlation can serve as a vital tool for CFD based containment analysis for the Indian NPPs using any of the general purpose CFD code. Additionally, it can be used on a stand-alone basis for quick offhand reference about the performance of PCRD.

6.7 Conclusions

The updated CFD based recombiner model was used for generating the data matrix required for mapping PCRD performance in terms of hydrogen conversion and correlation for outlet variables based on inlet conditions. For this purpose, the geometry was selected such that it sufficiently captures all the processes taking place inside the actual PCRD. Based on this model, a number of simulations were carried out with different inlet conditions for a range of velocity, temperature, hydrogen concentrations and steam concentrations that can be encountered by a PCRD in the reactor containment during severe accident scenarios. The results of all the cases were analyzed in detail to generate a correlation between inlet and outlet variables. Various combinations of inlet variables were tested by multi-linear regression analysis to represent hydrogen conversation efficiency as a function of inlet variables. Similar analysis was carried out for representing other outlet variables as a function of suitable combination of inlet variables. Thus outlet temperature and outlet velocity were also directly represented as a suitable function of the inlet variables instead of solving momentum and energy conservation equations inside PCRD. All these correlations were compiled in the form of an empirical model. The results of the developed empirical model were also compared against the CFD simulations. These were found to be within accuracy range of ±20% of the CFD results. These results indicate that conversion efficiency does not change significantly with concentration of steam at the inlet. On the other hand, it is highly dependent on the hydrogen concentration at inlet. This is because, higher hydrogen concentration causes faster reaction rate leading to the increase in catalyst temperature and in turn, further improvement in reaction kinetics. The empirical correlation thus developed can be used on a stand-alone basis for quick off-hand reference about the performance of PCRD. It can also be easily plugged into CFD based hydrogen distribution simulations inside closed enclosures having PCRD.

CHAPTER 7

Demonstration of the Hybrid Approach

7.1 Introduction

Containment analysis involving multiple Passive Catalytic Recombiner Devices (PCRDs) is focused on the influence of these PCRDs on the overall hydrogen distribution and thermodynamic state of gas mixture inside multi-compartment containment geometry of Nuclear Power Plants. Hence, innovative practical approaches need to be devised for carrying out such studies for hydrogen mitigation to capture multi physics phenomena using CFD in a more computationally economical manner. This can be achieved by using some sort of lumped model for the PCRD while modelling rest of the geometry using a detailed CFD approach. Use of such a coupled approach can obviate the need of using fine mesh for modelling recombiners and can serve as a vital tool to predict the effect of PCRDs on hydrogen distribution inside multi-compartment geometry of reactor containment. Analysis of the thermal hydraulic performance of recombiners and hydrogen distribution behaviour in the large multi-compartment containment volumes may thus become less time-intensive. Researchers world-wide, have reported few such approaches based on vivid assumptions. One such study reported by Halouane et al. (2018) implements a CFD model for recombiner in the ANSYS Fluent code using a correlation given by the PCRD manufacturer. In the model, PCRD unit was considered as a channel where the reaction takes place without any chemistry details.

Similar approach based on the empirical correlation formulated for our PCRD is also required to be formulated. This approach will facilitate a mechanism for speedy containment analysis involving hydrogen distribution in presence of multiple recombiners. This chapter aims to formulate such a new hybrid approach. Thus it will demonstrate the incorporation of empirical model developed for the PCRD into general-purpose CFD code to predict the performance of PCRD inside a closed geometry.

7.2 Description of Hybrid Approach

In the hybrid approach, the fluid domain of the environment (like the multi-compartment containment geometry) having PCRD is modeled using CFD, while the volume of PCRD inside the domain is not meshed. This creates internal boundary faces inside the fluid domain as shown in Figure 7.1. Since the empirical model is based on the steady state performance of PCRD for every inlet condition, the flow across the recombiner is assumed to be steady during each time step of the transient analysis. At each time step during the simulation, the space averaged values of different variables at the PCRD inlet (which is outlet boundary face inside the fluid domain) are derived from the CFD simulation of hydrogen distribution inside the closed geometry. These values are then passed on to the empirical PCRD model. Values of these variables at the PCRD outlet are calculated at each time step by the empirical model. The calculated outlet values at PCRD outlet (which serves as inlet for the fluid domain) are supplied as inflow boundary condition for the CFD calculations of fluid domain. Thus the empirical model runs in parallel with the CFD simulation. At each time-step, it exchanges the values of all the variables at PCRD inlet and outlet with the CFD calculations of the overall fluid domain. Figure 7.1 exhibits the comparison between the working philosophy of detailed CFD approach and the hybrid approach explained above.

This approach is different from other hybrid approaches reported elsewhere for PCRD in the sense that it does not have any mesh for the PCRD as compared to the coarse mesh used by other approaches. Hence, there is no requirement of lumping all the catalyst plates as single solid plate having thermal mass equal to the combined mass of individual catalytic plates. Thus, the error encountered due to neglecting thermal radiation between the parallel catalytic plates and the fluid between does not arise in this method. Similarly, the solution of the momentum equation can be avoided for the PCRD domain in this approach, as the outlet velocity gets calculated externally. Hence the pressure at the outlet of PCRD is considered the same as the inlet for each time step. Unlike other hybrid approaches, it obliviates the assumption of equivalent resistance coefficient for parallel catalyst plates inside PCRD, required for solving the momentum equation. This approach directly calculates the gas temperature and velocity at the outlet of PCRD by the use of their empirical correlations based on inlet variables. Here, the accuracy is more as the correlations are based on detailed CFD analysis taking care of the thermal radiation as well as velocity rise caused due to actual momentum balance including buoyancy between the parallel catalytic plates of PCRD.

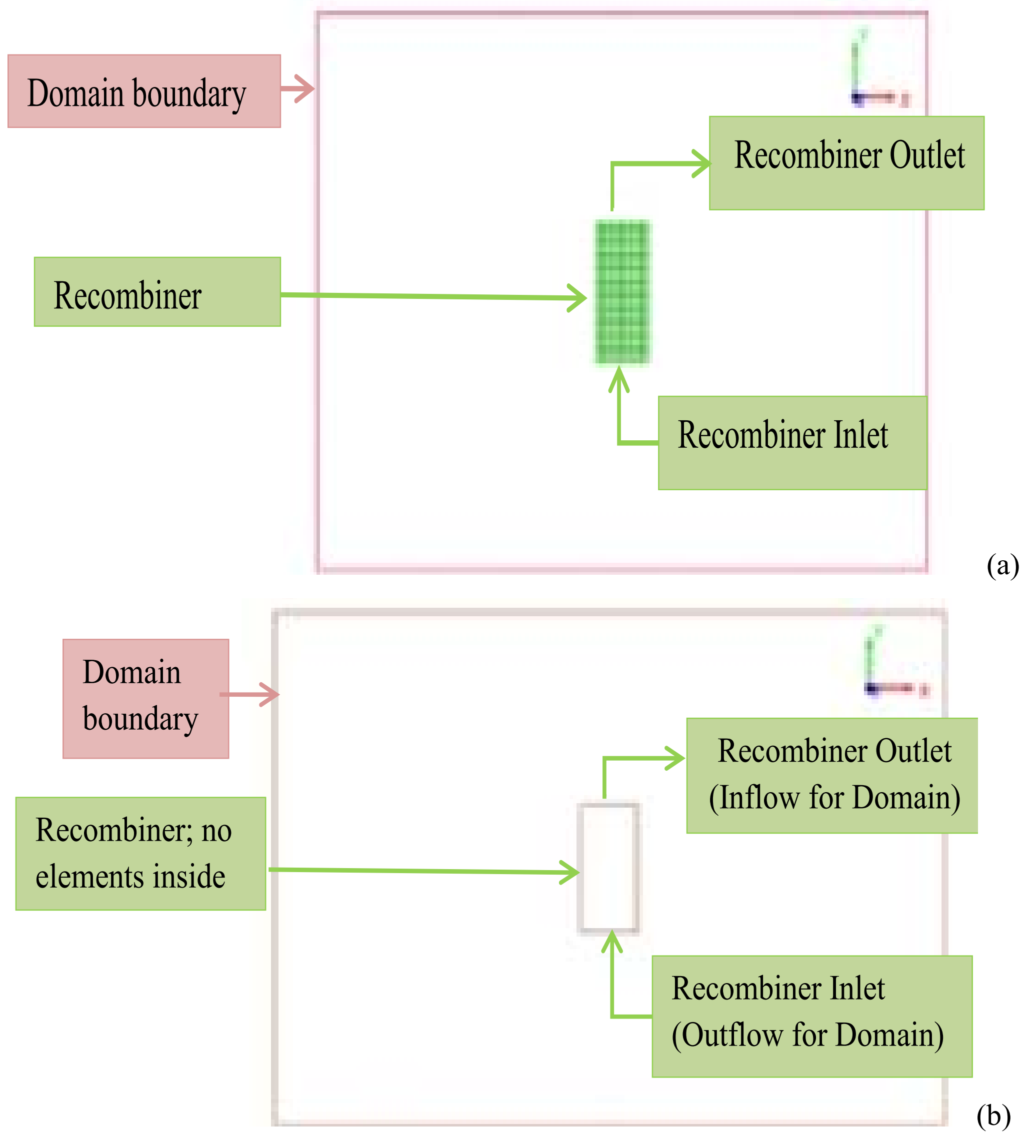

Fig. 7.1: Comparison of (a) conventional CFD approach and (b) Hybrid Approach for modeling of PCRD inside a closed geometry

7.3 Demonstration of the Hybrid Approach

The use of this hybrid approach for modeling of PCRD inside closed geometries has been demonstrated by plugging the empirical model for PCRD into the CFD software FLUIDYN+MP. However, it is a generic methodology and can be applied to any other commercially available general purpose CFD software having the necessary capabilities to model phenomena such as multispecies gas transport, two phase flows, turbulence, thermal radiation etc. The method has been demonstrated by simulating a room of 3 m × 3 m x 9 m having two compartments in vertical direction. Each compartment has a height of 4.5 m. The compartments are interconnected by an opening of 1 m x 1 m at the centre of the partition. Each compartment has a recombiner box of dimensions 0.4 m x 0.8 m x 1 m. The recombiners are placed near the centre of opposite walls in each of the compartment as shown in Figure 7.2. The domain is pre-filled with 8% v/v hydrogen and 50% v/v steam. Model geometry and other details are presented in Figure 7.2.

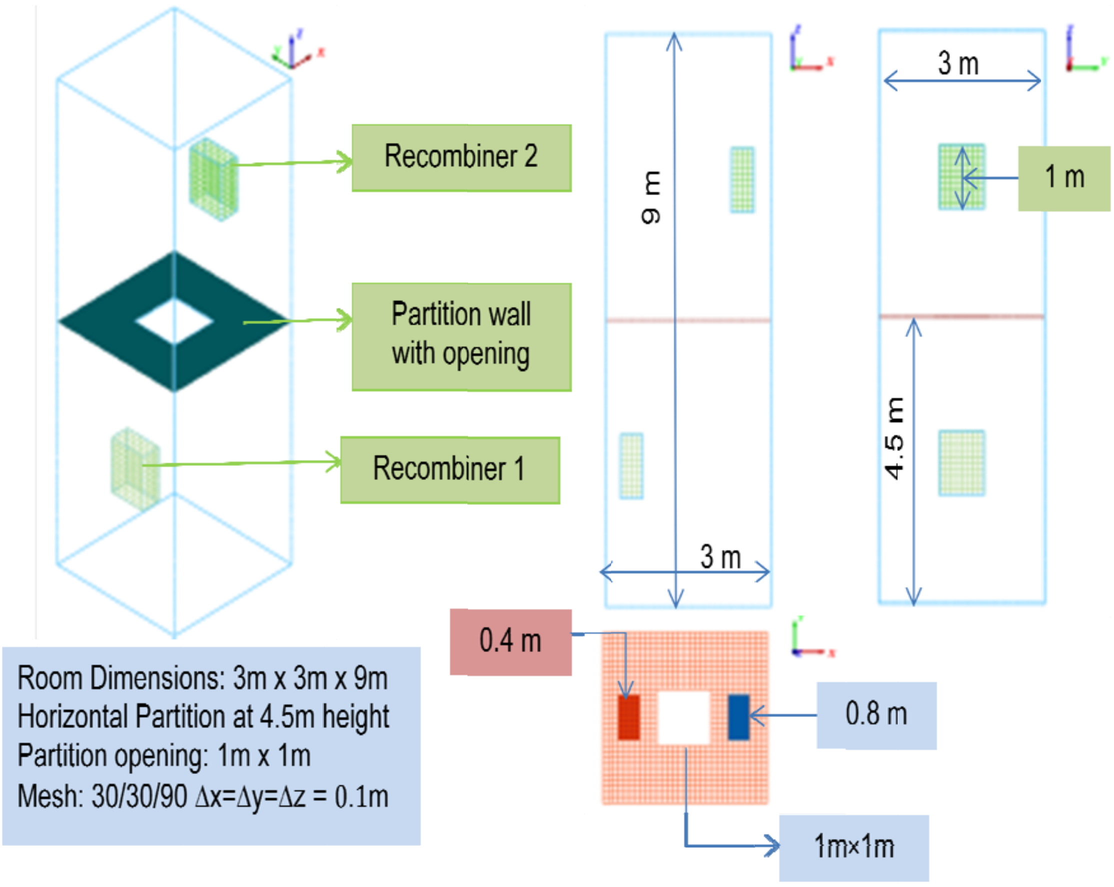

Fig. 7.2: Geometry and mesh details for the demonstration case on hybrid approach

7.3.1 Details of The Model Used in the Approach

The model geometry has been discretised using completely structured mesh. Since there is no requirement of fine mesh inside the PCRD, a uniform mesh has been used having hexahedral elements of 100 mm size in x, y and z direction. The values of all the variables across the cells present at the velocity outflow boundaries (inlet boundary for each recombiner) are space averaged at each time step and fed to the user sub routine based on the empirical model for PCRD. Values of velocity, temperature and species mass fractions at the velocity inflow boundaries (recombiner outlets) are assigned as 'user defined'. These values for the change in properties across the recombiner are calculated using the empirical correlations by the user sub routine and fed to the inflow boundaries at every time step. At each of the velocity outflow boundaries (recombiner inlets) the total mass flow rate is assumed to be equal to that through the corresponding recombiner outlets.

7.3.2 Boundary Conditions

All the walls of the two compartment room, including the partition wall and the recombiner walls are considered as adiabatic and no-slip wall. Bottom surfaces of both the recombiners are defined as velocity outflow boundaries. Top surfaces of both the recombiners are defined as velocity inflow boundaries.

7.3.3 Initial Conditions

Table 7.1 shows the initial conditions. This data corresponds to typical premixed wet conditions having 50% v/v steam. The initial conditions are taken similar to the wet cases presented in Table 3.5 of chapter 3. Hence, the pressure and temperature are taken is such that the gas mixture is thermodynamically sustainable for 50% v/v steam at ambient conditions of the simulation. Due to high initial temperature and adiabatic walls, no condensation is envisaged inside the domain.

Table 7.1: Initial conditions

Property	**Value**
Pressure	216. 837 kPa
Temperature	378 K
H_2 Volume fraction/Mass fraction	0.08/0.007521
O_2 Volume fraction/Mass fraction	0.0882/0.1327
N_2 Volume fraction/Mass fraction	0.3318/0.4367
H_2O Volume fraction/Mass fraction	0.5/0.4231
Specific Turbulent kinetic energy	10^{-8} m^2/s^2

7.3.4 Results & Discussions

Since the purpose the present simulation is only to demonstrate the applicability and working of the hybrid approach, the transient has been run for 120 s. The simulation starts with uniformly distributed hydrogen and steam as per the initial conditions presented in Table 7.1. The PCRD located in the upper compartment has been designated as 'Recombiner-1' and that in the lower compartment is designated as 'Recombiner-2'. Various chemical and thermodynamic variables are monitored, at the inlet and outlet of both the recombiners. At the inlet, space average values from the cells present at the PCRD inlet boundary face are plotted. On the other hand at the outlet, both the values calculated in the simulation and the values calculated using the standalone empirical correlation have been plotted to verify that the boundary conditions are calculated and applied properly.

Figures 7.3 (a) and 7.3 (b) present the variation of hydrogen concentration with respect to time at the inlet and outlet of Recombiner-1 and Recombiner-2 respectively.

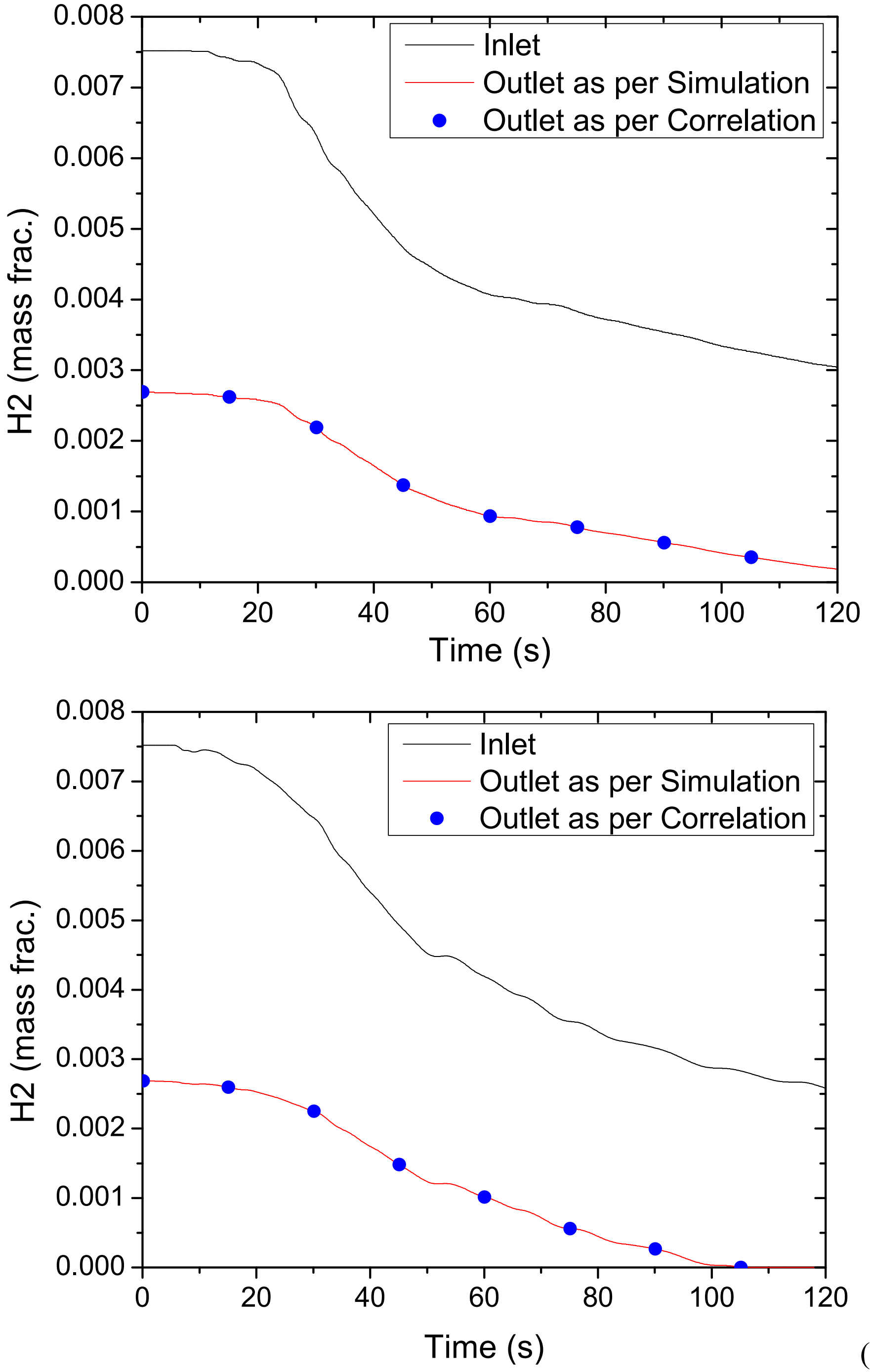

(a)

(b)

Fig. 7.3: Hydrogen concentration vs. Time for (a) recombiner 1 and (b) recombiner 2

It can be seen that both the recombiners start working from the beginning. In about 20 seconds the inlet values start getting affected by the recombiner operation. It is observed from Figure 7.3 that, for the conditions simulated, there is an initial conversion of around 5E-3 hydrogen mass faction across the inlet and outlet of both these recombiners. This is measured by the difference in hydrogen concentration between the inlet and outlet.

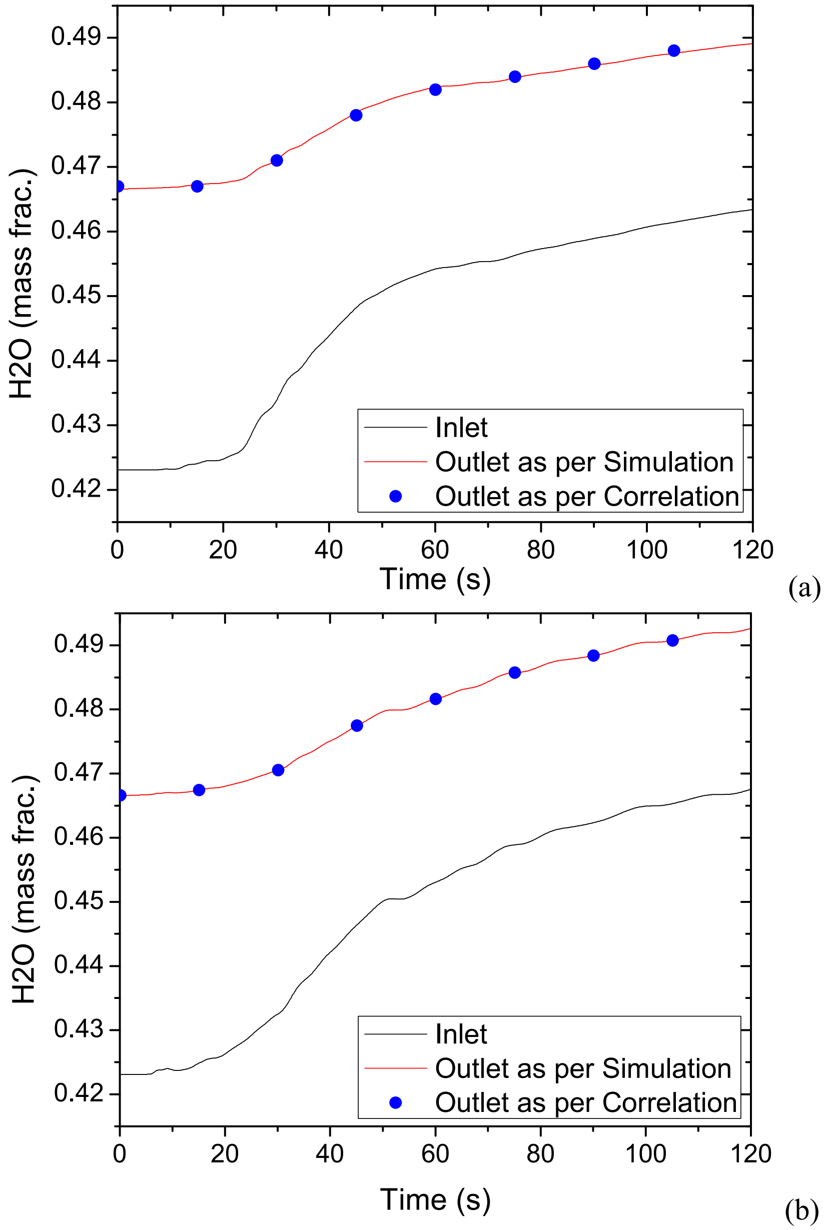

Fig. 7.4: Steam concentration vs. Time for (a) recombiner 1 and (b) recombiner 2

The conversion across recombiners starts dropping as the inlet hydrogen concentration decreases. This is due to drop in temperature as the heat of reaction decreases. Inverse trends are observed for the steam concentration as can be seen from Figures 7.4 (a) and 7.4 (b) which present steam mass fraction plots with respect to time for recombiner 1 and 2 respectively. This proportionally inverse trend compared to hydrogen is due to the fact that consumption of hydrogen with oxygen during recombination leads to the formation of water vapor causing proportional increase in its concentration.

The variation of gas temperature with respect to time, at the inlet and outlet of Recombiner-1 and Recombiner-2 is shown in Figure 7.5 (a) and 7.5 (b) respectively. Here it can be observed that, since the initial hydrogen mass fraction is 0.0076 (as per 8% v/v) during the beginning of the simulation itself, the recombination starts instantly. This leads to the gas temperatures near both the recombiners to increase. This temperature rise causes the natural convection flow to develop across the recombiners. The resulting difference in velocity across the inlet and outlet for both the recombiners is presented in Figures 7.6 (a) and 7.6 (b). As seen from these figures, the velocity rise across the recombiners at the start of the simulation is around 0.8 m/s. It can also be seen that as the simulation progresses, the velocity-change across the recombiner decreases. This is due the drop in hydrogen concentration. Additionally, as the gas temperature entering the recombiners rises, the relative affect of heat addition to the gas by the reaction decreases. Hence buoyancy comes down and leads to progressively lesser velocity change across the inlet and outlet.

From these figures, it is also evident that the values of different variables at the outlet of both recombiners as obtained during the simulation match very closely with the values calculated by the stand alone empirical correlation. These results demonstrate that the hybrid approach developed by plugging the empirical model for PCRD into CFD code for hydrogen distribution inside the large multi compartment domain has been correctly implemented and gives the results as intended.

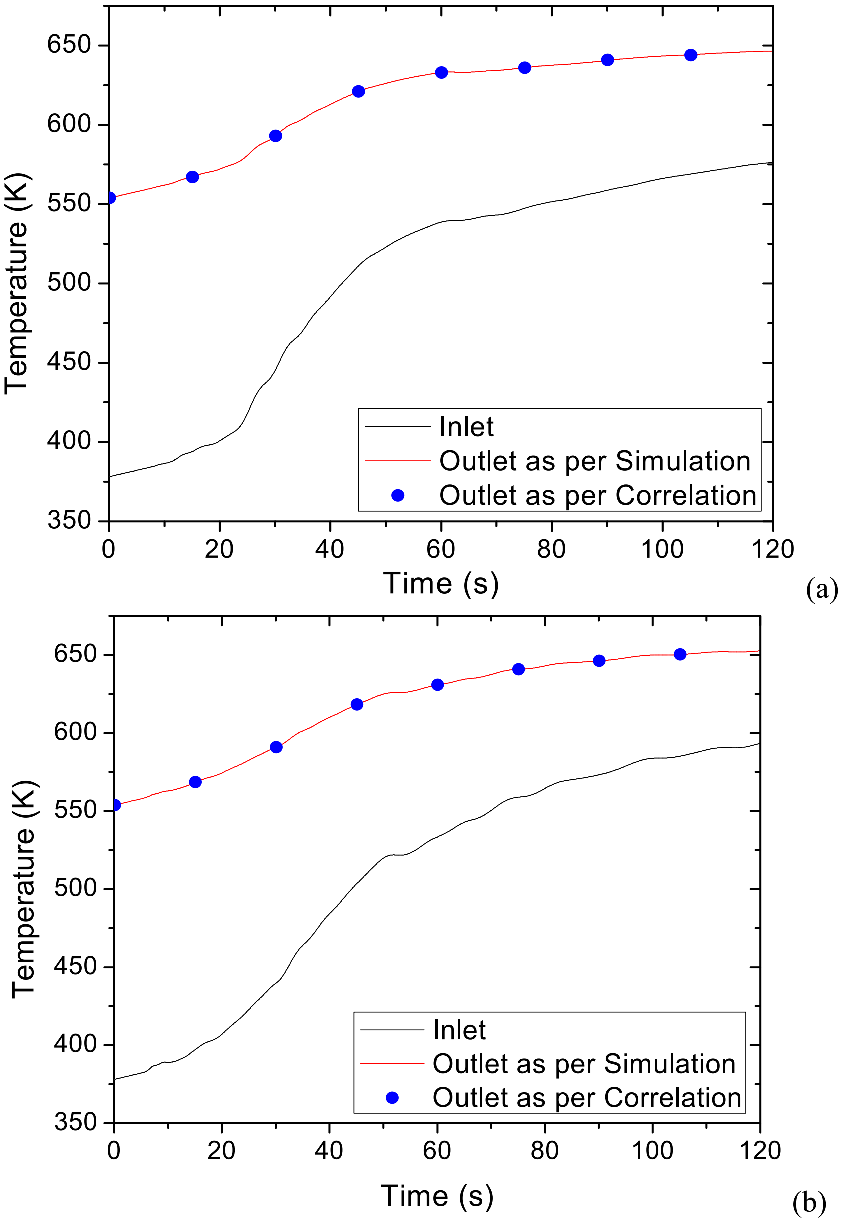

Fig. 7.5: Fluid temperature vs. Time for (a) recombiner 1 and (b) recombiner 2

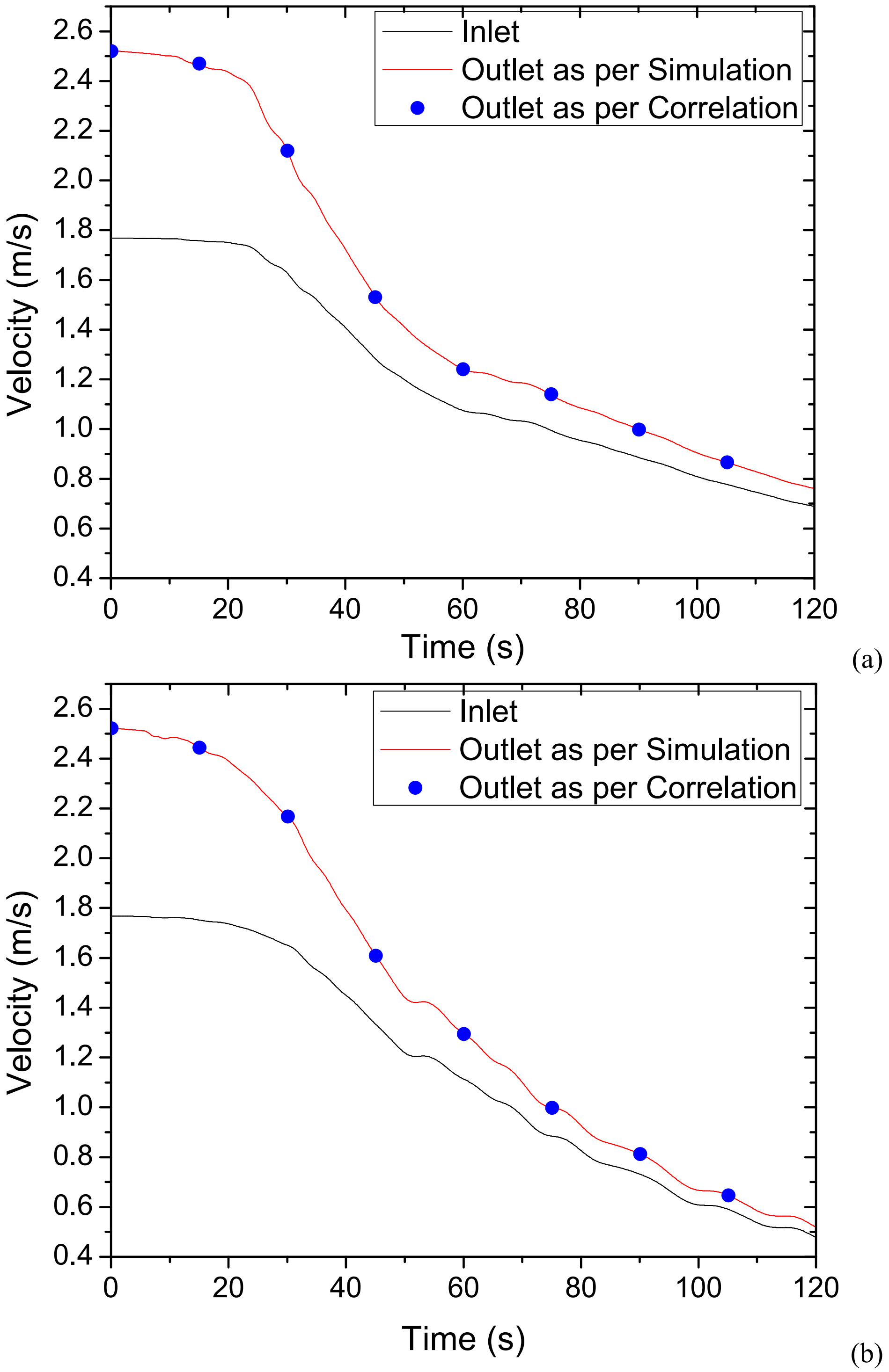

Fig. 7.6: Velocity vs. Time for (a) recombiner 1 and (b) recombiner 2

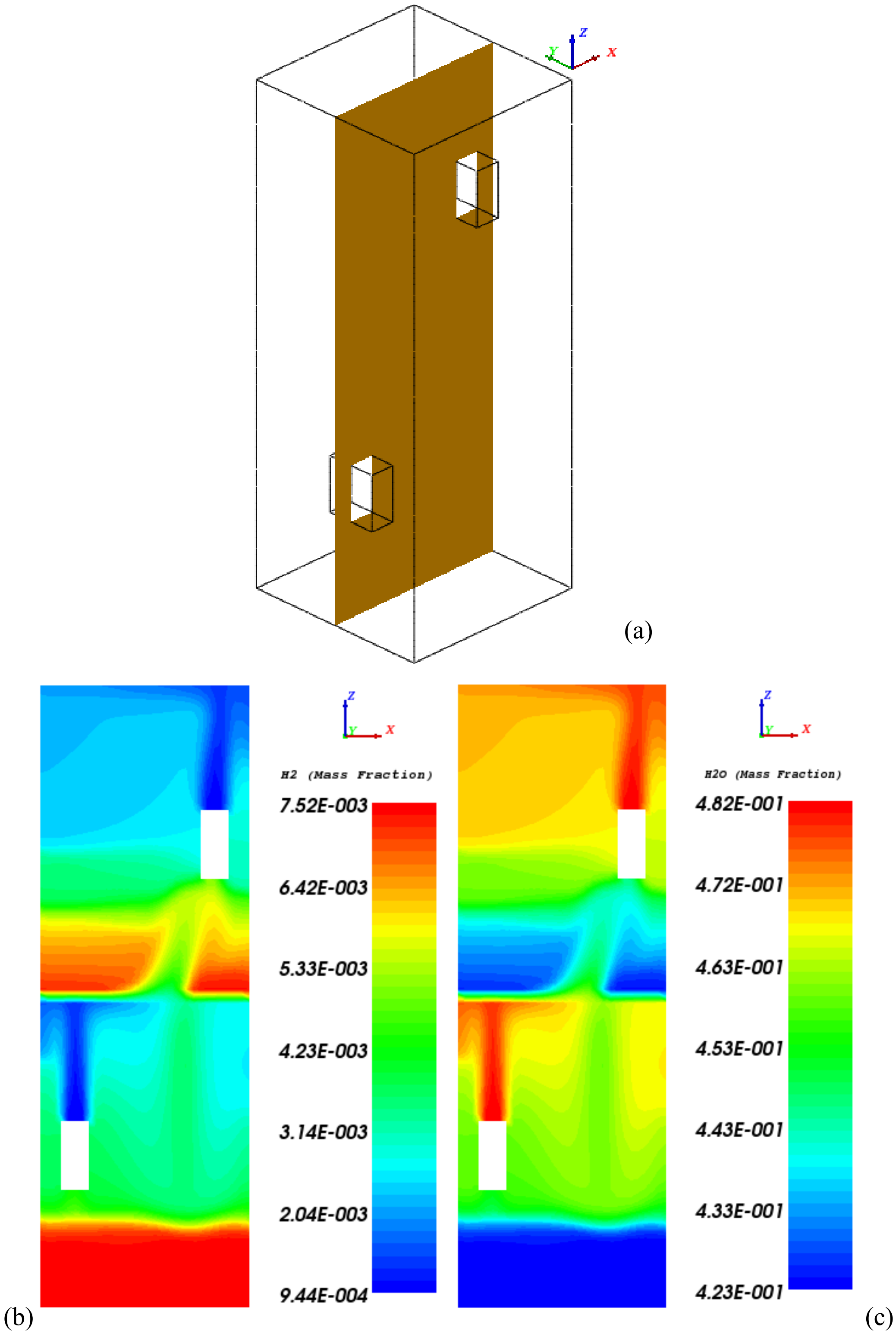

Fig. 7.7: (a) Position of sectional plane for contour plots, (b) H_2 concentration and (c) Steam concentration at 60 seconds during the transient

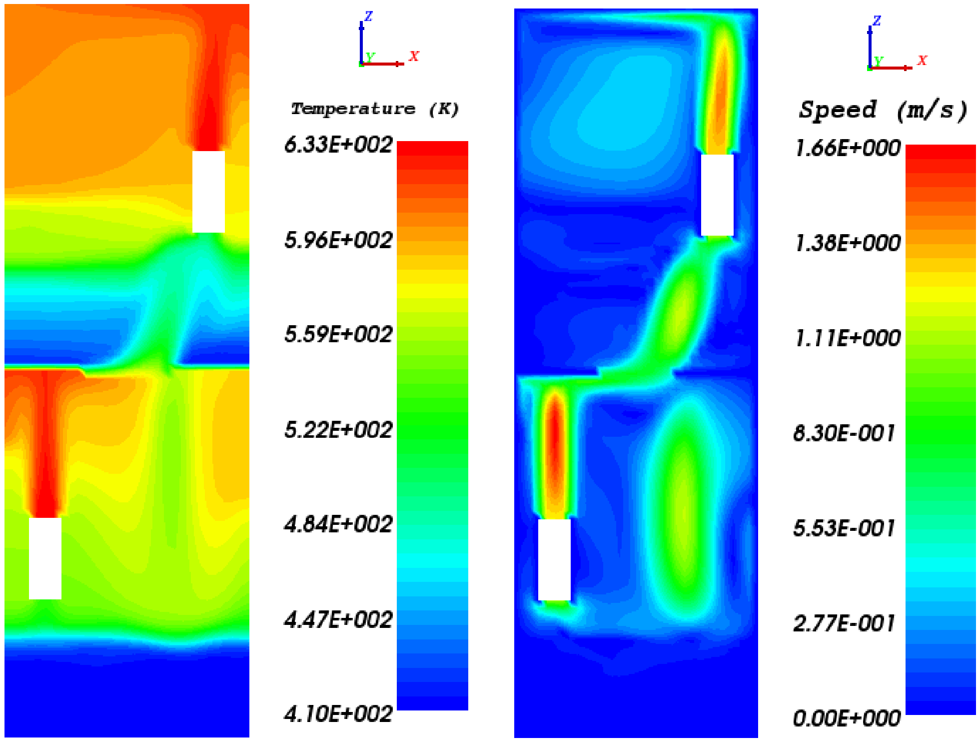

(a) (b)

Fig. 7.8: (a) Fluid temperature and (b) Velocity magnitude at 60 seconds during the transient

The contour plots for different variables have been presented in Figures 7.7 and 7.8. These contours have been plotted at a vertical sectional plane passing through the centre of the room. The direction of the plane is selected such that it passes through the centre of both the recombiners as shown in Figure 7.7 (a). These results have been plotted corresponding to 60 seconds during the transient. Figures 7.7 (b) and 7.7 (c) present the concentration profiles for hydrogen and steam respectively inside the domain. Similarly, Figures 7.8 (a) and 7.8 (b) present the temperature and velocity distribution inside the domain at 60 seconds. From these plots, it can be seen that in addition to the natural convection flow developed around the individual recombiners, the effect of the opening in the partition wall is also evident. The hot gases coming out from Recombiner 2 rise upwards and escape through the opening into the upper compartment. This causes temperature rise near the inlet of Recombiner 1. This flow pattern is expected to be dynamic with respect to time due to contiguously changing concentration and temperature profile inside the domain.

7.4 Conclusions

A new hybrid approach has been developed and its functioning has been demonstrated for prediction of PCRD behavior inside closed multi compartment geometry similar to those present inside the containment building of NPPs. This approach is different from other similar approaches reported in literature in the sense that it does not require any assumption for resistance coefficient and thermal mass for solving the momentum and energy equations inside PCRD. The method is based on generic empirical model for specific PCRD and hence can be used even with different number of catalytic plates inside the PCRD. This method obliviates the complexity of fine meshing for PCRD while using CFD for capturing hydrogen distribution as well as other thermodynamic processes inside closed geometry. The major conclusions that can be drawn are:

- As the simulation progresses, the hydrogen concentration inside the domain starts to decrease due to its consumption for recombination with oxygen. The steam concentration inside the domain increases proportionally with decrease in hydrogen concentration due to the former being produced by consumption of the later inside the recombiner.

- The meshing requirement for the CFD model based on the developed hybrid approach is significantly less and simpler as compared to detailed CFD model for hydrogen recombination studies.
- The results from this hybrid model indicate normal working of recombiner right from the beginning of the simulation as opposed to the results from detailed recombiner model presented in chapter 3 where the recombiner takes some time for start up. This is due to the initial heating of the catalyst plates which is captured by detailed model but is neglected by the hybrid approach. This difference in the depiction of startup recombiner behavior is very small and does not affect the overall prediction for hydrogen recombination and distribution.
- The new hybrid approach thus formulated, will serve as a vital tool for CFD-based severe accident containment analysis using any commercial CFD software by drastically reducing the meshing requirement in such studies.

CHAPTER 8

Conclusions & Recommendations

Release of hydrogen as a consequence of severe accident in a Nuclear Power Plant (NPP) can be a potential threat to the integrity of the containment building. One of the most promising technologies to mitigate the consequences of hydrogen buildup inside the containment of NPP under severe accident scenario is to deploy Passive Catalytic Recombiner Device (PCRD). They work on the principle of recombining hydrogen with oxygen from ambient air on catalytic surfaces to form steam and release exothermic heat of reaction. These devices are known to recombine hydrogen at much lower concentrations and at near-ambient temperatures, thus reducing the risk of gas phase ignition/deflagration/detonation of the hydrogen–air-steam mixtures at low hydrogen concentrations. Experimental studies together with well validated analytical models based on empirical, semi-empirical and more detailed 2D or 3D numerical approaches have gained significance for understanding the behavior and evaluating the performance of catalytic recombiners. However, for the real containment analysis, such models are usable only when they are built in conjunction with CFD based hydrogen transport codes, in order to resolve the stratification related issues in the typical post Loss Of Coolant Accident (LOCA) steam laden containment.

As a part of the research work related to this thesis, a detailed model has been developed for PCRD using commercial CFD software FLUIDYN. This model resolves the recombiner internals such the thin catalytic plates as well as the parallel flow channels into finely discretized space-time domain. For establishment of its accuracy, the model is validated against available results from open literature. This model is based on the reaction kinetics data from the literature to enable quantitative comparison of the results. The validated model is then applied to carry out simulations for assessment of the most suitable PCRD location within a closed geometry. These performance assessment simulations have been carried out under different atmospheric conditions in the vessel (i.e. dry and steam) with premixed hydrogen environment. Models for condensation in bulk as well as at the walls are used in the simulation owing to the steam formed during recombination reaction and also the steam already present in the atmosphere (as in case of reactor containment during severe accident scenarios). However due to the exothermic reaction, the water vapor formed during recombination gets heated up and does not condense in any of the cases presented. The study facilitated qualitative comparison of the performance efficiency of PCRD when placed at different locations inside a closed geometry. The findings reveal that PCRD location plays important role in its effectiveness to curtail hydrogen stratification inside the closed geometry. The investigation is vital for the hydrogen mitigation programme for severe accident scenarios as position of the recombiner box plays vital role in the mitigation scheme.

Second milestone of the research work is achieved in the form of reaction kinetics for the PCRD catalyst developed for Indian NPPs. The Reaction kinetics associated with SS wire mesh substrate based Pt-Pd catalyst is evaluated by the means of lab scale experiments. The activation energy calculated for the recombination reaction on the single catalyst plate is found to be in range 18.1 kJ/mol, a with pre exponential factor of 2.14. This value is in accordance with the values reported for similar catalyst in open literature. Behaviour of catalyst plates stacked in parallel inside PCRD is also evaluated experimentally. When catalytic plates are placed in parallel to each other and outer surface of the two side plates is blocked, the lateral diffusion of hydrogen from the sides is prohibited. This leads to inflow of hydrogen towards the central channels from the bottom only. Hence, for the catalytic plates placed in parallel, the activation energy is found out to be 20.6 kJ/mol, while the pre-exponential factor is 6.1. Thus, the overall phenomena occurring at the parallel catalytic plates, is approximated in the form of a single step Arrhenius equation.

As a next step, the reaction kinetics obtained for the in-house PCRD catalyst is used to fine tune the CFD based recombiner model. This is done by replacing the kinetics from open literature with the single step Arrhenius equation developed for the in-house catalyst. This is significant as the newly obtained kinetics for the parallel catalytic plates is different from the reaction kinetics available in open literature. The updated recombiner model is then validated against in-house experimental data to ascertain the accuracy of the CFD model.

The updated CFD model with the reaction kinetics of the developed catalyst is used to perform a detailed parametric study for mapping the performance of in-house PCRD. For this purpose, a number of simulations have been carried out with different inlet conditions, based on the expected ranges of velocity, temperature, hydrogen concentration, and steam concentration inside reactor containment during postulated severe accidents. This data matrix is processed using multi linear regression analysis to obtain correlations for PCRD outlet variables as suitable functions of different inlet variables. Thus outlet temperature and outlet velocity are also directly represented as a suitable function of the inlet variables. This approach is able to avoid the uncertainties in solution of the momentum equation based on assumed values for the resistance coefficient for PCRD. These correlations for hydrogen conversion inside PCRD and other outlet variables are than compiled into an empirical model for the Indian PCRD.

The empirical model thus developed can be easily plugged into any general purpose CFD software for prediction of PCRD behavior. In order to represent the applicability of this empirical model, a CFD based hybrid approach is developed and demonstrated. In this methodology, multiple PCRDs inside the CFD domain of large geometry are modeled as black-boxes. Their performances are predicted and merged into the CFD calculations with the help of empirical model run parallel to the CFD analysis. The method obliviates the complexity of fine meshing inside PCRD while using CFD for capturing hydrogen distribution as well as other thermodynamic processes inside closed geometry. Hence, this hybrid approach will serve as a vital tool for CFD based severe accident containment analysis using any commercial CFD software by drastically reducing the meshing requirement in such studies.

Major conclusions drawn from the work performed are as given below.

1. It has been found that the kinetic model of Schefer [2] available in literature, to simulate the recombiner behavior gives higher hydrogen recombination rates as compared to reaction kinetics data generated in-house for the developed PCRD catalyst.
2. It has been found that steam concentration does not affect the conversion efficiency of the recombiner within the range of steam concentration taken in

the studies performed. The efficiency increases with hydrogen concentration and temperature of gas mixture.

3. Recombiner placed towards lower elevation inside the closed vessel gives better recombination rates and uniform hydrogen distribution.
4. The empirical correlation developed for estimating hydrogen recombination rate for the in-house PCRD predicts similar recombiner performance as calculated by the detailed CFD model based on reaction kinetics.
5. The hybrid approach incorporating empirical correlations inside the CFD model gives faster results due to less meshing requirement in the fluid domain.

Major outcomes of the thesis are:

1. The catalyst developed for use in PCRD has been characterized in terms of particle size, morphology and chemical kinetics.
2. Reaction kinetics for hydrogen recombination associated with the developed catalyst plates arranged in parallel has been evaluated by in-house experiments.
3. The obtained reaction kinetics has been used to develop a detailed CFD model. This model has been validated against experimental results.
4. Empirical correlations for hydrogen conversion as well as other outlet variables have been formulated for the PCRD developed for Indian PHWRs.
5. A new Hybrid Approach has been formulated by incorporation of the developed empirical correlations into CFD code to analyze hydrogen distribution and PCRD performance inside reactor containment.

The demonstrated hybrid approach based on the empirical correlation developed for hydrogen recombiners can be applied for detailed containment analysis in future. This will involve performance of various parametric studies related to hydrogen distribution in presence of multiple PCRDs placed at different locations inside the multi-compartment containment geometry of Nuclear Power Plant. Additionally, the developed empirical correlation may be fine-tuned further by carrying out experiments for the steady state performance of standalone recombiner under different inlet conditions. These experimental studies shall be similar in approach to the parametric studies performed in this work for development the empirical correlation.

References

IAEA TecDoc 1196, Fineschi F., Koroll, G., Rohde J., Mitigation of hydrogen hazards in water cooled power reactors, VIENNA, February 2001

IAEA TecDoc 1661, Mitigation of Hydrogen Hazards in Severe Accidents in Nuclear Power Plants, VIENNA, July (2011)

OECD/NEA, Implementation of Hydrogen Mitigation Techniques, NEA/CSNI/R (96) 9

OECD/NEA, Status Report on Hydrogen Management and Related Computer Codes, NEA/CSNI/R (2014) 8

Shapiro Z. M, Moffette T. R. Hydrogen flammability data and application to PWR loss-of-coolant accident, WAPD-SC-545, September 1957, Bettis plant Pittsburgh, PA, USA.

Chakraborty A. K., Removal of Hydrogen with Catalytic Recombiners During Severe Accident Situations, Proceedings of Workshop on Hydrogen Behavior and Mitigation in Water cooled Nuclear Power Reactors, Brussels, March 4 – 8, 1991. 305-316

Baronov G.S., Grigoriev S.A., Kalinnikov A. A., Nikolaev I. I. and Fateev V. N., Development of hydrogen safety system, WHEC 16 / 13-16 June 2006 – Lyon France

Dewit W. A., Koroll G. W., Sitar J. L., Graham W. R. C., Knight C., Hydrogen recombiner development at AECL In: Proc. OECD/NEA/CSNI, AECL-11762, NEA/CSNI/R (96) 8. Pinawa, Manitoba: White Shell Laboratories (1996)

Belapurkar A. D., Gupta N. M., A hydrophobic catalyst for recombining H_2/D_2 and O_2 in nuclear reactors, Power Plant Chemistry 2 (2000) 452-457

Belapurkar A. D., Varma S., Shirole A., Sharma J., Cordierite supported platinum catalyst for hydrogen-oxygen recombination for use in nuclear reactors under LOCA, Power Plant Chemistry 10 (2008) 461-467

Sanap K. K., Varma S., Dalavi D., Patil P. S., Waghmode S. B., Bharadwaj S. R., Variation in noble metal morphology and its impact on functioning of hydrogen mitigation catalyst, International Journal of Hydrogen Energy 36 (2011) 10455 - 10467

Kweonha P., Chong L. K., CFD analysis of PAR performance as function of inlet design, Nuclear Engineering and Design 296 (2016) 38-50

Zhengfeng S., Hongzhi Z., Zhi Z., Zhenghua Z., Guohua M., Xinchun L., Rong L., Tao T., Jun F., Bo G., Supported Pd nano-clusters for the hydrogen mitigation application in severe accidents, Nuclear Engineering and Design 316 (2017) 93-98

Peijian Y., Junyin X., Wei Y., Chen Z., Xinhai Y., Shuangliang Z., Shenghu Z., Shan-Tung T., Super hydrophobic Pd@CeO2/Al2O3 catalyst coating for hydrogen mitigation systems in nuclear power plants, International Journal of Hydrogen Energy 44/39 (2019) 21746-21758

Markandeya S. G., Analytical Model Development for Predicting the Behavior of Catalytic Recombiners, Unpublished Report, GRS, Germany, 1993

Drinovac P., Experimental studies on catalytic recombiners for light water reactors, Ph. D. Dissertation RWTH Aachen University (2006)

Reinecke E. A., Tragsdorf I. Gierling M., K., Studies on innovative hydrogen recombiners as safety devices in the containments of light water reactors, Nuclear Engineering and Design 230 (2004) 49-59

Fischer K., Broeckerhoff P., Ahlers G., Gustavsson V., Herranz L., Polo J., Dominguez T. and Royl P., Hydrogen removal from LWR containments by catalytic-coated thermal insulation elements (THINCAT). Nuclear Engineering & Design, 221 (2003), pp. 137–149

Ganju Sunil et al., Experimental Studies On Hydrogen Distribution in a Large, Single Compartment Geometry, 15th NHMTC And 4th ISHMT/ASME Heat And Mass Transfer Conference, Pune India, Jan. 12 - 14, 2000,

Wolf L. and Holzbauer H., Comparison of FATHOMS Blind and Open Post-test Predictions with the Experimental Data of HDR -H_2-mlxing tests E.11.2 and E.11.4, Proceedings of Workshop on Hydrogen behavior and mitigation in water-cooled nuclear power reactors, Brussels Belgium, 4 - 8 Mar 1991

Andreani, M., Putz, F., Dury, T. V., Gjerloev C., Smith, B. L., On the Application of Field Codes to the Analysis of Gas Mixing in Large Volumes: Case studies using CFX and GOTHIC, Annals of Nuclear Energy, (2003), Vol. 30, pp. 685-714

Travis J. R., Spore J. W., Royl P., Lam K. L., Wilson T. L., Necker G. A., Nichols B. D., Redlinger R., Hughes E. D., Wilkening H., Baumann W., and Niederauer G. F., GASFLOW: A Computational Fluid Dynamics Code for Gases, Aerosols, and Combustion; Vol. 1, Theory and Computational Model; Vol. 2, User's Manual; and Vol. 3, Assessment Manual, Los Alamos National Laboratory report LA-13357-MS (1998), and Forschungszentrum Karlsruhe report FZKA-5994 (1998).

Royl P., Rochholz H., Travis J.R., Necker G., Breitung W., Three dimensional analysis of steam/hydrogen transport with catalytic recombiners in nuclear reactor containment using computer code GASFLOW, 15th International Conference on Structural Mechanics in Reactor Technology, Post-Conference Seminar on Containment of Nuclear Reactors, Hoam Convention Center, Seoul, Korea, 23-24 August 1999.

Royl, P., Rochholz, H., Breitung, W., Travis, J. R., Necker, G., Analysis of steam and hydrogen distributions with PAR mitigation in NPP containments, Nuclear Engineering and Design, Volume 202, 231-248 (2002)

Valdepenas J.M., Jimenez M.A., Fuertes F. M., Fernandez J. A., Improvements in a CFD code for analysis of hydrogen behavior within containments, Nuclear Engineering and Design, 237 (2007) 627-647

Royl P., Travis J. R., Breitung W., Jongtae K., Sang B. K., GASFLOW validation with Panda tests from the OECD SETH Benchmark covering steam/air and steam/helium/air mixtures, XCFD4NRS Workshop, Grenoble 10-12 September 2008

Breitung W., Analysis methodology for hydrogen behavior in accident scenarios, International Conference on Hydrogen Safety, 120009, Pisa, 8-10 September 2005

Heitsch M., Huhtanen R., Téchy Z., Fry C., Kostkac P., Niemi J., Schramm Berthold, CFD evaluation of hydrogen risk mitigation measures in a VVER 440/213 containment, Nuclear Engineering and Design, 240/ 2 (2010) 385-396

Gera B., Sharma P. K., Singh R. K. and Ghosh A. K., Numerical Simulation of Passive Catalytic Recombiner, KERNTECHNIK, 74/5-6 (2009) 286-291

Gera B., Sharma P. K., Singh R. K., and Vaze K. K., CFD Analysis of Passive Autocatalytic Recombiner, Science and Technology of Nuclear Installations (2011 a) 862812, 9 doi:10.1155/2011/862812

Mimouni S., Mechitoua N., Ouraou, M., CFD Recombiner Modeling and Validation on the H2-Par and Kali-H2 Experiments, Science and Technology of Nuclear Installations, 10.1155 (2011) 574514

Reinecke E. A., Bentaib A., Kelm S., Jahn W., Meynet N., Caroli C., Open issues in the applicability of recombiner experiments and modeling to reactor simulations, Progress in Nuclear Energy 52 (2010), 136–147

Reinecke E. A., Stephan K., Wilfried J., Christian J., Allelein H. J., Simulation of the efficiency of hydrogen recombiners as safety devices, International Conference on Hydrogen Safety, San Francisco, CA, 12-14 September 2011

Rożeń A., Modeling of a passive catalytic recombiner for hydrogen mitigation by CFD methods, 22nd International Conference Nuclear Energy for Europe, Bled Slovenia, 9-12 September 2013

Reinecke E. A., Stephan K., Wilfried J., Christian J., Allelein H. J., Simulation of the efficiency of hydrogen recombiners as safety devices, International Journal of Hydrogen Energy 38 (2013) 8117-8124

Meynet N., Ahmed B., Vincent G., Impact of oxygen starvation on operation and potential gas-phaseignition of passive auto-catalytic recombiners, Combustion and Flame, 161 (2014) 2192–2202

Klauck M., Reinecke E. A., Stephan K., Meynet N., Ahmed B., Allelein H. J., Passive auto-catalytic recombiners operation in the presence of hydrogen and carbon monoxide: Experimental study and model development, Nuclear Engineering and Design, 266 (2014) 137–147

Orszulik M., Adam F., Tomasz B., CFD modeling of passive autocatalytic recombiners, NUKLEONIKA: 60/2 (2015) 347-353

Reinecke E. A., Stephan K., Steffen P. M., Klauck M. and Allelein H. J., Validation and Application of the REKO-DIREKT Code for the Simulation of Passive Autocatalytic Recombiner Operational Behavior, Nuclear Technology, 196 (2016) 355-366

Hoyes J.R., Ivings M.J., CFD modeling of hydrogen stratification in enclosures: Model validation and application to PAR performance, Nuclear Engineering and Design, 310 (2016) 142 - 153

Mehdi D., Reza S., Mohammad R., Gholamreza J., Amir S. S., Investigation of a Hydrogen Mitigation System During Large Break Loss-Of-Coolant Accident for a Two-Loop Pressurized Water Reactor, Nuclear Engineering and Technology 48 (2016) 117-1183

Agrawal N., Seik M. A., Balasubramaniyan V., Innovative hydrogen recombiner concept for severe accident management in nuclear power plants, Nuclear Engineering and Design, 323 (2017) 359 - 366

Mahdi S., Faramarz Y., Kaveh K., Seyed M. H., Determination of PAR configuration for PWR containment design: A hydrogen mitigation strategy, International Journal of Hydrogen Energy 42 (2017) 7104-7119

McMinn P., Passive Autocatalytic Recombiners for Flammable Gas Control, Fauske & Associates, LLC, July (2017)

Halouane Y., Dehbi A., CFD simulation of hydrogen mitigation by a passive autocatalytic recombiner, Nuclear Engineering and Design, 330 (2018) 488 - 496

Rożeń A., Simulation of start-up behaviour of a passive autocatalytic hydrogen recombiner, NUKLEONIKA 63/2 (2018) 27-41

Avdeenkov A. V., Sergeev V., Stepanov A. V., Malakhov A. A., Koshmanov D. Y., Soloviev S. L., Bessarabov D. G., Math hydrogen catalytic recombiner: Engineering model for dynamic full-scale calculations, International Journal of Hydrogen Energy 43 (2018) 23523-23537

Revankar S. T., Passive containment cooling system with hydrogen recombiner for prolonged station blackout, International Journal of Nuclear Safety and Security, 1/1 (2019) 1-17

Zhi'ao H., Huifang M. Ning L., Xingwei S., Lei L., Analysis of hydrogen risk and its mitigation systems in CPR1000 during shutdown conditions, Progress in Nuclear Energy 115 (2019) 194-207

Allelein H. J., COCOSYS: status of development and validation of the German containment code system. Nuclear Engineering and Design, 238 (2008) 872–889

Heitsch M., Fluid dynamic analysis of a catalytic recombiner to remove hydrogen, Nuclear Engineering and Design 201 (2000) 1–10

Appel C., Mantzaras J., Schaeren R., Bombach R., Inauen A., Kaeppeli B., Hemmerling B., and Stampanoni A., An Experimental and Numerical Investigation of Homogeneous Ignition in Catalytically Stabilized Combustion of H2/Air Mixtures over Platinum, Combustion and Flame, 128/4 (2002) 340-368

Plumecocq W., Bentaib A. and Layley V., Modeling of the containment mitigation measures in the ASTEC code, focusing on spray and hydrogen recombiners, International Top. Mtg. Nuclear Reactor Thermal Hydraulics, (2005) NURETH-11, Avignon (France)

Kudriakov S., Dabbene F., Studer E., Beccantini A., Magnaud J. P., Paill`ere H., Bentaib A., Bleyer A., Malet J., Porcheron E., Caroli C., Kudriakov S., et al. The TONUS CFD code for hydrogen risk analysis: physical models, numerical schemes and validation matrix. Nuclear Engineering and Design, 238 (2008) 551–565

Bachellerie E., et al. Generic approach for designing and implementing a passive autocatalytic recombiner PAR-system in nuclear power plant containments. Nuclear Engineering and Design, 221 (2003) 151–165

Iyer K. N., Deoras P. M., Aghalayam P. A., Simulation of hydrogen mitigation in catalytic recombiner: Part-II: Formulation of a CFD model, Nuclear engineering and design 241/5 (2011) 1758-1767

Gera B., Sharma P. K., Singh R. K., Vaze K. K., Integrated CFD simulation of passive autocatalytic recombiner in an enclosure filled with hydrogen with two approaches, SMiRT 21, New Delhi (2011 b) III 299

Gera B., Sharma P. K., Singh R. K., Vaze K. K., CFD analysis of passive autocatalytic recombiner interaction with atmosphere, Kerntechnik 76 (2011 c) 2 98-103

Schefer R. W., Catalyzed Combustion of H2/Air Mixtures in a Flat Plate Boundary Layer: II, Numerical Model", Combustion and Flame, 45 (1982) 171–190

Chen Y. S., Kim S. W., Computation of turbulent flows using an extended k-ε turbulence closure model, NASA, CR (1987) 179204

Bird R. B., Stewart W. E., Lightfoot E. N., Transport Phenomena, John Wiley & Sons (2002)

Fluidyn MP GUI Users Manual, Transoft International, Version 5.2, October 2009

Bohm J., Modelling of catalytic processes in recombiners, Ph. D. Dissertation RWTH Aachen University (2007)

Sanap K. K., Varma S., Waghmode S. B., Bharadwaj S. R., Supported Pt nano particles for the hydrogen mitigation application, International Journal of Hydrogen Energy, 39 (2014) 15142 -15155

Barker B. D., Electroless deposition of metals, Surface Technology, 15 (1981) 77-88

Morfin F., Sabroux J. C., Renouprez A., Catalytic combustion of hydrogen for mitigating hydrogen risk in case of a severe accident in a nuclear power plant: study of catalysts poisoning in a representative atmosphere, Applied Catalysis B: Environ, 47 (2004) 47-58

Acres G. J. K., The reaction between hydrogen and oxygen on platinum, Platinum Metals, 10 (1966) 60-64

Kim K. R., Paek S. W., Chung H. Catalytic recombination of hydrogen and oxygen in air stream, Journal Industrial and Engineering Chemistry, 7 (2001) 116-120

Warnatz J., Allendorf M. D., Kee R. J., Coltrin M. E.. A model of elementary chemistry & fluid mechanics in combustion of hydrogen on platinum surfaces, Combustion and Flame, 96 (1994) 393-406

Hellsing B., Kasemo B., Zhdanov V. P., Kinetics of the hydrogen-oxygen reaction on platinum, Journal of Catalysis 132 (1991) 210-228

Seshadri K., Peters N., Williams F.A., Asymptotic analyses of stoechiometric and lean hydrogen-air flames, Combustion and Flame 96 (1994) 407-427

Clyne M. A. A., Thrush B. A., Reaction of oxygen atom with hydrogen. Nature 189 (1961) 135-136